



A search for prompt lepton-jets in pp collisions at $\sqrt{s}=8$ TeV with the ATLAS detector

Citation

ATLAS Collaboration. 2016. "A search for prompt lepton-jets in pp collisions at $\sqrt{s}=8$ TeV with the ATLAS detector." Journal of High Energy Physics 2016 (2) (February). doi:10.1007/jhep02(2016)062.

Published Version

doi:10.1007/JHEP02(2016)062

Permanent link

<http://nrs.harvard.edu/urn-3:HUL.InstRepos:34487706>

Terms of Use

This article was downloaded from Harvard University's DASH repository, and is made available under the terms and conditions applicable to Open Access Policy Articles, as set forth at <http://nrs.harvard.edu/urn-3:HUL.InstRepos:dash.current.terms-of-use#OAP>

Share Your Story

The Harvard community has made this article openly available.
Please share how this access benefits you. [Submit a story](#).

[Accessibility](#)

EUROPEAN ORGANISATION FOR NUCLEAR RESEARCH (CERN)



Submitted to: JHEP

CERN-PH-EP-2015-242
24th February 2016

A search for prompt lepton-jets in pp collisions at $\sqrt{s} = 8$ TeV with the ATLAS detector

The ATLAS Collaboration

Abstract

A search is presented for a new, light boson with a mass of about 1 GeV and decaying promptly to jets of collimated electrons and/or muons (lepton-jets). The analysis is performed with 20.3 fb^{-1} of data collected by the ATLAS detector at the Large Hadron Collider in proton–proton collisions at a centre-of-mass energy of 8 TeV. Events are required to contain at least two lepton-jets. This study finds no statistically significant deviation from predictions of the Standard Model and places 95% confidence-level upper limits on the contribution of new phenomena beyond the SM, including SUSY-portal and Higgs-portal models, on the number of events with lepton-jets.

1 Introduction

In several models of physics beyond the Standard Model (SM) [1–5], the so-called dark matter (see e.g. Ref. [6] and references therein) is charged under a non-Abelian, dark-sector, gauge symmetry that is broken at an energy scale $O(1 \text{ GeV})$. The dark-sector ground state can transition to and from excited states via the emission of a dark gauge boson, referred to as the dark photon (γ_d), that couples very weakly to the SM particles via kinetic mixing [7] with the SM photon. In these models, the Large Hadron Collider (LHC) could produce excited dark-sector states via their interactions with particles found in models of supersymmetry (SUSY) [1, 3] or with Higgs scalar bosons [4, 5] (here referred to as SUSY-portal and Higgs-portal models, respectively), which then decay via the emission of dark photons. If dark photons carry masses of $O(1 \text{ GeV})$, then the dark photon produced from the decay chain of heavier particles such as the SM Higgs boson or SUSY particles would be highly boosted. Depending on its mass, the dark photon would decay primarily into a collimated pair of leptons or light hadrons. The leptonic final-state is experimentally easier accessible, offering a distinct signature that stands out amongst large hadronic backgrounds. A collimated set of energetic leptons is referred to as a lepton-jet (LJ).

A search is carried out for final-states with two prompt lepton-jets using data accumulated in proton–proton collisions at a centre-of-mass energy $\sqrt{s} = 8 \text{ TeV}$ with the ATLAS detector [8]. Many new physics models predict at least two lepton-jets in the final-states as described in Refs. [3, 4]. The analysis focuses on the presence of lepton-jets and does not rely on the rest of the event topology. The dark-photon decay width, Γ_ℓ , and the kinetic mixing parameter, ϵ , are related through

$$\Gamma_\ell = \frac{1}{3} \alpha \epsilon^2 m_{\gamma_d} \sqrt{1 - \frac{4m_\ell^2}{m_{\gamma_d}^2}} \left(1 + \frac{2m_\ell^2}{m_{\gamma_d}^2} \right), \quad (1)$$

where α is the fine structure constant and m_{γ_d} and m_ℓ denote the masses of the dark photons and charged leptons, respectively [9, 10]. The analysis focuses on dark photons with prompt-decays, i.e. consistent with zero decay length within the experimental resolution. Previous searches for prompt lepton-jets, with ATLAS data at $\sqrt{s} = 7 \text{ TeV}$, resulted in upper limits on the production of two lepton-jets in a SUSY-portal model [11] and for a Higgs-portal model [12]. The CMS and D0 collaborations also set upper limits on prompt lepton-jet production [13–17]. Related searches for non-prompt lepton-jets [18] have been performed by ATLAS and have set constraints on smaller values of the kinetic mixing parameter, $\epsilon \leq 10^{-5}$. There are additional constraints on the kinetic mixing parameter and dark-photon mass, e.g. from beam-dump and fixed target experiments [9, 19–27], e^+e^- collider experiments [28–33], electron and muon magnetic moment measurements [34, 35] and astrophysical observations [36, 37].

2 The ATLAS detector

ATLAS is a multi-purpose detector [8] consisting of an inner tracking detector (ID), electromagnetic and hadronic calorimeters and a muon spectrometer (MS) that employs toroidal magnets. The ID provides

precision tracking of charged particles for pseudorapidity¹ $|\eta| < 2.5$ using silicon pixel and silicon microstrip (SCT) detectors and a straw-tube transition radiation tracker (TRT) that relies on transition radiation to distinguish electrons from pions in the range $|\eta| < 2.0$.

The sensors of the pixel detector have a typical pixel size of $50 \times 400 \mu\text{m}$ and typically provide three spatial measurements along the track of a charged particle. The innermost layer with a radial distance to the beamline of about 5 cm is known as the B-layer. The SCT has sensors with a strip pitch of $80 \mu\text{m}$ and provides eight measurements for a typical track. The fine-grained sensors of the semiconductor trackers permit the reconstruction of the closely aligned tracks of lepton-jet candidates (Section 5.1).

The liquid-argon (LAr) electromagnetic (EM) sampling calorimeters cover the range $|\eta| < 3.2$. The calorimeter's transverse granularity, typically $\Delta\eta \times \Delta\phi$ of 0.025×0.025 , and three-fold shower-depth segmentation are used to construct discriminating variables for evaluating the electromagnetic character of lepton-jet candidates (Section 5.4).

A scintillator-tile calorimeter, divided into a barrel and two extended-barrel cylinders, on each side of the central barrel, provides hadronic calorimetry in the range $|\eta| < 1.7$, while a LAr hadronic end-cap calorimeter provides coverage over $1.5 < |\eta| < 3.2$. The LAr forward calorimeters provide both, electromagnetic and hadronic energy measurements, and extend the coverage to $|\eta| \leq 4.9$. The calorimeter system has a minimum depth of 9.7 nuclear interaction lengths at $\eta = 0$. The MS is a large tracking system, consisting of three parts: a magnetic field provided by three toroidal magnets, a set of 1200 chambers measuring with high spatial precision the tracks of the outgoing muons, a set of triggering chambers with accurate time-resolution. It covers $|\eta| < 2.7$ and provides precision tracking and triggering for muons.

ATLAS has a three-level trigger system. The Level 1 (L1) trigger is implemented in hardware, and it uses information from the calorimeters and muon spectrometer to reduce the event rate to 75–100 kHz. The software-based Level 2 (L2) trigger and the Event Filter (EF) reduce the event rate to 300–500 Hz of events that are retained for offline analysis. The L1 trigger generates a list of region-of-interest (RoI) η – ϕ coordinates. The muon RoIs have a spatial extent of 0.2 in $\Delta\eta$ and $\Delta\phi$ in the MS barrel, and 0.1 in the MS endcap. Electromagnetic calorimeter RoIs have a spatial extent of 0.2 in $\Delta\eta$ and $\Delta\phi$. For the L2 trigger the reconstruction is mostly based on simplified algorithms running on data localized in the RoI which was reported by L1. At the EF level the trigger system has access to the full event for processing.

3 Signal models

Two benchmark models are used to interpret the data. In the SUSY-portal model (Section 3.1), a pair of squarks is produced and the cascade decays of the squarks include dark-sector particles and one or more dark photons. In the Higgs-portal model (Section 3.2), the SM Higgs boson decays into a pair of dark fermions, each of which decays into one or more dark photons in cascades. For both models, the dark photons decay into lepton pairs, that can be reconstructed as a lepton-jet, or light hadrons, depending on the branching fractions. Monte Carlo (MC) simulated samples are produced for the two models. All signal MC events are processed with the GEANT4-based ATLAS detector simulation [38, 39] and then

¹ ATLAS uses a right-handed coordinate system with its origin at the nominal interaction point (IP) in the centre of the detector. The z -axis points along the beam pipe. The x -axis points from the IP to the centre of the LHC ring, and the y axis points upward. Cylindrical coordinates (r, ϕ) are used in the transverse plane, ϕ being the azimuthal angle around the beam pipe. Pseudorapidity is defined in terms of the polar angle θ as $\eta = -\ln \tan(\theta/2)$.

analysed with the standard ATLAS reconstruction software. The branching ratio (BR) values for the dark-photon decays to leptons are taken from Ref. [4]. In all signal models used to interpret the results the dark photons are required to decay promptly with mean life time ($c\tau$) close to zero. For the Higgs-portal model, long-lived dark photon samples with $c\tau = 47$ mm are used to extrapolate the signal efficiency of zero $c\tau$ dark photons to non-zero $c\tau$ dark photons (Section 9).

3.1 SUSY-portal lepton-jet MC simulation

A benchmark SUSY model [3] is used to simulate SUSY production of dark-sector particles and dark photons. Simulated samples are produced in several steps. Squark (\tilde{q}) pair events are generated with MADGRAPH [40], version 5, in a simplified model with light-flavour squark pairs with decoupled gluinos [41, 42].² Then BRIDGE [44], interfaced with MADGRAPH, simulates squark decays into neutralinos. The neutralinos decay into dark-sector particles, which decay to SM particles as shown in Figure 1. The squarks are set to decay with a 100% BR into a quark and a neutralino ($\tilde{\chi}_1^0$). The neutralinos decay into dark-sector particles in two ways: $\tilde{\chi}_1^0 \rightarrow \gamma_d \tilde{\chi}_d$ or $\tilde{\chi}_1^0 \rightarrow s_d \tilde{\chi}_d$, where s_d is a dark scalar particle that decays to $\gamma_d \gamma_d$ and $\tilde{\chi}_d$ is a dark neutralino. In this model, the stable dark-matter particle is the dark neutralino which is invisible in the detector. For fragmentation and hadronization PYTHIA 8 [45, 46] is used, with the CTEQ6L1 1 [47] PDF parton distribution function (PDF) set, and the AUET2 [48] set of tuned parameters.

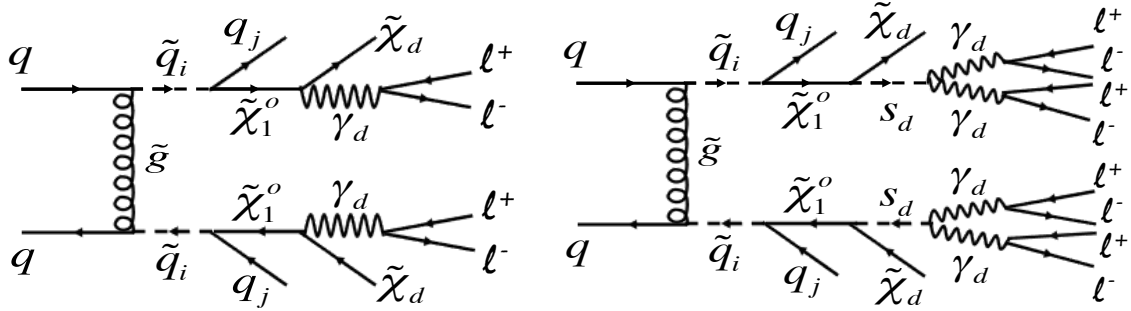


Figure 1: Feynman diagram illustrating the dark-photon production in the $2\gamma_d$ final-state (left), and $4\gamma_d$ final-state (right).

As the dark-sector is loosely constrained experimentally, the squark mass, the dark-photon mass, and all intermediate masses are chosen to correspond to well-motivated nominal values and ranges to which the search is sensitive. The squark-pair production cross section, and hence the signal model sensitivity, would decrease with an increase in the squark mass. The squark mass also affects the sensitivity through the boost of the final-state dark photon. The squark mass, $m_{\tilde{q}}$, is considered to be 700 GeV, which is motivated by the upper limit (17 fb) on the cross section times BR established by a previous search for prompt lepton-jets [11] at $\sqrt{s} = 7$ TeV. This translates into an upper limit of 77 fb on the squark pair-production cross section, which is the predicted cross section at a squark mass of nearly 700 GeV.

² This is the same simplified model used in a previous ATLAS search and shown in the third plot of Figure 10 in Ref. [43]. In the analysis context, the fact that gluinos are decoupled implies the $2 \rightarrow 2$ production, such that there are two SUSY particles at the hard scatter producing two lepton-jets per event.

For the dark-sector, a ~ 1 GeV dark-photon mass is considered, as predicted by the SUSY-portal and Higgs-portal models. For consistency with the $\mathcal{O}(1 \text{ GeV})$ scale for dark-sector particle masses, following the model described in Ref. [3], the set of mass values for the squark decay products is chosen as follows: the $\tilde{\chi}_1^0$ mass is set to 8 GeV, and a set of γ_d mass values is chosen between 0.1 GeV and 2 GeV. A dark photon that kinetically mixes with a SM photon would couple with the same strength to lepton–antilepton and $q\bar{q}$ pairs as the SM photon. The virtual photon conversion rates are measured in low-energy e^+e^- annihilations [49, 50] and a few sets of γ_d mass points are chosen for which the BRs into the leptons are large enough (e.g. 0.25–1.0) to be detectable. The BRs to leptons are in the range from 25% to 100% except when m_{γ_d} is close to either the ρ or ϕ mass. Table 1 summarizes the particle masses assumed.

Table 1: Mass points for SUSY and dark-sector particles in GeV.

$m_{\tilde{q}}$	$m_{\tilde{\chi}_1^0}$	$m_{\tilde{\chi}_d}$	m_{γ_d}	m_{s_d}
700	8	2	0.1, 0.2, 0.3, 0.4, 0.5, 0.7, 0.9, 1.2, 1.5, 2.0	2, 4, 4.5

The intermediate dark-sector masses are chosen such that all particles remain on-shell. The dark scalar s_d mass is set to 2 GeV for samples with γ_d masses below 0.9 GeV, and it is set to 4 GeV for samples with γ_d mass in the range from 0.9 to 1.5 GeV. A 4.5 GeV s_d mass is used for the MC sample with a γ_d mass of 2 GeV. The model sensitivity is mostly driven by the dark photons’ boost and BR to leptons.

3.2 Higgs-portal lepton-jet MC simulation

A hypothesized decay of the Higgs boson to a pair of dark fermions f_{d_2} is considered [4, 5] as shown in Figure 2. Dark fermions f_{d_2} decay to a dark photon (γ_d) and a lighter dark fermion (f_{d_1}) or the Hidden Lightest Stable Particle (HLSP) (Figure 2, left). In another process, a dark fermion f_{d_2} decays to a lighter dark fermion f_{d_1} (referred to as HLSP) and a dark scalar s_{d_1} . The s_{d_1} decays to a pair of dark photons (Figure 2, right). The same set of generators (MADGRAPH + BRIDGE + PYTHIA 8 chain) that are used to generate the SUSY samples are used to generate the Higgs-portal samples. Also the same PDF set and underlying event tune is used.

The Higgs boson ($m_H = 125 \text{ GeV}$) is generated through the gluon-fusion production mechanism with an estimated production cross section of $\sigma_{\text{SM}} = 19.2 \text{ pb}$ for pp collisions at $\sqrt{s} = 8 \text{ TeV}$ [51]. The mass of f_{d_2} is chosen to be 5 GeV, f_{d_1} and s_{d_1} masses are chosen to be 2 GeV, and the dark photon (γ_d) mass is chosen to be 0.4 GeV. For consistency, the choice of Higgs boson mass and the dark-sector particles’ masses in the cascade decay is the same as used in the ATLAS displaced lepton-jets analysis [18].

4 Pre-selection of events

Events are required to have a primary collision vertex containing at least three tracks with transverse momentum $p_T > 400 \text{ MeV}$. All events must satisfy the trigger, and offline reconstructed objects (electrons or muons) are required to match the leptons firing the trigger.

Unprescaled triggers with the lowest available trigger threshold are used, and a logical OR of triggers is taken to maximize the signal acceptance. For the electron channels, a single-electron trigger with a transverse energy threshold of 60 GeV as well as a trigger requiring two electromagnetic showers with

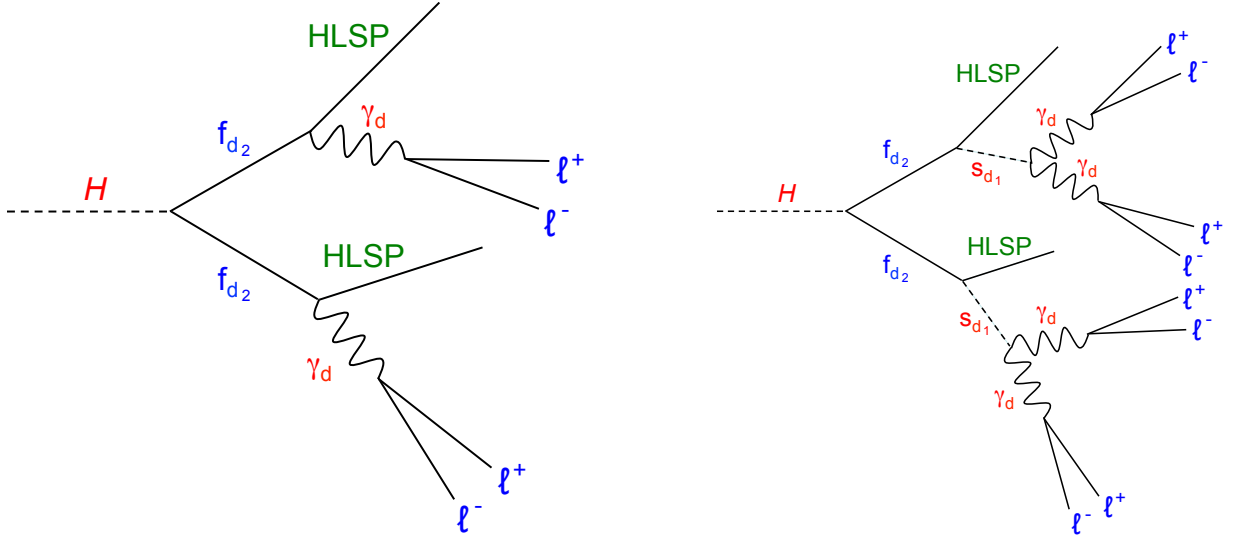


Figure 2: The Higgs boson decays to a pair of dark fermions f_{d_2} , each of which decays to a Hidden Lightest Stable Particle (HLSP) and a dark photon (left) or to a HLSP and a dark scalar s_{d_1} (right) that in turn decays to a pair of dark photons γ_d .

minimum transverse energies of $E_T > 35$ GeV and $E_T > 25$ GeV are used. For the muon channels, a dimuon trigger with a p_T threshold of 13 GeV as well as a single-muon trigger with a p_T threshold of 36 GeV are used. For the mixed channels where both electrons and muons are present, the single-electron, the single-muon and the dimuon triggers are used.

Electron candidates to be used to build lepton-jets are reconstructed from clusters of deposited energy with $E_T > 10$ GeV inside the EM calorimeter fiducial region, $|\eta| < 2.47$, excluding the barrel/end-cap transition region $1.37 < |\eta| < 1.52$ where there is substantial inactive material that is difficult to model accurately. Each cluster must have at least one inner detector track associated. The reconstructed electron is required to match an electron trigger object above the E_T trigger threshold in the trigger system within $\Delta R \equiv \sqrt{(\Delta\phi)^2 + (\Delta\eta)^2} < 0.2$. The transverse shower profiles of these reconstructed electrons differ with respect to an isolated electron from a W or Z boson because the electrons overlap.

Muon candidates to be used to build lepton-jets must be reconstructed in both the ID and the MS and have $|\eta| < 2.5$. Additional requirements are placed on the number of associated hits in the silicon pixel and microstrip detectors, as well as on the number of track segments in the MS. A requirement $|d_0| < 1$ mm with respect to the primary vertex is imposed on muons. Muon candidates are required to match to the muon trigger objects within $\Delta R < 0.2$.

4.1 Track selection

The track selection criteria are crucial for reconstruction of close pairs of tracks and for assessment of fake rates (e.g. when a single track is misreconstructed as two tracks). The criteria are as follows:

- $p_T > 5$ GeV, $|\eta| < 2.5$.

- Transverse impact parameter $|d_0| < 1$ mm.
- Number of B-layer hits ≥ 1 .
- Number of Pixel-layer hits ≥ 2 (includes the B-layer hit requirement).
- Number of Pixel + SCT-layer hits ≥ 7 .
- Longitudinal impact parameter $|z_0 \sin \theta| < 1.5$ mm.

All tracks are required to come from the same primary vertex.

5 Selection of lepton-jets

Signal MC events together with background MC events and background-dominated data from a jet-triggered sample are used to develop optimized criteria that are applied to pre-selected events to preferentially retain LJ events while rejecting backgrounds (Section 5.4). A data-driven method is used to determine the background content in the final sample of LJ candidate events (Section 6).

5.1 Lepton-jet definition

Lepton-jets are bundles of tightly collimated, high- p_T leptons. In the current study, only prompt γ_d leptonic decays (e^+e^- or $\mu^+\mu^-$) are selected. Hadronic γ_d decays cannot be distinguished from multijet background.³ Non-prompt-decays suffer lower multijet backgrounds and are treated elsewhere [18].

Two prompt-decay scenarios are considered. In the first, a single γ_d decays into e^+e^- , $\mu^+\mu^-$ or $\pi^+\pi^-$, with BRs determined by the mass of the γ_d and of the virtual SM photon with which the γ_d kinetically mixes. A γ_d mass range from 0.1–2 GeV is considered. In the second scenario, a dark scalar s_d decays to a pair of dark photons ($\gamma_d\gamma_d$) and each dark photon decays as described above. A MC generator tool, called the LJ gun [18], is used to generate these processes. For simplicity, the LJ gun samples are generated with only three dark-photon decay modes, e^+e^- , $\mu^+\mu^-$ or $\pi^+\pi^-$, and the branching ratios are assigned based on the mass of the dark photons. The BRs of the γ_d are determined with a single γ_d sample. The s_d masses considered range from 1 GeV to 10 GeV. The generated events are processed through the full ATLAS GEANT4-based simulation chain. Additional pp interactions in the same and nearby bunch crossings (pile-up) are included in the simulation. All Monte Carlo samples are re-weighted to reproduce the observed distribution of the number of interactions per bunch crossing in the data.

The separation between the leptons depends on the mass and the boost of their parent γ_d . Figure 3 shows the dependence of the average separation between muons, ΔR , on the γ_d or s_d transverse momentum for various mass values. In the left figure, the average ΔR is evaluated from the distribution for a given p_T slice of γ_d decaying into two truth⁴ muons. In the right figure, the average ΔR is evaluated from the distribution of six possible combinations of muon pairs from four muons for a given p_T bin of s_d decaying

³ The simulation does include the hadronic decays. However, no requirements are applied to select the hadronic decay products, as such selection would be masked by the multijet background.

⁴ The term "truth" is used to indicate objects derived directly from the Monte Carlo generator output, without considering the detector simulation.

into γ_d , where each γ_d decays into a muon pair. The average ΔR decreases with increasing p_T of the dark particle.

Lepton-jet candidates are formed from ID tracks, energy clusters in the EM calorimeter and muons. In order to minimize the background from processes producing low- p_T tracks, ID tracks are required to have a minimum p_T of 5 GeV.

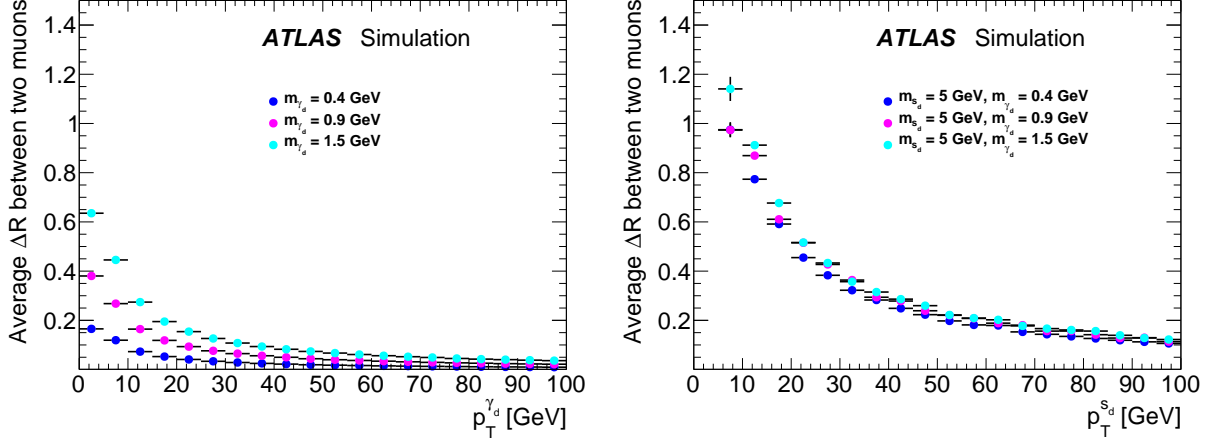


Figure 3: The average separation between two truth muons in the LJ gun samples for various masses of the γ_d (left) as a function of the p_T of γ_d , and (right) with respect to the p_T of a dark scalar particle s_d with a mass of 5 GeV.

5.2 Lepton-jet reconstruction

The reconstruction of lepton-jets starts by arranging the ID tracks from the primary vertex in order of decreasing p_T . The minimum p_T of all tracks in the list is 5 GeV. Starting from the first track in the list, the next track in the list within $\Delta R = 0.5$ of the seed track is found. The four-momenta of the two tracks are summed to give the four-momentum of the lepton-jet candidate. Subsequent tracks within $\Delta R = 0.5$ of the lepton-jet candidate are added iteratively, recomputing the momentum sum at each step. This procedure is repeated until the track list is exhausted. Tracks that are added to a lepton-jet candidate are removed from consideration for subsequent LJ candidates. Additional lepton-jets are built from the remaining tracks in the list following the same procedure. Each lepton-jet candidate contains at least two tracks.

The lepton-jet candidates are categorized as follows:

- **Electron-jet (eLJ):** If at least one reconstructed electron with $E_T > 10$ GeV is found within $\Delta R = 0.5$ of the lepton-jet but no muons, the lepton-jet candidate is called an electron-jet (eLJ). Due to the spatial resolution of the EM calorimeter, the two electrons from an $O(1 \text{ GeV})$ γ_d usually merge to form a single cluster. The two leading tracks must have $p_T > 10$ GeV, and all other tracks have $p_T > 5$ GeV.

- **Muon-jet (muLJ):** If at least two muons with $p_T > 10$ GeV are found within $\Delta R = 0.5$ of the lepton-jet but no electrons, the lepton-jet candidate is called a muon-jet (muLJ). The two muon tracks must have $p_T > 10$ GeV, and all other tracks have $p_T > 5$ GeV.
- **Mixed-jet (emuLJ):** If at least one reconstructed electron with $E_T > 10$ GeV and at least one muon with $p_T > 10$ GeV is found within $\Delta R = 0.5$ of the lepton-jet cone, the lepton-jet candidate is called a mixed-jet (emuLJ). Mixed-jets are reconstructed from the s_d producing two γ_d pairs where one γ_d decays to e^+e^- and the other to $\mu^+\mu^-$. The leading track must have $p_T > 10$ GeV, and the sub-leading track and all other tracks have $p_T > 5$ GeV.

Six categories of events are defined: those with two electron-jets (eLJ–eLJ), those with two muon-jets (muLJ–muLJ), and those with a mixed combination of jets (eLJ–muLJ, eLJ–emuLJ, muLJ–emuLJ, emuLJ–emuLJ).

5.3 Lepton-jet reconstruction efficiency

The characteristics of the reconstructed lepton-jets are studied using the LJ gun samples. The efficiency for lepton-jet reconstruction is p_T - and η - dependent. All efficiencies shown in this section are with respect to single lepton-jet events. The eLJ reconstruction efficiency (Figure 4) is defined as the fraction of events having at least one truth γ_d decaying to e^+e^- which contain a reconstructed eLJ matched to the direction of the γ_d (s_d) for single (double) γ_d samples. The matching criterion is that at least one of the LJ's clusters in the EM calorimeter lies within $\Delta R = 0.1$ of the truth γ_d (s_d) momentum direction.

The muLJ reconstruction efficiency (Figure 5) is defined as the fraction of events having at least one truth γ_d decaying to $\mu^+\mu^-$ which contain a reconstructed muLJ matched to the direction of γ_d (s_d) for single (double) γ_d samples. The matching criterion is that at least one of the LJ's muons lies within $\Delta R = 0.1$ of the truth γ_d (s_d) momentum.

For both single and double γ_d production, electron-jets have a higher reconstruction efficiency for higher p_T dark photons. The rise in efficiency with the dark photon p_T is due to the requiring at least two tracks with $p_T \geq 10$ GeV and at least one cluster with $E_T \geq 10$ GeV. Longitudinally polarized (LP) dark photons [18] have a higher probability for the decay products to have unbalanced momenta than the transversely polarized (TP) ones. For eLJ, LP dark photons are more likely than TP ones to satisfy the $p_T > 10$ GeV requirement as shown in Figure 4. The slight decrease in muLJ efficiency at high p_T in Figure 5 is due to the smaller ΔR of γ_d decays along the γ_d momentum direction. For higher p_T γ_d , the LP muLJ decay products are more often reconstructed as a single muon in the MS. As shown in Figure 5 (right), for the double γ_d case, the muLJ reconstruction efficiency improves with the dark-photon p_T , as only one of the γ_d needs to be reconstructed.

5.4 Background rejection at the lepton-jet level

The reconstructed sample of lepton-jets includes SM backgrounds, mostly hadronic jets that are misidentified as lepton-jets. The variables that discriminate between signal and background processes are based on the characteristics of the reconstructed lepton-jets. Electron LJs from dark particles are expected to

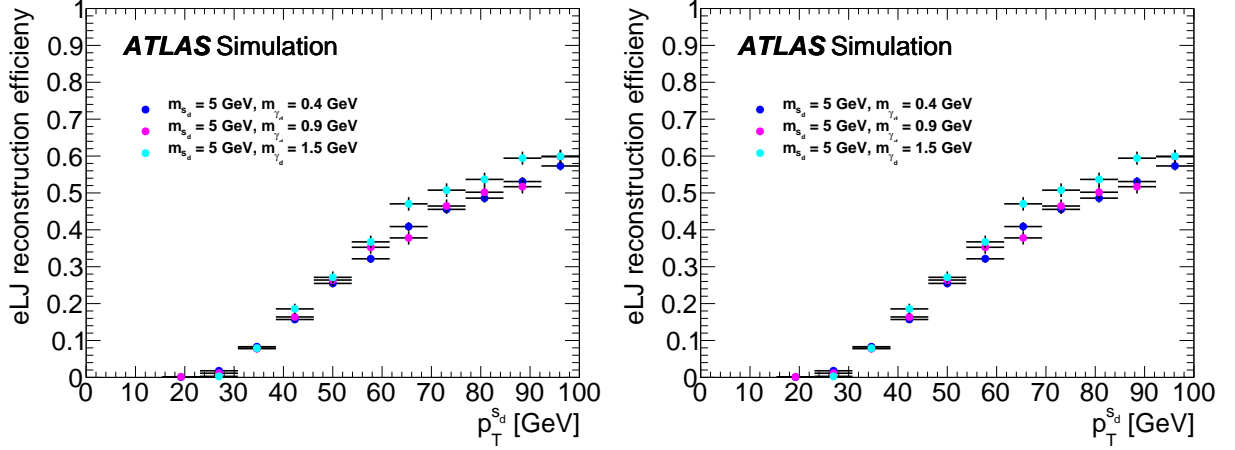


Figure 4: Efficiency of eLJ reconstruction as a function of p_T of longitudinally (LP) or transversely (TP) polarized γ_d for the process $\gamma_d \rightarrow e^+e^-$ (left) and for the process $s_d \rightarrow \gamma_d\gamma_d$, where at least one γ_d decays to e^+e^- (right).

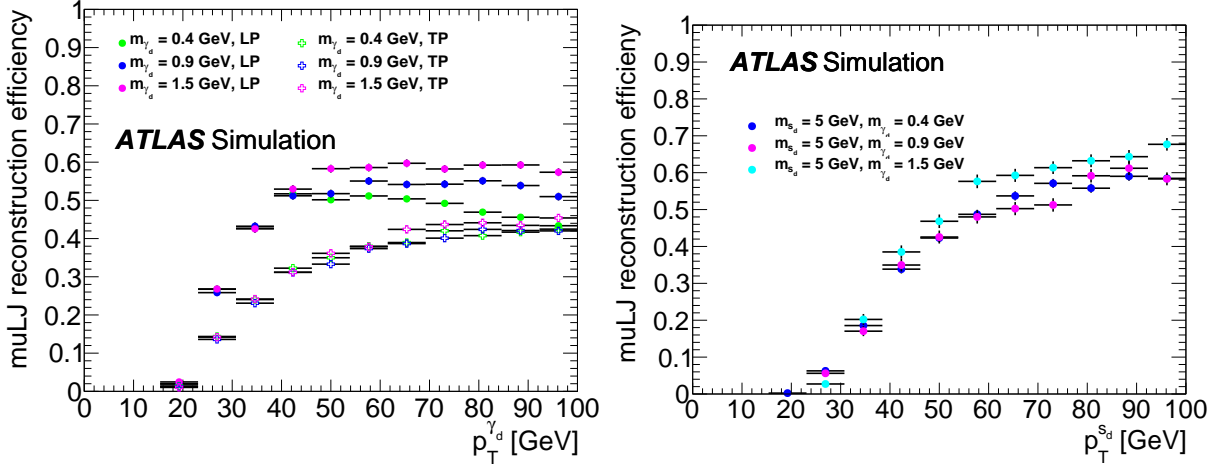


Figure 5: Efficiency of muLJ reconstruction as a function of p_T of longitudinally (LP) or transversely (TP) polarized γ_d for the process $\gamma_d \rightarrow \mu^+\mu^-$ (left) and for the process $s_d \rightarrow \gamma_d\gamma_d$, where at least one γ_d decays to $\mu^+\mu^-$ (right).

have a different isolation (defined below) around the electron tracks in the ID. They are also expected to have different shower shapes in the EM calorimeter when compared to hadronic jets from SM processes, due to the presence of multiple collimated electrons. The muons in the muLJs are more isolated in the ID and the calorimeter than the muLJ backgrounds from multijet processes. In Sections 5.4.1 to 5.4.3, all the variables considered for eLJ, muLJ and emuLJ are listed. Section 5.4.4 explains how the cut values are optimized. The shape of the distribution of each variable is qualitatively compared between data and simulation in a Z+jets sample. A few of these variables are shown in Figures 6 and 7. The Z+jets events are selected by requiring two opposite sign leptons, where the invariant mass of two leptons is within 10 GeV of the Z boson mass window.

5.4.1 eLJ variables

- **Track isolation:** Track isolation (Figure 6, left) is defined as the ratio of the scalar sum of the p_T of the ID tracks within $\Delta R = 0.5$ around the eLJ direction, excluding the EM cluster-matched tracks, to the eLJ p_T . Each ID track used for the isolation calculation must have $p_T \geq 1$ GeV and $|\eta| \leq 2.5$. To reduce pile-up dependence, each ID track must pass transverse and longitudinal impact parameter requirements, $|d_0| < 1$ mm and $|z_0 \sin \theta| < 1.5$ mm, respectively. The tracks matched to a cluster in the EM calorimeter are defined to be the ID tracks with $p_T \geq 5$ GeV that either lie within $\Delta R = 0.05$ from the cluster or are among the two tracks closest to the cluster.

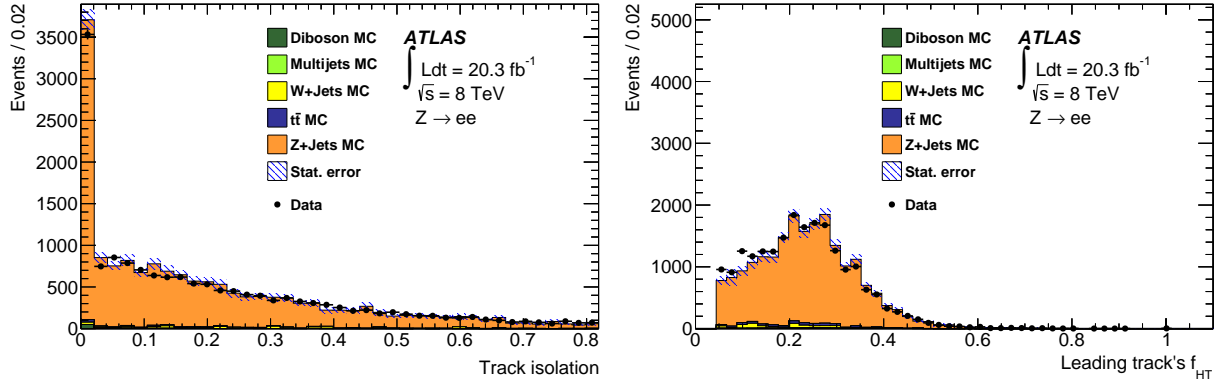


Figure 6: Distributions of track isolation and the fraction of high-threshold TRT hits f_{HT} of the leading track in a $Z \rightarrow e^+e^-$ sample.

- **Fraction of high-threshold TRT hits, f_{HT} (Figure 6, right):** Electrons deposit more energy in the TRT than pions due to transition radiation. The ratio of the number of high-threshold TRT hits (6 keV) on the track to the total number of TRT hits is a robust discriminating variable to identify electrons in an eLJ.
- **Energy of the strip with maximal energy deposit, E_{s1}^{max} (Figure 7, left):** The first sampling layer of the EM calorimeter has a finer granularity in η compared to the second sampling layer. This granularity is used to distinguish between electron and π^0 showers. An electron tends to deposit its energy in a single strip, while the $\pi^0 \rightarrow \gamma\gamma$ decays tend to share energy between two strips, providing a discriminant for π^0 rejection.
- **Fraction of energy deposited in the third sampling layer of the EM calorimeter, f_{s3} :** Electrons deposit most of their energy into the second sampling layer of the EM calorimeter, leaving only a small amount of energy in the third sampling layer. Hadrons deposit most of their energy in the hadronic section of the calorimeters and a small deposition in the second sampling layer of the electromagnetic calorimeter. Furthermore, hadrons deposit a relatively larger amount of energy in the third sampling layer compared to electrons. The fraction of energy found in the third sampling layer of the electromagnetic calorimeter is used to discriminate between electrons and hadrons.
- **Electromagnetic energy fraction, f_{EM} (Figure 7, right):** This is the fraction of the cluster's total transverse energy found in the EM calorimeter. An eLJ is expected to have a larger EM fraction than hadronic jets from SM processes. f_{EM} can be negative because the calibrated energy deposition in the hadronic calorimeter can be negative due to noise subtraction.

5.4.2 muLJ variables

- **Track isolation:** The ratio of the scalar sum of the p_T of the ID tracks, excluding the muon tracks, within $\Delta R = 0.5$ around the muLJ direction, to the p_T of the muLJ. Each ID track used for the isolation calculation must have $p_T \geq 1$ GeV and $|\eta| \leq 2.5$. To reduce pile-up dependence, each ID track must pass transverse and longitudinal impact parameter requirements, $|d_0| < 1$ mm and $|z_0 \sin \theta| < 1.5$ mm, respectively. The muon tracks are defined as the ID tracks with a tighter p_T requirement, $p_T \geq 5$ GeV, which are matched to the fitted muon tracks within $\Delta R = 0.05$.
- **Calorimeter isolation:** The ratio of the total transverse energy in the calorimeter within $\Delta R = 0.2$ from the leading muon of a muLJ to the p_T of that muon.

5.4.3 emuLJ variables

- **Track isolation:** The ratio of the scalar sum of the p_T of the ID tracks (excluding the electron tracks and muon tracks within $\Delta R = 0.5$ around the emuLJ direction) to the emuLJ p_T .
- **Energy of the strip with maximal energy deposit, E_{s1}^{\max} :** As described in Section 5.4.1.
- **Fraction of energy deposited in third sampling layer of EM calorimeter, f_{s3} :** As described in Section 5.4.1.
- **Hadronic leakage, E_T^{had} :** The transverse energy of the electron deposited in the first sampling layer of the hadronic calorimeter. The emuLJ is expected to have a small hadronic contribution due to the presence of a muon within the cone. The E_T^{had} is more sensitive than the f_{EM} variable for the emuLJ case.

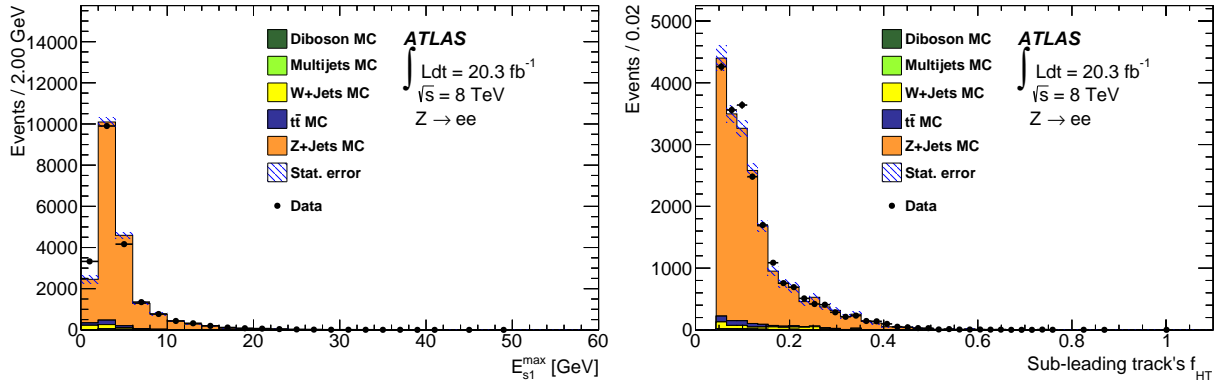


Figure 7: Distributions of the energy of the strip with maximal energy deposit E_{s1}^{\max} and the electromagnetic energy fraction f_{EM} in a $Z \rightarrow e^+e^-$ sample.

5.4.4 LJ variables optimization

Cuts on the variables described in Sections 5.4.1 to 5.4.3 are used to suppress SM backgrounds. A multi-dimensional space of cuts is explored. The optimal cut values are selected by maximizing the significance

expression [52],

$$\text{Significance} = \frac{n_S}{1 + \sqrt{n_B}}, \quad (2)$$

where n_S denotes the expected number of signal events, $n_S = \epsilon_s \times \sigma \times \mathcal{L}$, and n_B is the number of background events passing the selection cuts. The variable ϵ_s represents the signal efficiency formed by the product of the LJ reconstruction efficiency (Section 5.3), the efficiency of requirements on the discriminating variables and the LJ trigger efficiency. The optimized cuts for all LJ variables are given in Table 2. The optimization is performed for the efficiency of two-LJ events, which is obtained from the product of single LJ efficiencies. The cut efficiency variation as a function of the dark-photon mass is studied for the eLJ–eLJ, muLJ–muLJ and eLJ–muLJ channels in case of $2\gamma_d$ production. The variation is found to be small. For $2s_d$ production the cut efficiency variation with the dark-photon mass can be large when one of the γ_d originating from s_d decays into hadrons and the other into a lepton-pair. The size of the variation in this case depends on the branching ratio for γ_d decay to hadrons. Table 3 summarizes the signal acceptance \times efficiencies for the $m_{\gamma_d} = 0.4$ GeV benchmark, where efficiencies for events passing all the cuts are shown. These efficiencies take into account the trigger selection, primary vertex selection, lepton-jet reconstruction, and efficiencies of discriminating variable cuts, and do not include the BRs for γ_d decays into e^+e^- or $\mu^+\mu^-$ pairs in each channel. The difference between efficiencies for the Higgs-portal and SUSY-portal models are driven by the boost of the dark photon which depends on the mass of the parent particles, the squark or Higgs boson.

Table 2: Finalized set of cut values on the discriminating variables of eLJ, muLJ and emuLJ.

eLJ	muLJ	emuLJ
$E_{s1}^{\max} > 0.5 \text{ GeV}$ track isolation < 0.04 $f_{\text{HT}} > 0.14$ $f_{\text{EM}} > 0.99$ $f_{s3} < 0.015$	track isolation < 0.25 calorimeter isolation < 0.15	$E_{s1}^{\max} > 3 \text{ GeV}$ track isolation < 0.1 $E_T^{\text{had}} < 1 \text{ GeV}$ $f_{s3} < 0.015$

Table 3: Acceptance \times efficiency corresponding to $m_{\gamma_d} = 0.4$ GeV for all six channels in the SUSY-portal and Higgs-portal topologies.

State	eLJ–eLJ	muLJ–muLJ	eLJ–muLJ	eLJ–emuLJ	muLJ–emuLJ	emuLJ–emuLJ
SUSY-portal						
$2 \gamma_d + X$	$4.4 \pm 0.2 \%$	$6.4 \pm 0.3 \%$	$3.4 \pm 0.2 \%$	-	-	-
$2 (s_d \rightarrow \gamma_d \gamma_d) + X$	$6.3 \pm 0.4 \%$	$25.1 \pm 0.7 \%$	$7.2 \pm 0.3 \%$	$4.0 \pm 0.2 \%$	$8.1 \pm 0.3 \%$	$7.1 \pm 0.3 \%$
Higgs-portal						
$2 \gamma_d + X$	$0.23 \pm 0.02 \%$	$1.31 \pm 0.04 \%$	$0.20 \pm 0.01 \%$	-	-	-
$2 (s_d \rightarrow \gamma_d \gamma_d) + X$	$0.03 \pm 0.02 \%$	$0.50 \pm 0.07 \%$	$0.08 \pm 0.01 \%$	$0.05 \pm 0.01 \%$	$0.22 \pm 0.03 \%$	$0.08 \pm 0.02 \%$

6 Background estimation at the event level

All background contributions are estimated using the data-driven ABCD-likelihood method (Section 6.2), except for diboson top-quark pair ($t\bar{t}$), which are determined from MC simulations. The diboson estimation includes γ^* production with any mass. The MC simulations for other SM processes are used only to

investigate the shapes of the distributions of the LJ variables, and not for the background evaluation.

Various SM processes can mimic a LJ signal due to hadrons being misidentified as leptons. The following MC samples are considered: hadronic multijet events, γ + jets events, $W(\rightarrow \ell\nu)$ + jets, $Z(\rightarrow \ell^+\ell^-)$ + jets, $t\bar{t}$ and diboson (WW , WZ , ZZ , $\gamma\gamma$) events. PYTHIA 8 is used to generate these samples except for $t\bar{t}$, WW , WZ , ZZ for which MC@NLO [53] is used. The contribution from WZ and ZZ backgrounds, when one of the bosons is off-shell, is modelled with SHERPA [54].

Of the backgrounds considered, only the hadronic multijet, γ + jets and $Z(\rightarrow \ell^+\ell^-)$ + multijet events contribute significantly. The contribution from $t\bar{t}$ is negligible. The hadronization of the multijet, photon + jets and W/Z + jets samples is done with PYTHIA 8 using the CT10 NLO [55] PDF set. For the underlying event, the AUET2 set of tuned parameters [48] is used. As with the signal MC samples, the SM MC samples included the effect of multiple pp interactions per bunch crossing and are assigned an event weight such that the distribution of the number of pp interactions matches that in data. All MC events are processed with the GEANT4-based ATLAS detector simulation [38, 39] and then analysed with the standard ATLAS reconstruction software.

6.1 Low-mass Drell–Yan

The contribution from low-mass Drell–Yan events $\gamma^*(\rightarrow \ell^+\ell^-)$ + jets in the ranges $2 < m_{\ell\ell} < 8$ GeV and $10 < m_{\ell\ell} < 60$ GeV is investigated using MC simulation (SHERPA). This contribution is small because tracks from γ^* have a soft p_T spectra, while the analysis requires that the tracks present in a lepton-jet to have $p_T > 10$ GeV. Furthermore, the requirement of two lepton-jets per event makes this background small. The remaining background is taken into account in the ABCD data-driven estimation (Section 6.2), as the ABCD plane is defined based on the sub-leading lepton-jet, which for γ^* + jets is predominantly a hadronic jet. The $\gamma^* + \gamma^*$ background is evaluated from SHERPA MC simulations, and is subtracted from the event counts in the A , B , C and D regions while doing the fit for the hadronic jet background (see next section).

6.2 Background estimation with the ABCD-likelihood method

An ABCD-likelihood method is used to determine the lepton-jet backgrounds from SM processes. The method uses two nearly uncorrelated variables which have good discriminating power against background. By making a cut in each of the two variables, four non-overlapping regions are defined, of which one is the signal region, labelled region A . Ideally, most signal events are concentrated in region A , while the other regions B , C and D are the control regions dominated by background events. Using the event yields in the four regions, the background in the signal region is determined. Background processes contribute to the signal region selection because jets can be misidentified as lepton-jets. The dominant jet background originates from multijet processes, while $W/Z/\gamma/\gamma^*$ + jets production accounts for less than 1% in the signal region. The two discriminating variables used in the ABCD data-driven background estimation show a small correlation of about 6% in all LJ pairs except emuLJ–emuLJ. The emuLJ–emuLJ channel has fewer events, and the correlation between the variables is between 10% and 38%. All selections (Section 4) are applied, except for the two discriminating variables which are used

for the ABCD-likelihood method.

The ABCD-likelihood method estimates the expected background by fitting a likelihood function to the observed number of events in each of the four regions. The predicted event rates in each region are defined as follows:

- $\mu_A = \mu^U + \mu + \mu_A^K$
- $\mu_B = \mu^U \tau_B + \mu b + \mu_B^K$
- $\mu_C = \mu^U \tau_C + \mu c + \mu_C^K$
- $\mu_D = \mu^U \tau_B \tau_C + \mu d + \mu_D^K$

Here, μ is the signal yield, μ^U is the background yield from multijet and $W/Z/\gamma/\gamma^* + \text{jets}$ production in association with hadronic jets, while b , c , and d describe the signal contamination (fraction of signal events in the control regions B , C and D , divide by the fraction in the signal region). The variables τ_B and τ_C are the nuisance parameters that describe the ratio of the background expectation in the control region to the background expectation in the signal region. Lastly $\mu_A^K, \mu_B^K, \mu_C^K$ and μ_D^K represent the sum of the diboson and $t\bar{t}$ backgrounds, which are estimated from simulation since they are very small. These are taken as fixed parameters while doing the likelihood fit. The signal and background yields, as well as the values of the nuisance parameters, are obtained from the maximum-likelihood fit to the observed number of events (n_A, n_B, n_C , and n_D) in the four regions. The overall likelihood function is the product of the four likelihood functions in the four regions:

$$L(n_A, n_B, n_C, n_D | \mu, \mu^U, \tau_B, \tau_C) = \prod_{i=A,B,C,D} \frac{e^{-\mu_i} \mu_i^{n_i}}{n_i!}. \quad (3)$$

In the case of the eLJ–eLJ channel the least correlated variables, f_{EM} and f_{HT} , associated with the sub-leading eLJ are used for the ABCD plane after all other requirements are already applied. The two-dimensional distribution of these variables associated with the sub-leading eLJ is dominated by the multijet background in all four regions. Region A is defined for events where the eLJ passes the f_{EM} cut and its two leading tracks also pass the f_{HT} cut; region B for events where one or both leading tracks of that eLJ fail the f_{HT} cut, but the eLJ passes the f_{EM} requirement; region C for events where both leading tracks pass the f_{HT} cut, but the eLJ fails the f_{EM} cut; region D for events where that eLJ fails the f_{EM} and one or both leading tracks fail the f_{HT} cut. Similarly the B, C and D regions are shown in Figure 8 for other LJ pairs. Table 4 summarizes the variables used for the ABCD-method for each channel.

Table 4: List of nearly uncorrelated variables used in the ABCD-method for each channel.

Channel	Variable 1	Variable 2
eLJ–eLJ	sub-leading eLJ f_{EM}	sub-leading eLJ f_{HT}
muLJ–muLJ	leading muLJ calorimeter isolation	sub-leading muLJ calorimeter isolation
eLJ–muLJ	eLJ f_{EM}	muLJ calorimeter isolation
eLJ–emuLJ	eLJ f_{EM}	emuLJ E_T^{had}
muLJ–emuLJ	muLJ calorimeter isolation	emuLJ track isolation
emuLJ–emuLJ	emuLJ E_{s1}^{max}	emuLJ track isolation

Figure 8 shows a two-dimensional plot of the ABCD variables from the observed data used for the LJ search. The A , B , C and D regions are determined by the cuts applied, as described in Section 4, to the two variables given in Table 4. For visualization purposes, the 2D histogram shows only the leading track's f_{HT} distribution for the eLJ–eLJ channel.

7 Systematic uncertainties

The following effects are considered as possible sources of systematic uncertainty and are included as inputs to the likelihood.

- **Luminosity**

The overall normalization uncertainty on the integrated luminosity is 2.8% [56].

- **Trigger**

The modelling of the lepton triggers is checked for events containing collimated electrons by comparing the efficiency for matching eLJs to the offline "medium" or "loose" [57] electrons using photo-conversion events in the data and MC samples as a function of ΔR between the two tracks with high threshold TRT hit fractions. The photo-conversion events are selected by a trigger which requires at least two photons with E_{T} thresholds of 25 GeV and 35 GeV. The total systematic uncertainty of the signal efficiency due to the triggers used in the eLJ–eLJ channel is 13.5%. The systematic uncertainty on the efficiency of the dimuon triggers originates from two close muons which may fall in a single RoI and be identified as a single-muon at Level 1. The systematic uncertainty is determined as the difference between the ratio of data to simulation efficiencies and a straight line fit to the ratio vs. ΔR between two leading tracks in a lepton-jet. The systematic uncertainty associated with the single-muon trigger is small (0.6%), as described in Ref. [58]. The systematic uncertainty associated with the multi-muon triggers is evaluated using a data-driven method applied to $J/\psi \rightarrow \mu^+\mu^-$ data and simulated samples. This uncertainty is 5.8% of the signal acceptance.

The systematic uncertainty due to the triggers used in the mixed channel selection is evaluated as the weighted average uncertainty on the signal acceptance from the uncertainties associated with each of the relevant triggers. This uncertainty ranges from 3.3% to 5.4% depending on the γ_d mass for the mixed channels having eLJ–muLJ and muLJ–emuLJ combinations. For other mixed channels (eLJ–emuLJ and emuLJ–emuLJ) the uncertainty ranges from 3.1% to 4.8%. For events where the triggers overlap, the largest of the two uncertainties is used.

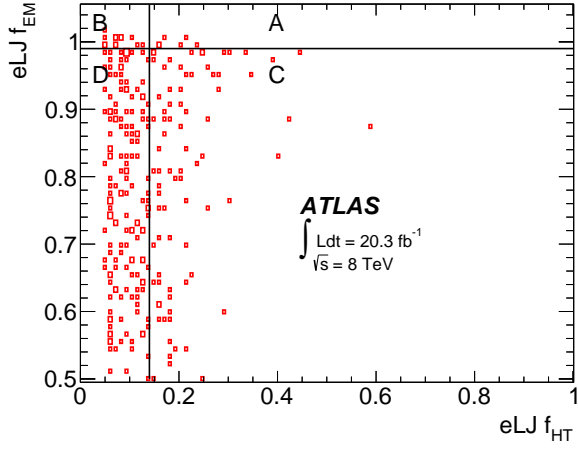
- **Lepton momentum resolution:** The systematic uncertainty for the lepton momentum resolution is evaluated by smearing and shifting the momentum of the leptons by scale factors derived from comparison of $Z \rightarrow \ell^+\ell^-$ in data and simulations, and by observing the effect of this shift on the signal efficiency. For electrons [57] the uncertainty is found to be less than 0.1%, whereas for muons [59] it is found to be in the range 1.9% to 5.2% depending on the dark-photon mass value.
- **Track reconstruction at small ΔR :** This systematic uncertainty is evaluated by studying differences in the track reconstruction efficiency between data and simulated samples. The efficiency is measured using a data-driven method for reconstructed $J/\psi \rightarrow \mu^+\mu^-$ candidates with a small ΔR (approximately between ΔR values of 0.05 and 0.3) between the two muons for data and simulated samples. The uncertainty due to this effect is found to be 8.4%.

- **Muon reconstruction at small ΔR :** The systematic uncertainty for the muon reconstruction in the muon spectrometer for small ΔR is described in Ref. [18]. It is evaluated using a data-driven method using J/ψ events to study the muon reconstruction efficiency estimation as a function of ΔR between two tracks, and the difference in efficiency between data and simulation is taken as a systematic uncertainty. The uncertainty is 5.4%.
- **LJ variables:** In order to assess the size of the systematic uncertainty due to the mismodelling of LJ variables, the shapes of the discriminating variables are compared for Z boson, photon conversions and multijet samples. Systematic uncertainties are assigned for each eLJ variable (f_{HT} , E_{s1}^{max} , f_{s3} , f_{EM} and scaled track isolation) based on the cut efficiency difference of each of those variables between the data and MC samples containing $Z \rightarrow e^+e^-$ events. The validity of this procedure is checked by comparing the shapes of the lepton-jet variable distributions in the signal MC simulation of dark photons with the $Z \rightarrow e^+e^-$ MC simulation for various intervals of cluster E_T and ΔR between two tracks in the lepton-jets. The electron cluster in the $Z \rightarrow e^+e^-$ process is comparable to the cluster of two overlapping electrons from a dark photon in the longitudinal shower profiles, track isolation, and f_{HT} variables. Since the emuLJ selection is based on variables very similar to those for the clusters in the EM calorimeter, the same sample of $Z \rightarrow e^+e^-$ events comprising reconstructed eLJs is used to evaluate the systematic uncertainties on emuLJ, and cross-check the emuLJ variables' (E_{s1}^{max} , f_{s3} , E_T^{had} and track isolation) distribution shapes in the multijet events from the data and MC simulation to see the impact of the presence of a muon in the LJ. The systematic uncertainties on the variables associated with the muLJ are obtained following a similar procedure to that for eLJ but instead using $J/\psi \rightarrow \mu^+\mu^-$ events, which are used given the lack of events for $Z \rightarrow \mu^+\mu^-$ where the muons should be within $\Delta R = 0.5$. The systematic uncertainties for the six types of LJ pairs are given in Table 5.

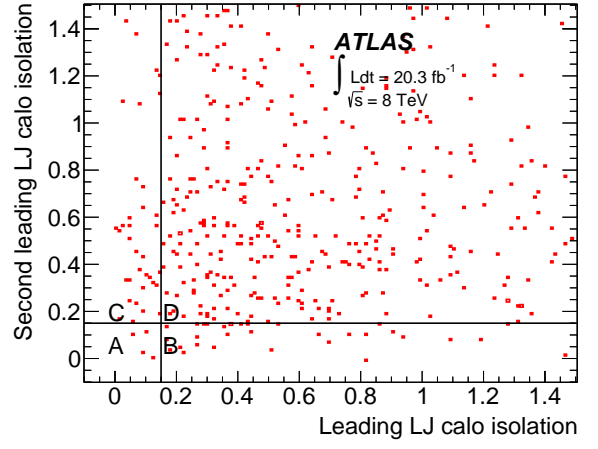
Table 5: The relative systematic uncertainties associated with the signal acceptance due to the modelling of the discriminating variables in the six types of LJ pairs.

Variables	eLJ-eLJ	muLJ-muLJ	eLJ-muLJ	eLJ-emuLJ	muLJ-emuLJ	emuLJ-emuLJ
f_{HT}	0.4 %	-	0.2 %	0.2 %	-	-
Track isolation	9.2 %	17.0 %	13.0 %	9.2 %	13.0 %	9.2 %
E_{s1}^{max}	0.2 %	-	0.1 %	5.5 %	5.4 %	11.1 %
f_{s3}	12.9 %	-	6.0 %	9.7 %	3.3 %	6.8 %
E_T^{had}	-	-	-	0.1 %	0.1 %	0.2 %
f_{EM}	0.9 %	-	0.4 %	0.4 %	-	-
Muon calorimeter isolation	-	6.7 %	3.3 %	-	3.3 %	-

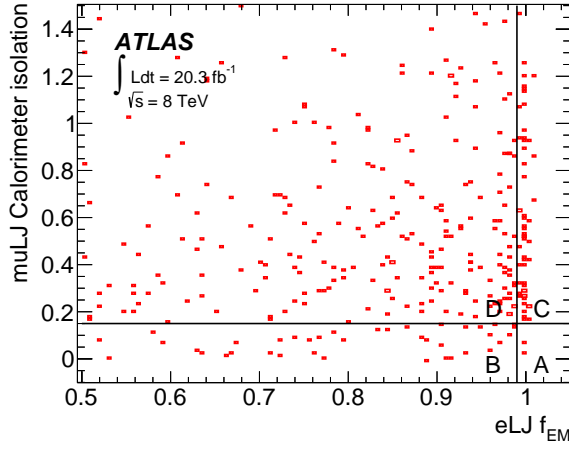
- **Backgrounds:** The two discriminating variables used in the ABCD data-driven background estimation show a small correlation of about 6% in all LJ pairs except emuLJ-emuLJ. The effect of this correlation is incorporated in the background estimation using the ABCD-likelihood method. This is done by introducing a nuisance parameter in the likelihood fit. The correlation is taken into account as a systematic uncertainty on the ABCD-likelihood estimation for the background originating from jets in the multijet and $W/Z/\gamma/\gamma^* + \text{jets}$ processes. An additional 4.5% uncertainty is assigned to the background estimate due to a small pile-up dependence of the track isolation variable (multijet background in region A could suffer from pile-up effects).



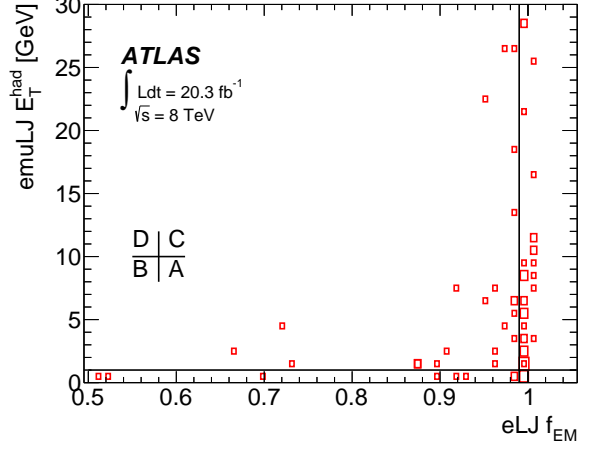
(a)



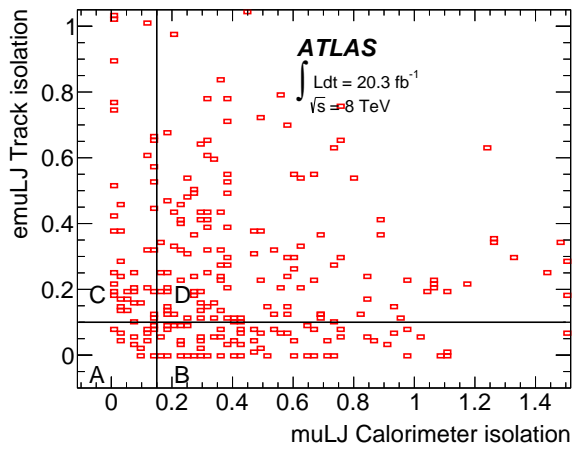
(b)



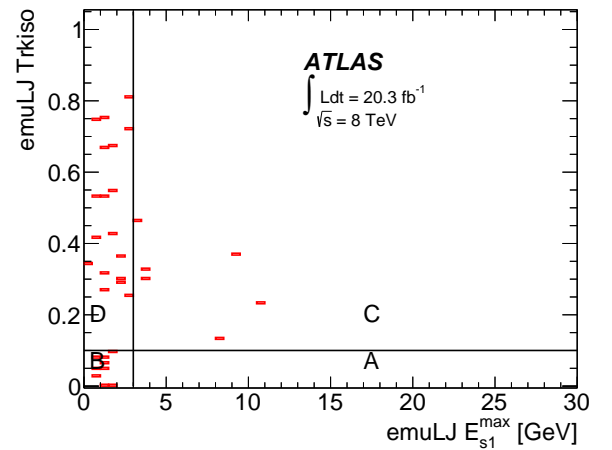
(c)



(d)



(e)



(f)

Figure 8: Scatter plot of the variables used in the ABCD-method for (a) eLJ–eLJ, (b) muLJ–muLJ, (c) eLJ–muLJ, (d) eLJ–emuLJ, (e) muLJ–emuLJ, (f) emuLJ–emuLJ. The horizontal and the vertical black lines indicate the cut values on both variables, as indicated in Table 2.

8 Observed events in data and background estimation

The number of observed events in data for all six channels in signal region A is shown in Table 6. The expected yields for background processes estimated from the data-driven ABCD-likelihood as well as the total background estimated in region A are also shown in this table. The difference between the number of events estimated with the ABCD-likelihood method and the total background comes from diboson and $t\bar{t}$ contributions. The expected number of events in the MC simulation is shown in the Appendix (Tables 7 and 8). The numbers shown for the background are for a dark-photon mass of 300 MeV and two dark-photon production in the SUSY-portal model. The variation of the total background estimate from changing the dark-photon multiplicity, the dark-photon mass or even considering a different model (Higgs-portal) is found to be less than 4%. The data are found to be in good agreement with the background prediction.

Table 6: Number of signal and background events in signal region A . The expected yields for background processes estimated from the data-driven ABCD-likelihood as well as the total background estimation taking into account diboson and $t\bar{t}$ contributions are also shown.

Channel	Background (ABCD-likelihood method)	Background (total)	Observed events in data
eLJ–eLJ	2.9 ± 0.9	4.4 ± 1.3	6
muLJ–muLJ	2.9 ± 0.6	4.4 ± 1.1	4
eLJ–muLJ	6.7 ± 1.4	7.1 ± 1.4	2
eLJ–emuLJ	7.8 ± 2.0	7.8 ± 2.0	5
muLJ–emuLJ	20.2 ± 4.5	20.3 ± 4.5	14
emuLJ–emuLJ	1.3 ± 0.8	1.9 ± 0.9	0

9 Interpretation and limits

No significant deviation from SM predictions is found, and 95% confidence-level upper limits are placed on the contribution of new phenomena beyond the SM on the number of events with lepton-jets. A likelihood-based approach is employed for hypothesis-testing and limit calculation, using the CL(s) technique [60].

All systematic uncertainties discussed in Section 7 are taken into account. The expectation and uncertainties are calculated using the HistFactory statistical tool [61]. A log-likelihood ratio (LLR) is used as the test statistic, defined as the ratio of the signal-plus-background hypothesis to the background-only hypothesis. Ensembles of pseudo-experiments were generated for the signal-only hypothesis and the signal+background hypothesis, varying the LLR according to the statistical and systematic uncertainties. For a given hypothesis, the combined likelihood is the product of the likelihoods for the channels considered, each resulting from the product of a Poisson distribution representing the statistical fluctuations of the expected total event yield, and of Gaussian distributions representing the effect of the systematic uncertainties. The upper limits were determined by performing a scan of p -values corresponding to LLR values larger than the one observed in data. Limits are placed for squark + squark $\rightarrow 2\gamma_d + X$, squark + squark $\rightarrow 2(s_d \rightarrow \gamma_d \gamma_d) + X$, $H \rightarrow 2\gamma_d + X$ and $H \rightarrow 2(s_d \rightarrow \gamma_d \gamma_d) + X$ processes in the electron, muon and mixed channels.

The 95% confidence-level upper limits on signal are expressed in terms of the cross section times BR for the production of two lepton-jets, which are shown in the Appendix (Tables 9–14) and are based on the following formula:

$$\sigma \times BR = \frac{N_{\text{limit}}}{\mathcal{L} \times \epsilon_s} \quad (4)$$

Here N_{limit} is the upper limit on the signal yield, \mathcal{L} represents the integrated luminosity, and ϵ_s represents the signal efficiency including the trigger efficiency, signal acceptance, the reconstruction efficiency for two LJs and the efficiency of the selection criteria for the discriminating variables on both LJs. The uncertainties on the luminosity and on the efficiencies are taken into account in the likelihood that derives N_{limit} .

The expected and observed limits on the number of signal events are shown in Figure 9 for all six channels. The theoretical predictions for the signal in the $2\gamma_d + X$ and $4\gamma_d + X$ final-states for the SUSY-portal model are also illustrated in this figure. At $m_{\gamma_d} = 0.7$ GeV, the branching fraction of dark photons into lepton pairs is around 15% due to higher decay probabilities into ρ and ϕ mesons, which is the reason why the signal expectation is small for this mass point. Figure 10 shows the 95% CL combined upper limit on the cross section times branching ratio for the $2\gamma_d + X$ topology.

The ratio of the average efficiency at a given $c\tau$ to the efficiency at $c\tau = 0$ mm is used to rescale the expected number of signal events estimated from the reference $H \rightarrow 2\gamma_d + X$ sample. Here $c\tau$ is the mean lifetime of the dark photon used in the simulation and the efficiency is the average efficiency for this mean lifetime. This efficiency scaling is shown in Figure 11. A large number of pseudo experiments is generated for $c\tau$ ranging from 0 - 100 mm. The average efficiency ratios are obtained based on the lepton-jet efficiency dependence on the proper decay length. The average efficiency curves are valid for all channels. This is due to the B-layer hit requirements of at least two tracks in the lepton-jets, which makes the lepton-jet reconstruction efficiency vanish for all lepton-jets types with the proper decay length > 52 mm. Therefore there is no further impact due to the lepton-jet reconstruction, their selection cuts and the triggers requirements.

The 95% confidence-level upper limit on the production cross section times BR to two lepton-jets in the $H \rightarrow 2\gamma_d + X$ model is obtained as a function of lifetime $c\tau$ as shown in Figure 12, after taking into account the uncertainty associated with the efficiency scaling for $c\tau$. A 45% uncertainty is assigned on the efficiency scaling based on a comparison of the extrapolated signal expectation at 47 mm $c\tau$ with the direct estimate of the expected signal for the dark-photon simulation sample generated with $c\tau = 47$ mm. The extrapolated signal expectation is obtained by scaling the signal expectation for the dark-photon sample with $c\tau = 0$ mm by the average efficiency ratio at $c\tau = 47$ mm as given by the curve in Figure 12. The decays of the dark photons into leptons are simulated with an exponential decay law. The limit is based on combined results from the eLJ–eLJ, muLJ–muLJ and eLJ–muLJ channels. The emuLJ channels are not used as they do not contribute to the $H \rightarrow 2\gamma_d + X$ topology, given that a single γ_d cannot decay into a pair of leptons of different flavour. The comparison with the theoretical prediction (dashed line) for 10% BR of Higgs boson decay to two dark photons⁵ shows that values of $c\tau$ below 3.2 mm are excluded at 95% confidence-level.

⁵ This is an arbitrary choice, as the BR of the Higgs boson to dark photons is not theoretically known.

The results are also interpreted as a two-dimensional exclusion contour in the plane of the kinetic mixing parameter ϵ and the γ_d mass for the $H \rightarrow 2\gamma_d + X$ topology. As only one mass benchmark ($m_{\gamma_d} = 0.4$ GeV) is generated for the $H \rightarrow 2\gamma_d + X$ topology, the signal efficiencies are derived from the MC sample for the Higgs-portal in the eLJ–eLJ, muLJ–muLJ and eLJ–muLJ channels for that benchmark. For other γ_d mass benchmarks, the extrapolation corrections for all γ_d masses are obtained using the SUSY-portal MC samples. These correction factors are then used to rescale the efficiency at 0.4 GeV in the $H \rightarrow 2\gamma_d + X$ topology to derive efficiencies for other γ_d masses in the [0.1–2.0] GeV interval. As the efficiency dependence is found to be small for the SUSY samples across various dark-photon mass points in the $2\gamma_d + X$ topology, it is assumed for the Higgs-portal model that the efficiencies scale the same way as for the SUSY-portal samples with respect to 0.4 GeV dark-photon sample. Based on the variations in efficiencies across different dark-photon masses with respect to 0.4 GeV dark-photon sample, the following uncertainties are assigned to the efficiencies: 60% on the eLJ–eLJ channel, 200% on the muLJ–muLJ and 30% on the eLJ–muLJ channel.

In order to allow a comparison with the displaced lepton-jets analysis [18], 90% confidence-level exclusion limits are derived for $H \rightarrow 2\gamma_d + X$ production for various (5%, 10%, 20%, 40%) branching fractions by combining the results from the eLJ–eLJ, muLJ–muLJ and eLJ–muLJ channels after taking into account all systematic uncertainties.

Figure 13 shows the 90% confidence-level exclusion contour interpreted in the ϵ and γ_d mass plane in the ϵ region 10^{-2} – 10^{-6} and in the mass region [0.1–2] GeV for 5%, 10%, 20%, 40% branching fractions of the Higgs boson decay to $2\gamma_d + X$. In the low-mass region, below the $\mu^+\mu^-$ threshold, only the results from the eLJ–eLJ channel contribute. The results shown in the figure depend on the coupling of the dark photon to the SM photon ϵ , and on the mass of the dark photon. The figure also shows other excluded regions from a search for non-prompt lepton-jets at ATLAS [18] and from other experiments. Shown are existing 90% confidence-level exclusion regions from beam-dump experiments E137, E141, and E774 [20,21,62], Orsay [63], U70 [19], CHARM [64], LSND [26], A1 [23], the electron and muon anomalous magnetic moment [34,35,65], HADES [25], KLOE [28–32], the test-run results reported by APEX [22], an estimate using BaBar results [9, 32, 33], and constraints from astrophysical observations [36, 37]. While other experiment’s results are independent of the topology of the dark-photon production, the ATLAS results depend on the topology, i.e Higgs boson mass and its production mechanism, and its decay into dark photons. The results from CMS are shown elsewhere [15]. The ϵ values are evaluated using Equation (1) combined with R-ratio measurements of e^+e^- collider data [28–33], where the R-ratio is the ratio of the hadronic cross section to the muon cross section in electron–positron collisions. The expression for ϵ with respect to these variables is

$$\epsilon^2 = \frac{\hbar c}{c\tau(\Gamma_{e^+e^-} + \Gamma_{\mu^+\mu^-} + R\Gamma_{\mu^+\mu^-})}, \quad (5)$$

where \hbar is the reduced Planck constant, R is the R-ratio, while $\Gamma_{e^+e^-}$ and $\Gamma_{\mu^+\mu^-}$ are given by Equation (1).

10 Conclusions

A search for prompt lepton-jets using 20.3 fb^{-1} of pp collision data collected with the ATLAS detector at the LHC at a centre-of-mass energy of 8 TeV is performed. Such lepton-jets are expected from decays of low-mass dark photons in some model extensions to the SM. The analysis requires events with at least two lepton-jets.

No significant excess of events compared to the SM expectation is observed in any of the analysed channels, and 95% confidence-level upper limits are computed on the production cross section times branching ratio for two prompt lepton-jets in SUSY-portal and Higgs-portal models. The results are also interpreted in terms of a 90% confidence-level exclusion region in kinetic mixing and dark-photon mass parameter space, based on combined results from the $H \rightarrow 2\gamma_d + X$ topology. These results provide exclusion in regions of parameter space previously unexplored and extend the results of other searches.

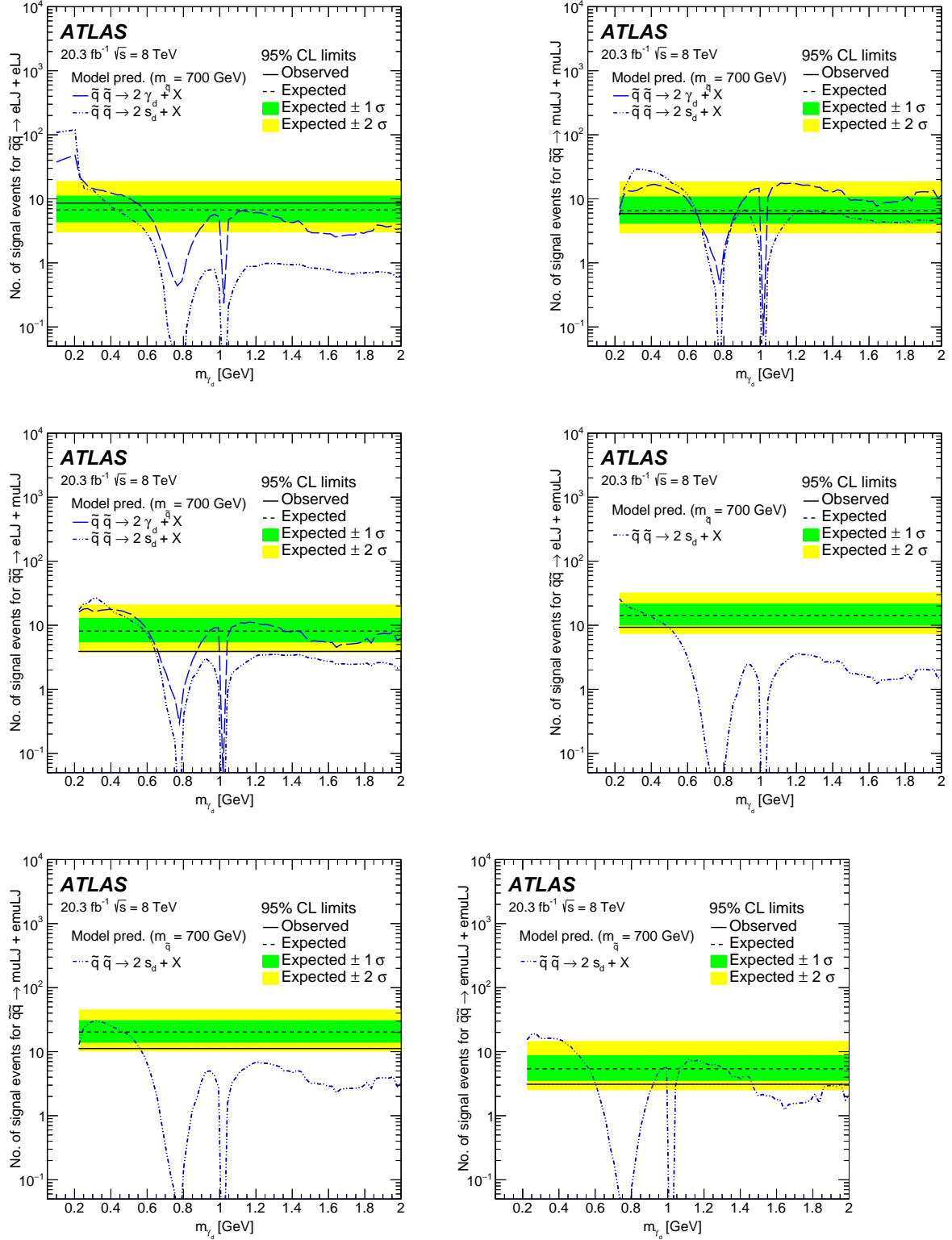


Figure 9: The 95% confidence-level observed and expected upper limits on the number of signal events for final-states consisting of two lepton-jets in the eLJ - eLJ , μLJ - μLJ , eLJ - μLJ , eLJ - emuLJ , μLJ - emuLJ and emuLJ - emuLJ channels. Results based on 20.3 fb $^{-1}$ of integrated luminosity are shown in these figures. The model predictions for the production of $2\gamma_d + X$ and $2(s_d \rightarrow \gamma_d \gamma_d) + X$ via SUSY-portal topologies for various γ_d mass values are also overlaid.

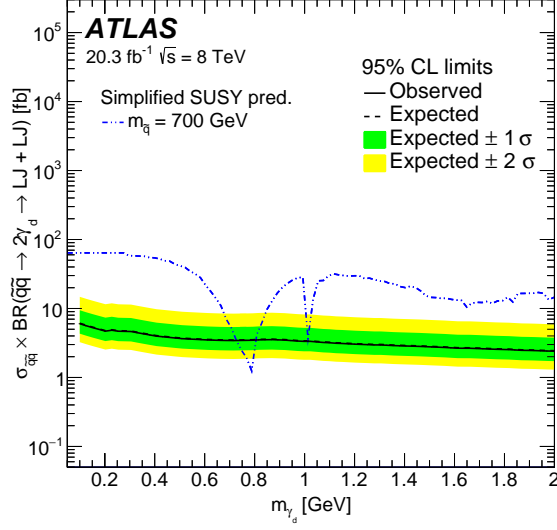


Figure 10: The 95% CL observed and expected upper limits on the cross section times branching ratio into final-states with two lepton-jets in the case of $2\gamma_d + X$ production via the SUSY-portal topology based on the combined results of the **eLJ–eLJ**, **muLJ–muLJ**, **eLJ–muLJ** channels. The limit is plotted as a function of dark-photon mass m_{γ_d} , and changes with mass due to a small dependence of signal efficiency on the γ_d mass.

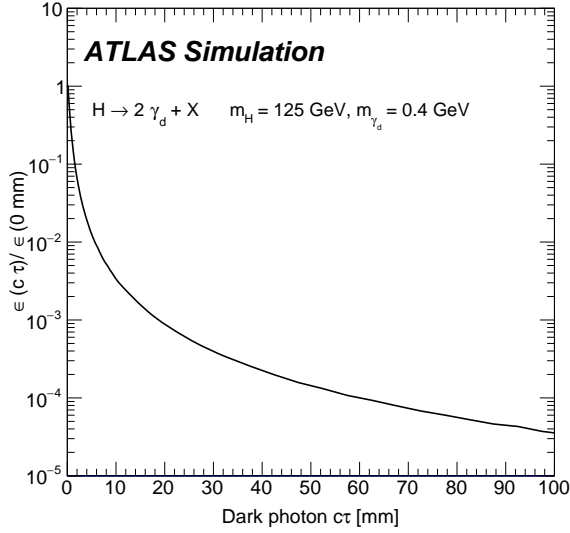


Figure 11: The detection efficiency ratio with respect to the reference model efficiency with zero mean life time is plotted as a function of γ_d mean lifetime $c\tau$. The extrapolated efficiency for other $c\tau$ is estimated from the $H \rightarrow 2\gamma_d + X$ MC sample generated with $c\tau = 47$ mm by studying the efficiency as a function of γ_d decay position. A 45% uncertainty is associated on this efficiency scaling as described in the text.

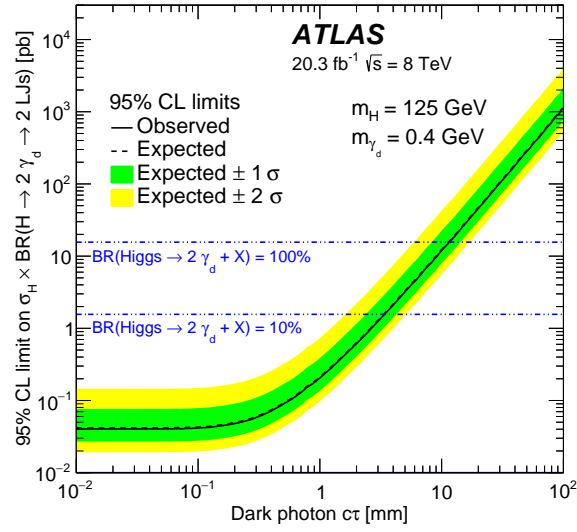


Figure 12: The 95% confidence-level observed and expected upper limits on the cross section times branching fractions into final-states consisting of two lepton-jets in the production of $2\gamma_d + X$ via Higgs-portal topology for $m_{\gamma_d} = 0.4$ GeV based on the combined results of the **eLJ-eLJ**, **muLJ-muLJ**, **eLJ-muLJ** channels. The limit is drawn as a function of lifetime $c\tau$. The results for various lifetimes ranging up to 100 mm are derived by extrapolating the detection efficiency using the curve as described in Figure 11. The comparison with the theoretical prediction (dashed line) for 10% BR of Higgs boson decay to two dark photons shows that values of $c\tau$ below 3.2 mm are excluded at 95% confidence-level.

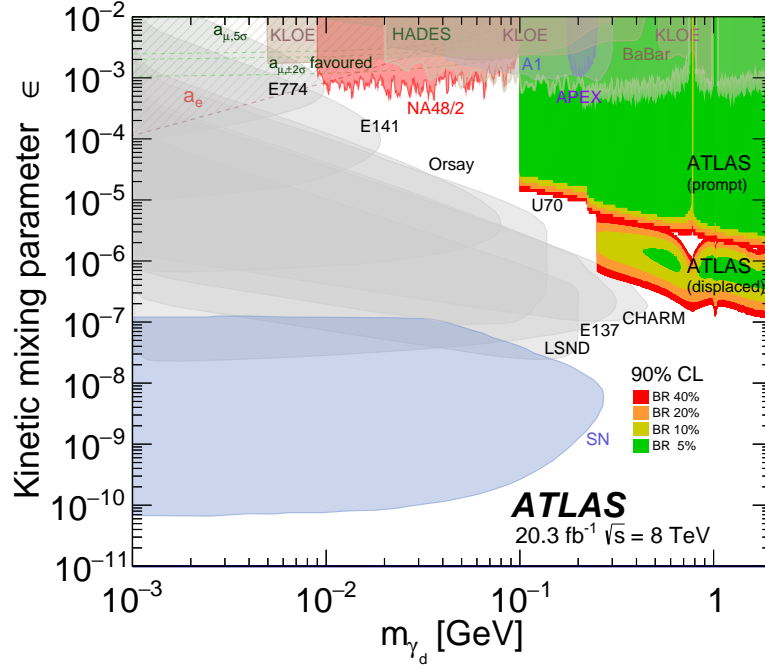


Figure 13: A two-dimensional exclusion plot in the dark-photon mass m_{γ_d} and the kinetic mixing ϵ parameter space, taken from Ref. [66]. The branching ratios are for $H \rightarrow 2\gamma_d + X$ decays. The 90% confidence-level exclusion region for prompt $H \rightarrow 2\gamma_d + X$ production with 5%, 10%, 20% and 40% branching fractions into $2\gamma_d + X$ decay are extracted based on the present combined results from the eLJ–eLJ, muLJ–muLJ and eLJ–muLJ channels using 8 TeV data at ATLAS. The excluded regions are derived based on comparing the total signal expectation for the $H \rightarrow 2\gamma_d + X$ production model with the 90% confidence-level upper limit on the signal expectation. The legend represents the ATLAS exclusions by both the prompt (this paper) and displaced lepton-jet analyses [18].

Acknowledgements

We thank CERN for the very successful operation of the LHC, as well as the support staff from our institutions without whom ATLAS could not be operated efficiently.

We acknowledge the support of ANPCyT, Argentina; YerPhI, Armenia; ARC, Australia; BMWFW and FWF, Austria; ANAS, Azerbaijan; SSTC, Belarus; CNPq and FAPESP, Brazil; NSERC, NRC and CFI, Canada; CERN; CONICYT, Chile; CAS, MOST and NSFC, China; COLCIENCIAS, Colombia; MSMT CR, MPO CR and VSC CR, Czech Republic; DNRF, DNSRC and Lundbeck Foundation, Denmark; IN2P3-CNRS, CEA-DSM/IRFU, France; GNSF, Georgia; BMBF, HGF, and MPG, Germany; GSRT, Greece; RGC, Hong Kong SAR, China; ISF, I-CORE and Benoziyo Center, Israel; INFN, Italy; MEXT and JSPS, Japan; CNRST, Morocco; FOM and NWO, Netherlands; RCN, Norway; MNiSW and NCN, Poland; FCT, Portugal; MNE/IFA, Romania; MES of Russia and NRC KI, Russian Federation; JINR; MESTD, Serbia; MSSR, Slovakia; ARRS and MIZŠ, Slovenia; DST/NRF, South Africa; MINECO, Spain; SRC and Wallenberg Foundation, Sweden; SERI, SNSF and Cantons of Bern and Geneva, Switzerland; MOST, Taiwan; TAEK, Turkey; STFC, United Kingdom; DOE and NSF, United States of America. In addition, individual groups and members have received support from BCKDF, the Canada Council, CANARIE, CRC, Compute Canada, FQRNT, and the Ontario Innovation Trust, Canada; EPLANET, ERC, FP7, Horizon 2020 and Marie Skłodowska-Curie Actions, European Union; Investissements d'Avenir Labex and Idex, ANR, Region Auvergne and Fondation Partager le Savoir, France; DFG and AvH Foundation, Germany; Herakleitos, Thales and Aristeia programmes co-financed by EU-ESF and the Greek NSRF; BSF, GIF and Minerva, Israel; BRF, Norway; the Royal Society and Leverhulme Trust, United Kingdom.

The crucial computing support from all WLCG partners is acknowledged gratefully, in particular from CERN and the ATLAS Tier-1 facilities at TRIUMF (Canada), NDGF (Denmark, Norway, Sweden), CC-IN2P3 (France), KIT/GridKA (Germany), INFN-CNAF (Italy), NL-T1 (Netherlands), PIC (Spain), ASGC (Taiwan), RAL (UK) and BNL (USA) and in the Tier-2 facilities worldwide.

11 Expected number of events in MC and 90% CL upper limits on the expected and observed number of signal events

Table 7: The number of expected signal events for the eLJ–eLJ, muLJ–muLJ and eLJ–muLJ channels in $2\gamma_d$ production. These numbers are obtained purely from simulations.

Sample ($n_{\gamma_d} = 2$)	eLJ–eLJ	muLJ–muLJ	eLJ–muLJ
<u>SUSY MC</u>			
$m_{\gamma_d} = 0.1$ GeV	37.5 ± 1.0	–	–
$m_{\gamma_d} = 0.3$ GeV	15.8 ± 0.6	14.7 ± 0.6	18.4 ± 0.7
$m_{\gamma_d} = 0.5$ GeV	10.0 ± 0.5	14.7 ± 0.7	15.3 ± 0.6
$m_{\gamma_d} = 0.9$ GeV	3.6 ± 0.2	9.3 ± 0.4	5.6 ± 0.3
$m_{\gamma_d} = 1.2$ GeV	6.3 ± 0.3	17.6 ± 0.5	10.2 ± 0.4
$m_{\gamma_d} = 1.5$ GeV	3.1 ± 0.2	9.6 ± 0.4	5.9 ± 0.3
$m_{\gamma_d} = 2.0$ GeV	3.6 ± 0.2	12.5 ± 0.5	6.8 ± 0.3
<u>Higgs MC</u>			
$m_{\gamma_d} = 0.4$ GeV with 10% BR	18.4 ± 1.2	103.7 ± 3.1	32.2 ± 1.7

Table 8: The number of expected signal events for all six LJ channels in $4\gamma_d$ production. These numbers are obtained purely from simulations.

Sample ($n_{\gamma_d} = 4$)	eLJ–eLJ	muLJ–muLJ	eLJ–muLJ	eLJ–emuLJ	muLJ–emuLJ	emuLJ–emuLJ
<u>SUSY MC</u>						
$m_{\gamma_d} = 0.1$ GeV	109.1 ± 1.6	–	–	–	–	–
$m_{\gamma_d} = 0.3$ GeV	12.0 ± 0.5	32.0 ± 0.9	21.5 ± 0.8	18.2 ± 0.7	30.0 ± 0.9	20.2 ± 0.8
$m_{\gamma_d} = 0.5$ GeV	4.5 ± 0.3	23.0 ± 0.8	11.2 ± 0.5	8.7 ± 0.5	17.3 ± 0.7	9.1 ± 0.5
$m_{\gamma_d} = 0.9$ GeV	0.7 ± 0.1	8.4 ± 0.4	3.0 ± 0.2	2.0 ± 0.2	4.1 ± 0.3	2.4 ± 0.2
$m_{\gamma_d} = 1.2$ GeV	2.1 ± 0.2	15.1 ± 0.5	6.8 ± 0.3	4.8 ± 0.3	11.6 ± 0.4	6.6 ± 0.3
$m_{\gamma_d} = 1.5$ GeV	0.8 ± 0.1	6.3 ± 0.3	3.1 ± 0.2	1.8 ± 0.2	3.3 ± 0.2	1.8 ± 0.2
$m_{\gamma_d} = 2.0$ GeV	0.6 ± 0.1	5.3 ± 0.3	2.3 ± 0.2	1.7 ± 0.2	3.4 ± 0.2	1.8 ± 0.2
<u>Higgs MC</u>						
$m_{\gamma_d} = 0.4$ GeV with 10% BR	0.9 ± 0.6	23.5 ± 3.4	4.1 ± 1.4	3.3 ± 1.4	15.8 ± 2.7	4.0 ± 1.4

eLJ-eLJ

Table 9: This table shows the 95% CL upper limit on the number of expected and observed events for various signal benchmarks in the **eLJ-eLJ** channel. The standard deviations (σ) relates to the expected limit.

Signal bench- marks γ_d mass [GeV]	$2\gamma_d + X$						$2(s_d \rightarrow \gamma_d \gamma_d) + X$					
	Obs.	Exp.	-2σ	-1σ	$+1\sigma$	$+2\sigma$	Obs.	Exp.	-2σ	-1σ	$+1\sigma$	$+2\sigma$
SUSY ($m_{\tilde{q}} = 700$ GeV)												
0.1	8.4	6.6	3.0	4.3	10.9	18.1	8.3	6.5	2.9	4.2	10.7	17.9
0.2	8.4	6.6	3.0	4.3	10.9	18.1	8.3	6.5	2.9	4.2	10.7	17.9
0.3	8.4	6.6	3.0	4.3	10.9	18.2	8.4	6.6	3.0	4.3	10.8	18.1
0.4	8.4	6.6	3.0	4.3	10.9	18.3	9.0	7.1	3.2	4.6	11.7	19.5
0.5	8.4	6.6	3.0	4.3	11.0	18.4	9.2	7.2	3.3	4.7	12.0	20.1
0.7	8.5	6.7	3.0	4.3	11.0	18.6	9.3	7.3	3.3	4.7	12.1	20.4
0.9	8.5	6.7	3.0	4.3	11.0	18.7	9.9	7.8	3.6	5.0	13.0	21.9
1.2	8.6	6.7	3.0	4.3	11.2	18.9	9.3	7.3	3.3	4.7	12.1	20.5
1.5	8.6	6.7	3.0	4.3	11.2	18.9	9.1	7.2	3.2	4.7	12.0	20.2
2	8.5	6.7	3.0	4.3	11.1	18.8	9.1	7.2	3.2	4.7	12.0	20.3
Higgs ($m_H = 125$ GeV)												
0.4	8.5	6.7	3.0	4.3	10.9	18.3	8.5	6.7	3.0	4.3	11.0	18.3

muLJ-muLJ

Table 10: This table shows the 95% CL upper limit on the number of expected and observed events for various signal benchmarks in the **muLJ-muLJ** channel. The standard deviations (σ) relates to the expected limit.

Signal bench- marks γ_d mass [GeV]	$2\gamma_d + X$						$2(s_d \rightarrow \gamma_d \gamma_d) + X$					
	Obs.	Exp.	-2σ	-1σ	$+1\sigma$	$+2\sigma$	Obs.	Exp.	-2σ	-1σ	$+1\sigma$	$+2\sigma$
SUSY ($m_{\tilde{q}} = 700$ GeV)												
0.3	5.9	6.5	2.9	4.1	10.9	18.7	6.3	6.9	3	4.4	11.6	19.9
0.4	5.9	6.5	2.9	4.1	10.9	18.7	6.3	6.9	3	4.4	11.6	19.8
0.5	5.9	6.5	2.9	4.1	10.9	18.7	6.4	6.9	3	4.4	11.7	19.9
0.7	6	6.6	2.9	4.1	11	19	7	7.6	3.4	4.9	12.8	21.9
0.9	5.9	6.5	2.9	4.1	10.9	18.7	6.7	7.3	3.3	4.7	12.3	21
1.2	5.9	6.5	2.9	4.1	10.9	18.7	6.8	7.4	3.3	4.7	12.5	21.3
1.5	5.9	6.5	2.9	4.1	10.9	18.7	7.1	7.8	3.5	4.9	13	22.1
2	5.9	6.5	2.9	4.1	10.9	18.7	7.6	8.3	3.8	5.3	13.8	23.3
Higgs ($m_H = 125$ GeV)												
0.4	5.9	6.5	2.9	4.1	11	18.8	6.5	7	3.1	4.5	11.9	20.3

eLJ–muLJ

Table 11: This table shows the 95% CL upper limit on the number of expected and observed events for various signal benchmarks in the **eLJ–muLJ** channel. The standard deviations (σ) relates to the expected limit.

Signal bench- marks γ_d mass [GeV]	$2\gamma_d + X$						$2(s_d \rightarrow \gamma_d \gamma_d) + X$					
	Obs.	Exp.	-2σ	-1σ	$+1\sigma$	$+2\sigma$	Obs.	Exp.	-2σ	-1σ	$+1\sigma$	$+2\sigma$
SUSY ($m_{\tilde{q}} = 700$ GeV)												
0.3	3.9	8	3.8	5.3	12.9	21	4.1	8.6	4	5.7	13.8	22.3
0.4	3.9	8	3.8	5.3	12.9	20.9	4.1	8.6	4	5.7	13.8	22.4
0.5	3.9	8	3.8	5.3	12.9	20.9	4.3	8.8	4.1	5.8	14.1	22.8
0.7	3.9	8.2	3.8	5.4	13.1	21.3	5.3	10.7	5	7.1	16.9	27
0.9	3.9	8.1	3.8	5.4	13	21.1	5	10.2	4.8	6.8	16.1	25.8
1.2	3.9	8.1	3.8	5.4	13	21	4.7	9.7	4.6	6.5	15.4	24.7
1.5	3.9	8.1	3.8	5.4	13	21	5	10.1	4.8	6.8	16.1	25.7
2	3.9	8.1	3.8	5.4	13	21.1	5.6	11.1	5.4	7.4	17.4	27.5
Higgs ($m_H = 125$ GeV)												
0.4	3.9	8.1	3.8	5.4	13	21.1	4.5	9.2	4.4	6.1	14.7	23.8

eLJ–emuLJ

Table 12: This table shows the 95% CL upper limit on the number of expected and observed events for various signal benchmarks in the **eLJ–emuLJ** channel. The standard deviations (σ) relates to the expected limit.

Signal bench- marks γ_d mass [GeV]	$2(s_d \rightarrow \gamma_d \gamma_d) + X$					
	Obs.	Exp.	-2σ	-1σ	$+1\sigma$	$+2\sigma$
SUSY ($m_{\tilde{q}} = 700$ GeV)						
0.3	6.9	11.0	5.6	7.6	17.0	26.4
0.4	7.3	11.7	5.9	8.0	17.8	27.7
0.5	7.6	11.9	6.0	8.2	18.3	28.4
0.7	6.5	4.5	2.3	3.0	7.0	10.7
0.9	9.3	14.3	7.3	9.9	21.8	32.5
1.2	10.1	14.9	7.8	10.4	22.2	32.7
1.5	12.6	17.3	9.9	13.2	23.3	32.3
2	13.7	17.4	10.7	13.5	23.1	32.0
Higgs ($m_H = 125$ GeV)						
0.4	5.9	9.7	4.8	6.6	15.0	23.6

muLJ-emuLJ

Table 13: This table shows the 95% CL upper limit on the number of expected and observed events for various signal benchmarks in the **muLJ-emuLJ** channel. The standard deviations (σ) relates to the expected limit.

Signal bench- marks γ_d mass [GeV]	$2(s_d \rightarrow \gamma_d \gamma_d) + X$					
	Obs.	Exp.	-2σ	-1σ	$+1\sigma$	$+2\sigma$
SUSY ($m_{\tilde{q}} = 700$ GeV)						
0.3	8.8	16.5	7.9	11	26.1	41.6
0.4	8.8	16.5	7.9	11	26.2	42
0.5	9	16.8	8.1	11.3	26.6	42.2
0.7	26.1	42.4	19.8	28	54.6	74.4
0.9	10.5	19.3	9.4	12.9	30.6	46.3
1.2	9.3	17.1	8.4	11.6	26.9	42.3
1.5	11.3	20.5	10.1	13.9	31.9	46.8
2	11.2	20.2	10.1	13.8	31	45.6
Higgs ($m_H = 125$ GeV)						
0.4	11.5	20.8	10.2	14	32.8	47.8

emuLJ-emuLJ

Table 14: This table shows the 95% CL upper limit on the number of expected and observed events for various signal benchmarks in the **emuLJ-emuLJ** channel. The standard deviations (σ) relates to the expected limit.

Signal bench- marks γ_d mass [GeV]	$2(s_d \rightarrow \gamma_d \gamma_d) + X$					
	Obs.	Exp.	-2σ	-1σ	$+1\sigma$	$+2\sigma$
SUSY ($m_{\tilde{q}} = 700$ GeV)						
0.3	2.9	5.1	2.4	3.3	8.4	14.0
0.4	2.9	5.1	2.4	3.3	8.4	14.0
0.5	3.0	5.2	2.4	3.4	8.6	14.2
0.7	3.1	5.4	2.5	3.5	8.8	14.7
0.9	2.9	5.0	2.4	3.3	8.3	13.8
1.2	2.9	5.1	2.4	3.4	8.5	14.1
1.5	2.9	5.0	2.4	3.3	8.4	13.9
2	3.0	5.3	2.5	3.5	8.7	14.4
Higgs ($m_H = 125$ GeV)						
0.4	3.9	6.1	2.9	4.0	9.0	13.3

References

- [1] N. Arkani-Hamed, D. P. Finkbeiner, T. R. Slatyer, and N. Weiner, *A Theory of Dark Matter*, [*Phys. Rev.* **D79** \(2009\) 015014](#), [arXiv:0810.0713 \[hep-ph\]](#).
- [2] M. Baumgart, C. Cheung, J. T. Ruderman, L.-T. Wang, and I. Yavin, *Non-Abelian Dark Sectors and Their Collider Signatures*, [*JHEP* **0904** \(2009\) 014](#), [arXiv:0901.0283 \[hep-ph\]](#).
- [3] C. Cheung, J. T. Ruderman, L.-T. Wang, and I. Yavin, *Lepton Jets in (Supersymmetric) Electroweak Processes*, [*JHEP* **1004** \(2010\) 116](#), [arXiv:0909.0290 \[hep-ph\]](#).
- [4] A. Falkowski, J. T. Ruderman, T. Volansky, and J. Zupan, *Hidden Higgs Decaying to Lepton Jets*, [*JHEP* **1005** \(2010\) 077](#), [arXiv:1002.2952 \[hep-ph\]](#).
- [5] A. Falkowski, J. T. Ruderman, T. Volansky, and J. Zupan, *Discovering Higgs Boson Decays to Lepton Jets at Hadron Colliders*, [*Phys. Rev. Lett.* **105** \(2010\) 241801](#), [arXiv:1007.3496 \[hep-ph\]](#).
- [6] X.-J. Bi, P.-F. Yin, and Q. Yuan, *Status of Dark Matter Detection*, [*Front. Phys. China* **8** \(2013\) 794–827](#), [arXiv:1409.4590 \[hep-ph\]](#).
- [7] B. Holdom, *Two $U(1)$'s and Epsilon Charge Shifts*, [*Phys. Lett.* **B166** \(1986\) 196](#).
- [8] ATLAS Collaboration,, *The ATLAS Experiment at the CERN Large Hadron Collider*, [*JINST* **3** \(2008\) S08003](#).
- [9] M. Reece and L.-T. Wang, *Searching for the light dark gauge boson in GeV-scale experiments*, [*JHEP* **0907** \(2009\) 051](#), [arXiv:0904.1743 \[hep-ph\]](#).
- [10] Y. F. Chan et al., *LHC Signatures of a Minimal Supersymmetric Hidden Valley*, [*JHEP* **1205** \(2014\) 155](#), [arXiv:1112.2705 \[hep-ph\]](#).
- [11] ATLAS Collaboration,, *A search for prompt lepton-jets in pp collisions at $\sqrt{s} = 7$ TeV with the ATLAS detector*, [*Phys.Lett.* **B719** \(2013\) 299–317](#), [arXiv:1212.5409](#).
- [12] ATLAS Collaboration,, *Search for WH production with a light Higgs boson decaying to prompt electron-jets in proton-proton collisions at $\sqrt{s}=7$ TeV with the ATLAS detector*, [*New J.Phys.* **15** \(2013\) 043009](#), [arXiv:1302.4403 \[hep-ex\]](#).
- [13] CMS Collaboration,, *Search for Light Resonances Decaying into Pairs of Muons as a Signal of New Physics*, [*JHEP* **1107** \(2011\) 098](#), [arXiv:1106.2375 \[hep-ex\]](#).
- [14] CMS Collaboration,, *Search for a non-standard-model Higgs boson decaying to a pair of new light bosons in four-muon final states*, [*Phys. Lett. B* **726** \(2013\) 564–586](#), [arXiv:1210.7619 \[hep-ex\]](#).
- [15] CMS Collaboration, *A Search for Pair Production of New Light Bosons Decaying into Muons*, [arXiv:1506.00424 \[hep-ex\]](#).
- [16] D0 Collaboration, V. M. Abazov et al., *Search for dark photons from supersymmetric hidden valleys*, [*Phys. Rev. Lett.* **103** \(2009\) 081802](#), [arXiv:0905.1478 \[hep-ex\]](#).

- [17] D0 Collaboration, V. M. Abazov et al., *Search for events with leptonic jets and missing transverse energy in $p\bar{p}$ collisions at $\sqrt{s} = 1.96$ TeV*, *Phys. Rev. Lett.* **105** (2010) 211802, [arXiv:1008.3356 \[hep-ex\]](#).
- [18] ATLAS Collaboration,, *Search for long-lived neutral particles decaying into lepton jets in proton–proton collisions at $\sqrt{s} = 8$ TeV with the ATLAS detector*, *JHEP* **1411** (2014) 088, [arXiv:1409.0746 \[hep-ex\]](#).
- [19] J. Bluemlein and J. Brunner, *New Exclusion Limits on Dark Gauge Forces from Proton Bremsstrahlung in Beam-Dump Data*, *Phys. Lett. B* **731** no. 4, (2014) 320–326, [arXiv:1311.3870](#), <http://dx.doi.org/10.1016/j.physletb.2014.02.029>.
- [20] E. M. Riordan et al., *Search for short-lived axions in an electron-beam-dump experiment*, *Phys. Rev. D* **59** no. 17, (1987) 755, <http://dx.doi.org/10.1103/PhysRevLett.59.755>.
- [21] A. Bross et al., *Search for short-lived particles produced in an electron beam dump*, *Phys. Rev. Lett.* **67** no. 18, (1991) 2942, <http://dx.doi.org/10.1103/PhysRevLett.67.2942>.
- [22] APEX Collaboration, S. Abrahamyan et al., *Search for a New Gauge Boson in Electron-Nucleus Fixed-Target Scattering by the APEX Experiment*, *Phys. Rev. Lett.* **107** (2011) 191804, [arXiv:1108.2750 \[hep-ex\]](#).
- [23] A1 Collaboration, H. Merkel et al., *Search for Light Gauge Bosons of the Dark Sector at the Mainz Microtron*, *Phys. Rev. Lett.* **106** (2011) 251802, [arXiv:1101.4091 \[nucl-ex\]](#).
- [24] WASA-at-COSY Collaboration, P. Adlarson et al., *Search for a dark photon in the $\pi^0 \rightarrow e^+ e^- \gamma$ decay*, *Phys. Lett. B* **726** no. 7, (2013) 187–193, [arXiv:1304.0671](#), <http://dx.doi.org/10.1016/j.physletb.2013.08.055>.
- [25] HADES Collaboration, G. Agakishiev et al., *Searching a dark photon with HADES*, *Phys. Lett. B* **731** no. 4, (2014) 265–271, [arXiv:1311.0216](#), <http://dx.doi.org/10.1016/j.physletb.2014.02.035>.
- [26] S. N. Gninenko, *Constraints on sub-GeV hidden sector gauge bosons from a search for heavy neutrino decays*, *Phys. Lett. B* **713** no. 9, (2012) 244–248, [arXiv:1204.3583](#), <http://dx.doi.org/10.1016/j.physletb.2012.06.002>.
- [27] J. D. Bjorken, R. Essig, P. Schuster, and N. Toro, *New Fixed-Target Experiments to Search for Dark Gauge Forces*, *Phys. Rev. D* **80** (2009) 075018, [arXiv:0906.0580 \[hep-ph\]](#).
- [28] KLOE-2 Collaboration, F. Archilli et al., *Search for a vector gauge boson in phi meson decays with the KLOE detector*, *Phys. Lett. B* **706** (2012) 251–255, [arXiv:1110.0411 \[hep-ex\]](#).
- [29] KLOE-2 Collaboration, D. Babusci et al., *Limit on the production of a light vector gauge boson in phi meson decays with the KLOE detector*, *Phys. Lett. B* **720** (2013) 111–115, [arXiv:1210.3927 \[hep-ex\]](#).
- [30] KLOE-2 Collaboration, D. Babusci et al., *Search for light vector boson production in $e^+e^- \rightarrow \mu^+\mu^-\gamma$ interactions with the KLOE experiment*, *Phys. Lett. B* **736** (2014) 459–464, [arXiv:1404.7772 \[hep-ex\]](#).
- [31] A. Anastasi et al., *Limit on the production of a low-mass vector boson in $e^+e^- \rightarrow U\gamma$, $U \rightarrow e^+e^-$ with the KLOE experiment*, *Phys. Lett. B* **750** (2015) 633–637, [arXiv:1509.00740 \[hep-ex\]](#).

- [32] BaBar Collaboration, B. Aubert et al., *Search for Dimuon Decays of a Light Scalar Boson in Radiative Transitions $\Upsilon \rightarrow \gamma A^0$* , *Phys. Rev. Lett.* **103** (2009) 081803, [arXiv:0905.4539 \[hep-ex\]](#).
- [33] BaBar Collaboration, J. P. Lees et al., *Search for a dark photon in e^+e^- collisions at BABAR*, *Phys. Rev. Lett.* **113** no. 11, (2014) 201801, [arXiv:1406.2980](#), <http://dx.doi.org/10.1103/PhysRevLett.113.201801>.
- [34] H. Davoudiasl, H.-S. Lee, and M. W. J., *Dark side of Higgs diphoton decays and muon $g-2$* , *Phys. Rev. Lett.* **86** no. 5, (2012) 095009, [arXiv:1208.2973](#), <http://dx.doi.org/10.1103/PhysRevD.86.095009>.
- [35] M. Endo, K. Hamaguchi, and G. Mishima, *Constraints on hidden photon models from electron $g-2$ and hydrogen spectroscopy*, *Phys. Rev. Lett.* **86** no. 27, (2012) 095029, [arXiv:1209.2558](#), <http://dx.doi.org/10.1103/PhysRevD.86.095029>.
- [36] J. B. Dent, F. Ferrer, and L. M. Krauss, *Constraints on Light Hidden Sector Gauge Bosons from Supernova Cooling*, [arXiv:1201.2683](#).
- [37] H. K. Dreiner, J.-F. Fortin, C. Hanhart, and L. Ubaldi, *Supernova constraints on MeV dark sectors from e^+e^- annihilations*, *Phys. Rev. D* **89** no. 16, (2014) 105015, [arXiv:1310.3826](#), <http://dx.doi.org/10.1103/PhysRevD.89.105015>.
- [38] GEANT4 Collaboration, S. Agostinelli et al., *GEANT4: A Simulation toolkit*, *Nucl. Instrum. Meth.* **A506** (2003) 250–303.
- [39] ATLAS Collaboration, *The ATLAS Simulation Infrastructure*, *Eur. Phys. J.* **C70** (2010) 823–874, [arXiv:1005.4568 \[physics.ins-det\]](#).
- [40] J. Alwall et al., *New Developments in MadGraph/MadEvent*, *AIP Conf. Proc.* **1078** (2009) 84–89, [arXiv:0809.2410 \[hep-ph\]](#).
- [41] J. Alwall, P. Schuster, and N. Toro, *Simplified Models for a First Characterization of New Physics at the LHC*, *Phys.Rev.* **D79** (2009) 075020, [arXiv:0810.3921 \[hep-ph\]](#).
- [42] LHC New Physics Working Group Collaboration, D. Alves et al., *Simplified Models for LHC New Physics Searches*, *J.Phys.* **G39** (2012) 105005, [arXiv:1105.2838 \[hep-ph\]](#).
- [43] ATLAS Collaboration, *Search for squarks and gluinos with the ATLAS detector in final states with jets and missing transverse momentum using $\sqrt{s} = 8$ TeV proton–proton collision data*, *JHEP* **1409** (2014) 176, [arXiv:1405.7875 \[hep-ex\]](#).
- [44] P. Meade and M. Reece, *BRIDGE: Branching ratio inquiry / decay generated events*, [arXiv:hep-ph/0703031 \[hep-ph\]](#).
- [45] T. Sjostrand, S. Mrenna, and P. Z. Skands, *PYTHIA 6.4 Physics and Manual*, *JHEP* **0605** (2006) 026, [arXiv:hep-ph/0603175 \[hep-ph\]](#).
- [46] T. Sjostrand, S. Mrenna, and P. Z. Skands, *A Brief Introduction to PYTHIA 8.1*, *Comput. Phys. Commun.* **178** (2008) 852–867, [arXiv:0710.3820 \[hep-ph\]](#).
- [47] J. Pumplin et al., *New generation of parton distributions with uncertainties from global QCD analysis*, *JHEP* **0207** (2002) 012, [arXiv:hep-ph/0201195 \[hep-ph\]](#).

- [48] ATLAS Collaboration,, *New ATLAS event generator tunes to 2010 data*, ATL-PHYS-PUB-2011-008 (2011), <https://cds.cern.ch/record/1345343>.
- [49] Particle Data Group Collaboration, K. A. Olive et al., *Review of Particle Physics*, *Chin. Phys.* **C38** (2014) 090001.
- [50] BaBar Collaboration, E. Solodov, *Study of the $e^+ e^-$ to hadrons via ISR at BaBar*, *Chin.Phys.* **C34** (2010) 660–668.
- [51] LHC Higgs Cross Section Working Group Collaboration, S. Heinemeyer et al., *Handbook of LHC Higgs Cross Sections: 3. Higgs Properties*, [arXiv:1307.1347](https://arxiv.org/abs/1307.1347) [[hep-ph](#)].
- [52] G. Punzi, *Sensitivity of searches for new signals and its optimization*, eConf **C030908** (2003) MODT002, [arXiv:hep-ph/0308063](https://arxiv.org/abs/hep-ph/0308063) [[physics](#)], [79(2003)].
- [53] S. Frixione and B. R. Webber, *Matching NLO QCD computations and parton shower simulations*, *JHEP* **0206** (2002) 029, [arXiv:hep-ph/0204244](https://arxiv.org/abs/hep-ph/0204244).
- [54] T. Gleisberg et al., *Event generation with SHERPA 1.1*, *JHEP* **0902** (2009) 007, [arXiv:0811.4622](https://arxiv.org/abs/0811.4622) [[hep-ph](#)].
- [55] H.-L. Lai et al., *New parton distributions for collider physics*, *Phys.Rev.* **D82** (2010) 074024, [arXiv:1007.2241](https://arxiv.org/abs/1007.2241) [[hep-ph](#)].
- [56] ATLAS Collaboration,, *Luminosity Determination in pp Collisions at $\sqrt{s} = 7$ TeV Using the ATLAS Detector at the LHC*, *Eur. Phys. J.* **C71** (2011) 1630, [arXiv:1101.2185](https://arxiv.org/abs/1101.2185) [[hep-ex](#)].
- [57] ATLAS Collaboration,, *Electron reconstruction and identification efficiency measurements with the ATLAS detector using the 2011 LHC proton-proton collision data*, *Eur. Phys. J.* **C74** (2014) 2941, [arXiv:1404.2240](https://arxiv.org/abs/1404.2240) [[hep-ex](#)].
- [58] ATLAS Collaboration,, *Performance of the ATLAS muon trigger in pp collisions at $\sqrt{s} = 8$ TeV*, *Eur. Phys. J.* **C75** (2015) 120, [arXiv:1408.3179](https://arxiv.org/abs/1408.3179) [[hep-ex](#)].
- [59] ATLAS Collaboration,, *Measurement of the muon reconstruction performance of the ATLAS detector using 2011 and 2012 LHC proton–proton collision data*, *Eur. Phys. J.* **C74** (2014) 3130, [arXiv:1407.3935](https://arxiv.org/abs/1407.3935) [[hep-ex](#)].
- [60] A. L. Read, *Presentation of search results: The CL(s) technique*, *J. Phys. G* **28** (2002) 2693–2704.
- [61] K. Cranmer, G. Lewis, L. Moneta, A. Shibata, and W. Verkerke, *HistFactory: A tool for creating statistical models for use with RooFit and RooStats*, CERN-OPEN-2012-016 (2012).
- [62] J. Bluemlein and J. Brunner, *New Exclusion Limits for Dark Gauge Forces from Beam-Dump Data*, *Phys. Lett. B* **701** no. 4, (2011) 155–159, [arXiv:1104.2747](https://arxiv.org/abs/1104.2747), <http://dx.doi.org/10.1016/j.physletb.2011.05.046>.
- [63] M. Davier and H. N. Ngoc, *An Unambiguous Search for a Light Higgs Boson*, *Phys. Lett. B* **229** no. 5, (1989) 150–155, [http://dx.doi.org/10.1016/0370-2693\(89\)90174-3](http://dx.doi.org/10.1016/0370-2693(89)90174-3).
- [64] R. Essig, R. Harnik, J. Kaplan, and N. Toro, *Discovering New Light States at Neutrino Experiments*, *Phys. Rev.* **D82** (2010) 113008, [arXiv:1008.0636](https://arxiv.org/abs/1008.0636) [[hep-ph](#)].
- [65] M. Pospelov, *Secluded U(1) below the weak scale*, *Phys. Rev. D* **80** no. 2, (2009) 095002, [arXiv:0811.1030](https://arxiv.org/abs/0811.1030), <http://dx.doi.org/10.1103/PhysRevD.80.095002>.

- [66] R. Essig et al., *Working Group Report: New Light Weakly Coupled Particles*, in *Community Summer Study 2013: Snowmass on the Mississippi (CSS2013) Minneapolis, MN, USA, July 29-August 6, 2013*. 2013. [arXiv:1311.0029 \[hep-ph\]](#).
<http://inspirehep.net/record/1263039/files/arXiv:1311.0029.pdf>.

The ATLAS Collaboration

G. Aad⁸⁵, B. Abbott¹¹³, J. Abdallah¹⁵¹, O. Abdinov¹¹, R. Aben¹⁰⁷, M. Abolins⁹⁰, O.S. AbouZeid¹⁵⁸, H. Abramowicz¹⁵³, H. Abreu¹⁵², R. Abreu¹¹⁶, Y. Abulaiti^{146a,146b}, B.S. Acharya^{164a,164b,a}, L. Adamczyk^{38a}, D.L. Adams²⁵, J. Adelman¹⁰⁸, S. Adomeit¹⁰⁰, T. Adye¹³¹, A.A. Affolder⁷⁴, T. Agatonovic-Jovin¹³, J. Agricola⁵⁴, J.A. Aguilar-Saavedra^{126a,126f}, S.P. Ahlen²², F. Ahmadov^{65,b}, G. Aielli^{133a,133b}, H. Akerstedt^{146a,146b}, T.P.A. Åkesson⁸¹, A.V. Akimov⁹⁶, G.L. Alberghi^{20a,20b}, J. Albert¹⁶⁹, S. Albrand⁵⁵, M.J. Alconada Verzini⁷¹, M. Aleksa³⁰, I.N. Aleksandrov⁶⁵, C. Alexa^{26b}, G. Alexander¹⁵³, T. Alexopoulos¹⁰, M. Alhroob¹¹³, G. Alimonti^{91a}, L. Alio⁸⁵, J. Alison³¹, S.P. Alkire³⁵, B.M.M. Allbrooke¹⁴⁹, P.P. Allport¹⁸, A. Aloisio^{104a,104b}, A. Alonso³⁶, F. Alonso⁷¹, C. Alpigiani⁷⁶, A. Altheimer³⁵, B. Alvarez Gonzalez³⁰, D. Álvarez Piqueras¹⁶⁷, M.G. Alviggi^{104a,104b}, B.T. Amadio¹⁵, K. Amako⁶⁶, Y. Amaral Coutinho^{24a}, C. Amelung²³, D. Amidei⁸⁹, S.P. Amor Dos Santos^{126a,126c}, A. Amorim^{126a,126b}, S. Amoroso⁴⁸, N. Amram¹⁵³, G. Amundsen²³, C. Anastopoulos¹³⁹, L.S. Ancu⁴⁹, N. Andari¹⁰⁸, T. Andeen³⁵, C.F. Anders^{58b}, G. Anders³⁰, J.K. Anders⁷⁴, K.J. Anderson³¹, A. Andreazza^{91a,91b}, V. Andrei^{58a}, S. Angelidakis⁹, I. Angelozzi¹⁰⁷, P. Anger⁴⁴, A. Angerami³⁵, F. Anghinolfi³⁰, A.V. Anisenkov^{109,c}, N. Anjos¹², A. Annovi^{124a,124b}, M. Antonelli⁴⁷, A. Antonov⁹⁸, J. Antos^{144b}, F. Anulli^{132a}, M. Aoki⁶⁶, L. Aperio Bella¹⁸, G. Arabidze⁹⁰, Y. Arai⁶⁶, J.P. Araque^{126a}, A.T.H. Arce⁴⁵, F.A. Arduh⁷¹, J-F. Arguin⁹⁵, S. Argyropoulos⁶³, M. Arik^{19a}, A.J. Armbruster³⁰, O. Arnaez³⁰, V. Arnal⁸², H. Arnold⁴⁸, M. Arratia²⁸, O. Arslan²¹, A. Artamonov⁹⁷, G. Artoni²³, S. Asai¹⁵⁵, N. Asbah⁴², A. Ashkenazi¹⁵³, B. Åsman^{146a,146b}, L. Asquith¹⁴⁹, K. Assamagan²⁵, R. Astalos^{144a}, M. Atkinson¹⁶⁵, N.B. Atlay¹⁴¹, K. Augsten¹²⁸, M. Aurousseau^{145b}, G. Avolio³⁰, B. Axen¹⁵, M.K. Ayoub¹¹⁷, G. Azuelos^{95,d}, M.A. Baak³⁰, A.E. Baas^{58a}, M.J. Baca¹⁸, C. Bacci^{134a,134b}, H. Bachacou¹³⁶, K. Bachas¹⁵⁴, M. Backes³⁰, M. Backhaus³⁰, P. Bagiacchi^{132a,132b}, P. Bagnaia^{132a,132b}, Y. Bai^{33a}, T. Bain³⁵, J.T. Baines¹³¹, O.K. Baker¹⁷⁶, E.M. Baldin^{109,c}, P. Balek¹²⁹, T. Balestri¹⁴⁸, F. Balli⁸⁴, W.K. Balunas¹²², E. Banas³⁹, Sw. Banerjee¹⁷³, A.A.E. Bannoura¹⁷⁵, H.S. Bansil¹⁸, L. Barak³⁰, E.L. Barberio⁸⁸, D. Barberis^{50a,50b}, M. Barbero⁸⁵, T. Barillari¹⁰¹, M. Barisonzi^{164a,164b}, T. Barklow¹⁴³, N. Barlow²⁸, S.L. Barnes⁸⁴, B.M. Barnett¹³¹, R.M. Barnett¹⁵, Z. Barnovska⁵, A. Baroncelli^{134a}, G. Barone²³, A.J. Barr¹²⁰, F. Barreiro⁸², J. Barreiro Guimarães da Costa⁵⁷, R. Bartoldus¹⁴³, A.E. Barton⁷², P. Bartos^{144a}, A. Basalae¹²³, A. Bassalat¹¹⁷, A. Basye¹⁶⁵, R.L. Bates⁵³, S.J. Batista¹⁵⁸, J.R. Batley²⁸, M. Battaglia¹³⁷, M. Baue^{132a,132b}, F. Bauer¹³⁶, H.S. Bawa^{143,e}, J.B. Beacham¹¹¹, M.D. Beattie⁷², T. Beau⁸⁰, P.H. Beauchemin¹⁶¹, R. Beccherle^{124a,124b}, P. Bechtel²¹, H.P. Beck^{17,f}, K. Becker¹²⁰, M. Becker⁸³, M. Beckingham¹⁷⁰, C. Becot¹¹⁷, A.J. Beddall^{19b}, A. Beddall^{19b}, V.A. Bednyakov⁶⁵, C.P. Bee¹⁴⁸, L.J. Beemster¹⁰⁷, T.A. Beermann³⁰, M. Begel²⁵, J.K. Behr¹²⁰, C. Belanger-Champagne⁸⁷, W.H. Bell⁴⁹, G. Bella¹⁵³, L. Bellagamba^{20a}, A. Bellerive²⁹, M. Bellomo⁸⁶, K. Belotskiy⁹⁸, O. Beltramello³⁰, O. Benary¹⁵³, D. Bencheikroun^{135a}, M. Bender¹⁰⁰, K. Bendtz^{146a,146b}, N. Benekos¹⁰, Y. Benhammou¹⁵³, E. Benhar Noccioli⁴⁹, J.A. Benitez Garcia^{159b}, D.P. Benjamin⁴⁵, J.R. Bensinger²³, S. Bentvelsen¹⁰⁷, L. Beresford¹²⁰, M. Beretta⁴⁷, D. Berge¹⁰⁷, E. Bergeaas Kuutmann¹⁶⁶, N. Berger⁵, F. Berghaus¹⁶⁹, J. Beringer¹⁵, C. Bernard²², N.R. Bernard⁸⁶, C. Bernius¹¹⁰, F.U. Bernlochner²¹, T. Berry⁷⁷, P. Berta¹²⁹, C. Bertella⁸³, G. Bertoli^{146a,146b}, F. Bertolucci^{124a,124b}, C. Bertsche¹¹³, D. Bertsche¹¹³, M.I. Besana^{91a}, G.J. Besjes³⁶, O. Bessidskaia Bylund^{146a,146b}, M. Bessner⁴², N. Besson¹³⁶, C. Betancourt⁴⁸, S. Bethke¹⁰¹, A.J. Bevan⁷⁶, W. Bhimji¹⁵, R.M. Bianchi¹²⁵, L. Bianchini²³, M. Bianco³⁰, O. Biebel¹⁰⁰, D. Biedermann¹⁶, S.P. Bieniek⁷⁸, M. Biglietti^{134a}, J. Bilbao De Mendizabal⁴⁹, H. Bilokon⁴⁷, M. Bindi⁵⁴, S. Binet¹¹⁷, A. Bingul^{19b}, C. Bini^{132a,132b}, S. Biondi^{20a,20b}, D.M. Bjergaard⁴⁵, C.W. Black¹⁵⁰, J.E. Black¹⁴³, K.M. Black²², D. Blackburn¹³⁸, R.E. Blair⁶, J.-B. Blanchard¹³⁶, J.E. Blanco⁷⁷, T. Blazek^{144a}, I. Bloch⁴², C. Blocker²³, W. Blum^{83,*}, U. Blumenschein⁵⁴, G.J. Bobbink¹⁰⁷,

V.S. Bobrovnikov^{109,c}, S.S. Bocchetta⁸¹, A. Bocci⁴⁵, C. Bock¹⁰⁰, M. Boehler⁴⁸, J.A. Bogaerts³⁰, D. Bogavac¹³, A.G. Bogdanchikov¹⁰⁹, C. Bohm^{146a}, V. Boisvert⁷⁷, T. Bold^{38a}, V. Boldea^{26b}, A.S. Boldyrev⁹⁹, M. Bomben⁸⁰, M. Bona⁷⁶, M. Boonekamp¹³⁶, A. Borisov¹³⁰, G. Borissov⁷², S. Borroni⁴², J. Bortfeldt¹⁰⁰, V. Bortolotto^{60a,60b,60c}, K. Bos¹⁰⁷, D. Boscherini^{20a}, M. Bosman¹², J. Boudreau¹²⁵, J. Bouffard², E.V. Bouhova-Thacker⁷², D. Boumediene³⁴, C. Bourdarios¹¹⁷, N. Bousson¹¹⁴, S.K. Boutle⁵³, A. Boveia³⁰, J. Boyd³⁰, I.R. Boyko⁶⁵, I. Bozic¹³, J. Bracinik¹⁸, A. Brandt⁸, G. Brandt⁵⁴, O. Brandt^{58a}, U. Bratzler¹⁵⁶, B. Brau⁸⁶, J.E. Brau¹¹⁶, H.M. Braun^{175,*}, S.F. Brazzale^{164a,164c}, W.D. Breaden Madden⁵³, K. Brendlinger¹²², A.J. Brennan⁸⁸, L. Brenner¹⁰⁷, R. Brenner¹⁶⁶, S. Bressler¹⁷², K. Bristow^{145c}, T.M. Bristow⁴⁶, D. Britton⁵³, D. Britzger⁴², F.M. Brochu²⁸, I. Brock²¹, R. Brock⁹⁰, J. Bronner¹⁰¹, G. Brooijmans³⁵, T. Brooks⁷⁷, W.K. Brooks^{32b}, J. Brosamer¹⁵, E. Brost¹¹⁶, J. Brown⁵⁵, P.A. Bruckman de Renstrom³⁹, D. Bruncko^{144b}, R. Bruneliere⁴⁸, A. Bruni^{20a}, G. Bruni^{20a}, M. Bruschi^{20a}, N. Bruscino²¹, L. Bryngemark⁸¹, T. Buanes¹⁴, Q. Buat¹⁴², P. Buchholz¹⁴¹, A.G. Buckley⁵³, S.I. Buda^{26b}, I.A. Budagov⁶⁵, F. Buehrer⁴⁸, L. Bugge¹¹⁹, M.K. Bugge¹¹⁹, O. Bulekov⁹⁸, D. Bullock⁸, H. Burckhart³⁰, S. Burdin⁷⁴, C.D. Burgard⁴⁸, B. Burghgrave¹⁰⁸, S. Burke¹³¹, I. Burmeister⁴³, E. Busato³⁴, D. Büscher⁴⁸, V. Büscher⁸³, P. Bussey⁵³, J.M. Butler²², A.I. Butt³, C.M. Buttar⁵³, J.M. Butterworth⁷⁸, P. Butti¹⁰⁷, W. Buttinger²⁵, A. Buzatu⁵³, A.R. Buzykaev^{109,c}, S. Cabrera Urbán¹⁶⁷, D. Caforio¹²⁸, V.M. Cairo^{37a,37b}, O. Cakir^{4a}, N. Calace⁴⁹, P. Calafiura¹⁵, A. Calandri¹³⁶, G. Calderini⁸⁰, P. Calfayan¹⁰⁰, L.P. Caloba^{24a}, D. Calvet³⁴, S. Calvet³⁴, R. Camacho Toro³¹, S. Camarda⁴², P. Camarri^{133a,133b}, D. Cameron¹¹⁹, R. Caminal Armadans¹⁶⁵, S. Campana³⁰, M. Campanelli⁷⁸, A. Campoverde¹⁴⁸, V. Canale^{104a,104b}, A. Canepa^{159a}, M. Cano Bret^{33e}, J. Cantero⁸², R. Cantrill^{126a}, T. Cao⁴⁰, M.D.M. Capeans Garrido³⁰, I. Caprini^{26b}, M. Caprini^{26b}, M. Capua^{37a,37b}, R. Caputo⁸³, R. Cardarelli^{133a}, F. Cardillo⁴⁸, T. Carli³⁰, G. Carlino^{104a}, L. Carminati^{91a,91b}, S. Caron¹⁰⁶, E. Carquin^{32a}, G.D. Carrillo-Montoya³⁰, J.R. Carter²⁸, J. Carvalho^{126a,126c}, D. Casadei⁷⁸, M.P. Casado¹², M. Casolino¹², E. Castaneda-Miranda^{145a}, A. Castelli¹⁰⁷, V. Castillo Gimenez¹⁶⁷, N.F. Castro^{126a,g}, P. Catastini⁵⁷, A. Catinaccio³⁰, J.R. Catmore¹¹⁹, A. Cattai³⁰, J. Caudron⁸³, V. Cavaliere¹⁶⁵, D. Cavalli^{91a}, M. Cavalli-Sforza¹², V. Cavasinni^{124a,124b}, F. Ceradini^{134a,134b}, B.C. Cerio⁴⁵, K. Cerny¹²⁹, A.S. Cerqueira^{24b}, A. Cerri¹⁴⁹, L. Cerrito⁷⁶, F. Cerutti¹⁵, M. Cerv³⁰, A. Cervelli¹⁷, S.A. Cetin^{19c}, A. Chafaq^{135a}, D. Chakraborty¹⁰⁸, I. Chalupkova¹²⁹, P. Chang¹⁶⁵, J.D. Chapman²⁸, D.G. Charlton¹⁸, C.C. Chau¹⁵⁸, C.A. Chavez Barajas¹⁴⁹, S. Cheatham¹⁵², A. Chegwidan⁹⁰, S. Chekanov⁶, S.V. Chekulaev^{159a}, G.A. Chelkov^{65,h}, M.A. Chelstowska⁸⁹, C. Chen⁶⁴, H. Chen²⁵, K. Chen¹⁴⁸, L. Chen^{33d,i}, S. Chen^{33c}, S. Chen¹⁵⁵, X. Chen^{33f}, Y. Chen⁶⁷, H.C. Cheng⁸⁹, Y. Cheng³¹, A. Cheplakov⁶⁵, E. Cheremushkina¹³⁰, R. Cherkaoui El Moursli^{135e}, V. Chernyatin^{25,*}, E. Cheu⁷, L. Chevalier¹³⁶, V. Chiarella⁴⁷, G. Chiarelli^{124a,124b}, G. Chiodini^{73a}, A.S. Chisholm¹⁸, R.T. Chislett⁷⁸, A. Chitan^{26b}, M.V. Chizhov⁶⁵, K. Choi⁶¹, S. Chouridou⁹, B.K.B. Chow¹⁰⁰, V. Christodoulou⁷⁸, D. Chromek-Burckhart³⁰, J. Chudoba¹²⁷, A.J. Chuinard⁸⁷, J.J. Chwastowski³⁹, L. Chytka¹¹⁵, G. Ciapetti^{132a,132b}, A.K. Ciftci^{4a}, D. Cinca⁵³, V. Cindro⁷⁵, I.A. Cioara²¹, A. Cicio¹⁵, F. Ciotto^{104a,104b}, Z.H. Citron¹⁷², M. Ciubancan^{26b}, A. Clark⁴⁹, B.L. Clark⁵⁷, P.J. Clark⁴⁶, R.N. Clarke¹⁵, W. Cleland¹²⁵, C. Clement^{146a,146b}, Y. Coadou⁸⁵, M. Cobal^{164a,164c}, A. Coccaro⁴⁹, J. Cochran⁶⁴, L. Coffey²³, J.G. Cogan¹⁴³, L. Colasurdo¹⁰⁶, B. Cole³⁵, S. Cole¹⁰⁸, A.P. Colijn¹⁰⁷, J. Collot⁵⁵, T. Colombo^{58c}, G. Compostella¹⁰¹, P. Conde Muiño^{126a,126b}, E. Coniavitis⁴⁸, S.H. Connell^{145b}, I.A. Connelly⁷⁷, V. Consorti⁴⁸, S. Constantinescu^{26b}, C. Conta^{121a,121b}, G. Conti³⁰, F. Conventi^{104a,j}, M. Cooke¹⁵, B.D. Cooper⁷⁸, A.M. Cooper-Sarkar¹²⁰, T. Cornelissen¹⁷⁵, M. Corradi^{20a}, F. Corriveau^{87,k}, A. Corso-Radu¹⁶³, A. Cortes-Gonzalez¹², G. Cortiana¹⁰¹, G. Costa^{91a}, M.J. Costa¹⁶⁷, D. Costanzo¹³⁹, D. Côte⁸, G. Cottin²⁸, G. Cowan⁷⁷, B.E. Cox⁸⁴, K. Cranmer¹¹⁰, G. Cree²⁹, S. Crépe-Renaudin⁵⁵, F. Crescioli⁸⁰, W.A. Cribbs^{146a,146b}, M. Crispin Ortuzar¹²⁰, M. Cristinziani²¹, V. Croft¹⁰⁶, G. Crosetti^{37a,37b}, T. Cuhadar Donszelmann¹³⁹, J. Cummings¹⁷⁶, M. Curatolo⁴⁷, J. Cúth⁸³, C. Cuthbert¹⁵⁰, H. Czirr¹⁴¹, P. Czodrowski³, S. D'Auria⁵³, M. D'Onofrio⁷⁴,

M.J. Da Cunha Sargedas De Sousa^{126a,126b}, C. Da Via⁸⁴, W. Dabrowski^{38a}, A. Dafinca¹²⁰, T. Dai⁸⁹, O. Dale¹⁴, F. Dallaire⁹⁵, C. Dallapiccola⁸⁶, M. Dam³⁶, J.R. Dandoy³¹, N.P. Dang⁴⁸, A.C. Daniells¹⁸, M. Danninger¹⁶⁸, M. Dano Hoffmann¹³⁶, V. Dao⁴⁸, G. Darbo^{50a}, S. Darmora⁸, J. Dassoulas³, A. Dattagupta⁶¹, W. Davey²¹, C. David¹⁶⁹, T. Davidek¹²⁹, E. Davies^{120,l}, M. Davies¹⁵³, P. Davison⁷⁸, Y. Davygora^{58a}, E. Dawe⁸⁸, I. Dawson¹³⁹, R.K. Daya-Ishmukhametova⁸⁶, K. De⁸, R. de Asmundis^{104a}, A. De Benedetti¹¹³, S. De Castro^{20a,20b}, S. De Cecco⁸⁰, N. De Groot¹⁰⁶, P. de Jong¹⁰⁷, H. De la Torre⁸², F. De Lorenzi⁶⁴, D. De Pedis^{132a}, A. De Salvo^{132a}, U. De Sanctis¹⁴⁹, A. De Santo¹⁴⁹, J.B. De Vivie De Regie¹¹⁷, W.J. Dearnaley⁷², R. Debbe²⁵, C. Debenedetti¹³⁷, D.V. Dedovich⁶⁵, I. Deigaard¹⁰⁷, J. Del Peso⁸², T. Del Prete^{124a,124b}, D. Delgove¹¹⁷, F. Deliot¹³⁶, C.M. Delitzsch⁴⁹, M. Deliyergiyev⁷⁵, A. Dell'Acqua³⁰, L. Dell'Asta²², M. Dell'Orso^{124a,124b}, M. Della Pietra^{104a,j}, D. della Volpe⁴⁹, M. Delmastro⁵, P.A. Delsart⁵⁵, C. Deluca¹⁰⁷, D.A. DeMarco¹⁵⁸, S. Demers¹⁷⁶, M. Demichev⁶⁵, A. Demilly⁸⁰, S.P. Denisov¹³⁰, D. Derendarz³⁹, J.E. Derkaoui^{135d}, F. Derue⁸⁰, P. Dervan⁷⁴, K. Desch²¹, C. Deterre⁴², P.O. Deviveiros³⁰, A. Dewhurst¹³¹, S. Dhaliwal²³, A. Di Ciaccio^{133a,133b}, L. Di Ciaccio⁵, A. Di Domenico^{132a,132b}, C. Di Donato^{132a,132b}, A. Di Girolamo³⁰, B. Di Girolamo³⁰, A. Di Mattia¹⁵², B. Di Micco^{134a,134b}, R. Di Nardo⁴⁷, A. Di Simone⁴⁸, R. Di Sipio¹⁵⁸, D. Di Valentino²⁹, C. Diaconu⁸⁵, M. Diamond¹⁵⁸, F.A. Dias⁴⁶, M.A. Diaz^{32a}, E.B. Diehl⁸⁹, J. Dietrich¹⁶, S. Diglio⁸⁵, A. Dimitrievska¹³, J. Dingfelder²¹, P. Dita^{26b}, S. Dita^{26b}, F. Dittus³⁰, F. Djama⁸⁵, T. Djobava^{51b}, J.I. Djuvsland^{58a}, M.A.B. do Vale^{24c}, D. Dobos³⁰, M. Dobre^{26b}, C. Doglioni⁸¹, T. Dohmae¹⁵⁵, J. Dolejsi¹²⁹, Z. Dolezal¹²⁹, B.A. Dolgoshein^{98,*}, M. Donadelli^{24d}, S. Donati^{124a,124b}, P. Dondero^{121a,121b}, J. Donini³⁴, J. Dopke¹³¹, A. Doria^{104a}, M.T. Dova⁷¹, A.T. Doyle⁵³, E. Drechsler⁵⁴, M. Dris¹⁰, E. Dubreuil³⁴, E. Duchovni¹⁷², G. Duckeck¹⁰⁰, O.A. Ducu^{26b,85}, D. Duda¹⁰⁷, A. Dudarev³⁰, L. Duflo¹¹⁷, L. Duguid⁷⁷, M. Dührssen³⁰, M. Dunford^{58a}, H. Duran Yildiz^{4a}, M. Düren⁵², A. Durglishvili^{51b}, D. Duschinger⁴⁴, M. Dyndal^{38a}, C. Eckardt⁴², K.M. Ecker¹⁰¹, R.C. Edgar⁸⁹, W. Edson², N.C. Edwards⁴⁶, W. Ehrenfeld²¹, T. Eifert³⁰, G. Eigen¹⁴, K. Einsweiler¹⁵, T. Ekelof¹⁶⁶, M. El Kacimi^{135c}, M. Ellert¹⁶⁶, S. Elles⁵, F. Ellinghaus¹⁷⁵, A.A. Elliot¹⁶⁹, N. Ellis³⁰, J. Elmsheuser¹⁰⁰, M. Elsing³⁰, D. Emelianov¹³¹, Y. Enari¹⁵⁵, O.C. Endner⁸³, M. Endo¹¹⁸, J. Erdmann⁴³, A. Ereditato¹⁷, G. Ernis¹⁷⁵, J. Ernst²⁵, M. Ernst²⁵, S. Errede¹⁶⁵, E. Ertel⁸³, M. Escalier¹¹⁷, H. Esch⁴³, C. Escobar¹²⁵, B. Esposito⁴⁷, A.I. Etienne¹³⁶, E. Etzion¹⁵³, H. Evans⁶¹, A. Ezhilov¹²³, L. Fabbri^{20a,20b}, G. Facini³¹, R.M. Fakhruddinov¹³⁰, S. Falciano^{132a}, R.J. Falla⁷⁸, J. Faltova¹²⁹, Y. Fang^{33a}, M. Fanti^{91a,91b}, A. Farbin⁸, A. Farilla^{134a}, T. Farooque¹², S. Farrell¹⁵, S.M. Farrington¹⁷⁰, P. Farthouat³⁰, F. Fassi^{135e}, P. Fassnacht³⁰, D. Fassouliotis⁹, M. Fauci Giannelli⁷⁷, A. Favareto^{50a,50b}, L. Fayard¹¹⁷, P. Federic^{144a}, O.L. Fedin^{123,m}, W. Fedorko¹⁶⁸, S. Feigl³⁰, L. Feligioni⁸⁵, C. Feng^{33d}, E.J. Feng⁶, H. Feng⁸⁹, A.B. Fenyuk¹³⁰, L. Feremenga⁸, P. Fernandez Martinez¹⁶⁷, S. Fernandez Perez³⁰, J. Ferrando⁵³, A. Ferrari¹⁶⁶, P. Ferrari¹⁰⁷, R. Ferrari^{121a}, D.E. Ferreira de Lima⁵³, A. Ferrer¹⁶⁷, D. Ferrere⁴⁹, C. Ferretti⁸⁹, A. Ferretto Parodi^{50a,50b}, M. Fiascaris³¹, F. Fiedler⁸³, A. Filipčič⁷⁵, M. Filipuzzi⁴², F. Filthaut¹⁰⁶, M. Fincke-Keeler¹⁶⁹, K.D. Finelli¹⁵⁰, M.C.N. Fiolhais^{126a,126c}, L. Fiorini¹⁶⁷, A. Firan⁴⁰, A. Fischer², C. Fischer¹², J. Fischer¹⁷⁵, W.C. Fisher⁹⁰, E.A. Fitzgerald²³, N. Flaschel⁴², I. Fleck¹⁴¹, P. Fleischmann⁸⁹, S. Fleischmann¹⁷⁵, G.T. Fletcher¹³⁹, G. Fletcher⁷⁶, R.R.M. Fletcher¹²², T. Flick¹⁷⁵, A. Floderus⁸¹, L.R. Flores Castillo^{60a}, M.J. Flowerdew¹⁰¹, A. Formica¹³⁶, A. Forti⁸⁴, D. Fournier¹¹⁷, H. Fox⁷², S. Fracchia¹², P. Francavilla⁸⁰, M. Franchini^{20a,20b}, D. Francis³⁰, L. Franconi¹¹⁹, M. Franklin⁵⁷, M. Frate¹⁶³, M. Fraternali^{121a,121b}, D. Freeborn⁷⁸, S.T. French²⁸, F. Friedrich⁴⁴, D. Froidevaux³⁰, J.A. Frost¹²⁰, C. Fukunaga¹⁵⁶, E. Fullana Torregrosa⁸³, B.G. Fulsom¹⁴³, T. Fusayasu¹⁰², J. Fuster¹⁶⁷, C. Gabaldon⁵⁵, O. Gabizon¹⁷⁵, A. Gabrielli^{20a,20b}, A. Gabrielli¹⁵, G.P. Gach¹⁸, S. Gadatsch³⁰, S. Gadomski⁴⁹, G. Gagliardi^{50a,50b}, P. Gagnon⁶¹, C. Galea¹⁰⁶, B. Galhardo^{126a,126c}, E.J. Gallas¹²⁰, B.J. Gallop¹³¹, P. Gallus¹²⁸, G. Galster³⁶, K.K. Gan¹¹¹, J. Gao^{33b,85}, Y. Gao⁴⁶, Y.S. Gao^{143,e}, F.M. Garay Walls⁴⁶, F. Garberson¹⁷⁶, C. García¹⁶⁷, J.E. García Navarro¹⁶⁷, M. Garcia-Sciveres¹⁵, R.W. Gardner³¹, N. Garelli¹⁴³, V. Garonne¹¹⁹, C. Gatti⁴⁷, A. Gaudiello^{50a,50b}, G. Gaudio^{121a}, B. Gaur¹⁴¹,

L. Gauthier⁹⁵, P. Gauzzi^{132a,132b}, I.L. Gavrilenko⁹⁶, C. Gay¹⁶⁸, G. Gaycken²¹, E.N. Gazis¹⁰, P. Ge^{33d},
 Z. Gecse¹⁶⁸, C.N.P. Gee¹³¹, Ch. Geich-Gimbel²¹, M.P. Geisler^{58a}, C. Gemme^{50a}, M.H. Genest⁵⁵,
 S. Gentile^{132a,132b}, M. George⁵⁴, S. George⁷⁷, D. Gerbaudo¹⁶³, A. Gershon¹⁵³, S. Ghasemi¹⁴¹,
 H. Ghazlane^{135b}, B. Giacobbe^{20a}, S. Giagu^{132a,132b}, V. Giangiobbe¹², P. Giannetti^{124a,124b}, B. Gibbard²⁵,
 S.M. Gibson⁷⁷, M. Gilchriese¹⁵, T.P.S. Gillam²⁸, D. Gillberg³⁰, G. Gilles³⁴, D.M. Gingrich^{3,d},
 N. Giokaris⁹, M.P. Giordani^{164a,164c}, F.M. Giorgi^{20a}, F.M. Giorgi¹⁶, P.F. Giraud¹³⁶, P. Giromini⁴⁷,
 D. Giugni^{91a}, C. Giuliani⁴⁸, M. Giulini^{58b}, B.K. Gjølsten¹¹⁹, S. Gkaitatzis¹⁵⁴, I. Gkialas¹⁵⁴,
 E.L. Gkoukousis¹¹⁷, L.K. Gladilin⁹⁹, C. Glasman⁸², J. Glatzer³⁰, P.C.F. Glaysheer⁴⁶, A. Glazov⁴²,
 M. Goblirsch-Kolb¹⁰¹, J.R. Goddard⁷⁶, J. Godlewski³⁹, S. Goldfarb⁸⁹, T. Golling⁴⁹, D. Golubkov¹³⁰,
 A. Gomes^{126a,126b,126d}, R. Gonçalo^{126a}, J. Goncalves Pinto Firmino Da Costa¹³⁶, L. Gonella²¹,
 S. González de la Hoz¹⁶⁷, G. Gonzalez Parra¹², S. Gonzalez-Sevilla⁴⁹, L. Goossens³⁰,
 P.A. Gorbounov⁹⁷, H.A. Gordon²⁵, I. Gorelov¹⁰⁵, B. Gorini³⁰, E. Gorini^{73a,73b}, A. Gorišek⁷⁵,
 E. Gornicki³⁹, A.T. Goshaw⁴⁵, C. Gössling⁴³, M.I. Gostkin⁶⁵, D. Goudami^{135c}, A.G. Goussiou¹³⁸,
 N. Govender^{145b}, E. Gozani¹⁵², H.M.X. Grabas¹³⁷, L. Graber⁵⁴, I. Grabowska-Bold^{38a}, P.O.J. Gradin¹⁶⁶,
 P. Grafström^{20a,20b}, K.-J. Grahm⁴², J. Gramling⁴⁹, E. Gramstad¹¹⁹, S. Grancagnolo¹⁶, V. Gratchev¹²³,
 H.M. Gray³⁰, E. Graziani^{134a}, Z.D. Greenwood^{79,n}, C. Grefe²¹, K. Gregersen⁷⁸, I.M. Gregor⁴²,
 P. Grenier¹⁴³, J. Griffiths⁸, A.A. Grillo¹³⁷, K. Grimm⁷², S. Grinstein^{12,o}, Ph. Gris³⁴, J.-F. Grivaz¹¹⁷,
 J.P. Grohs⁴⁴, A. Grohsjean⁴², E. Gross¹⁷², J. Grosse-Knetter⁵⁴, G.C. Grossi⁷⁹, Z.J. Grout¹⁴⁹, L. Guan⁸⁹,
 J. Guenther¹²⁸, F. Guescini⁴⁹, D. Guest¹⁷⁶, O. Gueta¹⁵³, E. Guido^{50a,50b}, T. Guillemin¹¹⁷, S. Guindon²,
 U. Gul⁵³, C. Gumpert⁴⁴, J. Guo^{33e}, Y. Guo^{33b,p}, S. Gupta¹²⁰, G. Gustavino^{132a,132b}, P. Gutierrez¹¹³,
 N.G. Gutierrez Ortiz⁷⁸, C. Gutschow⁴⁴, C. Guyot¹³⁶, C. Gwenlan¹²⁰, C.B. Gwilliam⁷⁴, A. Haas¹¹⁰,
 C. Haber¹⁵, H.K. Hadavand⁸, N. Haddad^{135e}, P. Haefner²¹, S. Hageböck²¹, Z. Hajduk³⁹,
 H. Hakobyan¹⁷⁷, M. Haleem⁴², J. Haley¹¹⁴, D. Hall¹²⁰, G. Halladjian⁹⁰, G.D. Hallowell⁸⁵,
 K. Hamacher¹⁷⁵, P. Hamal¹¹⁵, K. Hamano¹⁶⁹, A. Hamilton^{145a}, G.N. Hamity¹³⁹, P.G. Hamnett⁴²,
 L. Han^{33b}, K. Hanagaki^{66,q}, K. Hanawa¹⁵⁵, M. Hance¹⁵, B. Haney¹²², P. Hanke^{58a}, R. Hanna¹³⁶,
 J.B. Hansen³⁶, J.D. Hansen³⁶, M.C. Hansen²¹, P.H. Hansen³⁶, K. Hara¹⁶⁰, A.S. Hard¹⁷³,
 T. Harenberg¹⁷⁵, F. Hariri¹¹⁷, S. Harkusha⁹², R.D. Harrington⁴⁶, P.F. Harrison¹⁷⁰, F. Hartjes¹⁰⁷,
 M. Hasegawa⁶⁷, Y. Hasegawa¹⁴⁰, A. Hasib¹¹³, S. Hassani¹³⁶, S. Haug¹⁷, R. Hauser⁹⁰, L. Hauswald⁴⁴,
 M. Havranek¹²⁷, C.M. Hawkes¹⁸, R.J. Hawking³⁰, A.D. Hawkins⁸¹, T. Hayashi¹⁶⁰, D. Hayden⁹⁰,
 C.P. Hays¹²⁰, J.M. Hays⁷⁶, H.S. Hayward⁷⁴, S.J. Haywood¹³¹, S.J. Head¹⁸, T. Heck⁸³, V. Hedberg⁸¹,
 L. Heelan⁸, S. Heim¹²², T. Heim¹⁷⁵, B. Heinemann¹⁵, L. Heinrich¹¹⁰, J. Hejbal¹²⁷, L. Helary²²,
 S. Hellman^{146a,146b}, D. Hellmich²¹, C. Helsens¹², J. Henderson¹²⁰, R.C.W. Henderson⁷², Y. Heng¹⁷³,
 C. Hengler⁴², S. Henkelmann¹⁶⁸, A. Henrichs¹⁷⁶, A.M. Henriques Correia³⁰, S. Henrot-Versille¹¹⁷,
 G.H. Herbert¹⁶, Y. Hernández Jiménez¹⁶⁷, R. Herrberg-Schubert¹⁶, G. Herten⁴⁸, R. Hertenberger¹⁰⁰,
 L. Hervas³⁰, G.G. Hesketh⁷⁸, N.P. Hessey¹⁰⁷, J.W. Hetherly⁴⁰, R. Hickling⁷⁶, E. Higón-Rodríguez¹⁶⁷,
 E. Hill¹⁶⁹, J.C. Hill²⁸, K.H. Hiller⁴², S.J. Hillier¹⁸, I. Hinchliffe¹⁵, E. Hines¹²², R.R. Hinman¹⁵,
 M. Hirose¹⁵⁷, D. Hirschbuehl¹⁷⁵, J. Hobbs¹⁴⁸, N. Hod¹⁰⁷, M.C. Hodgkinson¹³⁹, P. Hodgson¹³⁹,
 A. Hoecker³⁰, M.R. Hoferkamp¹⁰⁵, F. Hoenig¹⁰⁰, M. Hohlfield⁸³, D. Hohn²¹, T.R. Holmes¹⁵,
 M. Homann⁴³, T.M. Hong¹²⁵, W.H. Hopkins¹¹⁶, Y. Horii¹⁰³, A.J. Horton¹⁴², J.-Y. Hostachy⁵⁵, S. Hou¹⁵¹,
 A. Hoummada^{135a}, J. Howard¹²⁰, J. Howarth⁴², M. Hrabovsky¹¹⁵, I. Hristova¹⁶, J. Hrivnac¹¹⁷,
 T. Hryn'ova⁵, A. Hrynevich⁹³, C. Hsu^{145c}, P.J. Hsu^{151,r}, S.-C. Hsu¹³⁸, D. Hu³⁵, Q. Hu^{33b}, X. Hu⁸⁹,
 Y. Huang⁴², Z. Hubacek¹²⁸, F. Hubaut⁸⁵, F. Huegging²¹, T.B. Huffman¹²⁰, E.W. Hughes³⁵, G. Hughes⁷²,
 M. Huhtinen³⁰, T.A. Hülsing⁸³, N. Huseynov^{65,b}, J. Huston⁹⁰, J. Huth⁵⁷, G. Iacobucci⁴⁹, G. Iakovidis²⁵,
 I. Ibragimov¹⁴¹, L. Iconomidou-Fayard¹¹⁷, E. Ideal¹⁷⁶, Z. Idrissi^{135e}, P. Iengo³⁰, O. Igonkina¹⁰⁷,
 T. Iizawa¹⁷¹, Y. Ikegami⁶⁶, K. Ikematsu¹⁴¹, M. Ikeno⁶⁶, Y. Ilchenko^{31,s}, D. Iliadis¹⁵⁴, N. Ilic¹⁴³,
 T. Ince¹⁰¹, G. Introzzi^{121a,121b}, P. Ioannou⁹, M. Iodice^{134a}, K. Iordanidou³⁵, V. Ippolito⁵⁷,
 A. Irles Quiles¹⁶⁷, C. Isaksson¹⁶⁶, M. Ishino⁶⁸, M. Ishitsuka¹⁵⁷, R. Ishmukhametov¹¹¹, C. Issever¹²⁰,

S. Istin^{19a}, J.M. Iturbe Ponce⁸⁴, R. Iuppa^{133a,133b}, J. Ivarsson⁸¹, W. Iwanski³⁹, H. Iwasaki⁶⁶, J.M. Izen⁴¹, V. Izzo^{104a}, S. Jabbar³, B. Jackson¹²², M. Jackson⁷⁴, P. Jackson¹, M.R. Jaekel³⁰, V. Jain², K. Jakobs⁴⁸, S. Jakobsen³⁰, T. Jakoubek¹²⁷, J. Jakubek¹²⁸, D.O. Jamin¹¹⁴, D.K. Jana⁷⁹, E. Jansen⁷⁸, R. Jansky⁶², J. Janssen²¹, M. Janus⁵⁴, G. Jarlskog⁸¹, N. Javadov^{65,b}, T. Javůrek⁴⁸, L. Jeanty¹⁵, J. Jejelava^{51a,t}, G.-Y. Jeng¹⁵⁰, D. Jennens⁸⁸, P. Jenni^{48,u}, J. Jentzsch⁴³, C. Jeske¹⁷⁰, S. Jézéquel⁵, H. Ji¹⁷³, J. Jia¹⁴⁸, Y. Jiang^{33b}, S. Jiggins⁷⁸, J. Jimenez Pena¹⁶⁷, S. Jin^{33a}, A. Jinaru^{26b}, O. Jinnouchi¹⁵⁷, M.D. Joergensen³⁶, P. Johansson¹³⁹, K.A. Johns⁷, K. Jon-And^{146a,146b}, G. Jones¹⁷⁰, R.W.L. Jones⁷², T.J. Jones⁷⁴, J. Jongmanns^{58a}, P.M. Jorge^{126a,126b}, K.D. Joshi⁸⁴, J. Jovicevic^{159a}, X. Ju¹⁷³, C.A. Jung⁴³, P. Jussel⁶², A. Juste Rozas^{12,o}, M. Kaci¹⁶⁷, A. Kaczmarzka³⁹, M. Kado¹¹⁷, H. Kagan¹¹¹, M. Kagan¹⁴³, S.J. Kahn⁸⁵, E. Kajomovitz⁴⁵, C.W. Kalderon¹²⁰, S. Kama⁴⁰, A. Kamenshchikov¹³⁰, N. Kanaya¹⁵⁵, S. Kaneti²⁸, V.A. Kantserov⁹⁸, J. Kanzaki⁶⁶, B. Kaplan¹¹⁰, L.S. Kaplan¹⁷³, A. Kapliy³¹, D. Kar^{145c}, K. Karakostas¹⁰, A. Karamaoun³, N. Karastathis^{10,107}, M.J. Kareem⁵⁴, E. Karentzos¹⁰, M. Karnevskiy⁸³, S.N. Karpov⁶⁵, Z.M. Karpova⁶⁵, K. Karthik¹¹⁰, V. Kartvelishvili⁷², A.N. Karyukhin¹³⁰, K. Kasahara¹⁶⁰, L. Kashif¹⁷³, R.D. Kass¹¹¹, A. Kastanas¹⁴, Y. Kataoka¹⁵⁵, C. Kato¹⁵⁵, A. Katre⁴⁹, J. Katzy⁴², K. Kawagoe⁷⁰, T. Kawamoto¹⁵⁵, G. Kawamura⁵⁴, S. Kazama¹⁵⁵, V.F. Kazanin^{109,c}, R. Keeler¹⁶⁹, R. Kehoe⁴⁰, J.S. Keller⁴², J.J. Kempster⁷⁷, H. Keoshkerian⁸⁴, O. Kepka¹²⁷, B.P. Kerševan⁷⁵, S. Kersten¹⁷⁵, R.A. Keyes⁸⁷, F. Khalil-zada¹¹, H. Khandanyan^{146a,146b}, A. Khanov¹¹⁴, A.G. Kharlamov^{109,c}, T.J. Khoo²⁸, V. Khovanskiy⁹⁷, E. Khramov⁶⁵, J. Khubua^{51b,v}, S. Kido⁶⁷, H.Y. Kim⁸, S.H. Kim¹⁶⁰, Y.K. Kim³¹, N. Kimura¹⁵⁴, O.M. Kind¹⁶, B.T. King⁷⁴, M. King¹⁶⁷, S.B. King¹⁶⁸, J. Kirk¹³¹, A.E. Kiryunin¹⁰¹, T. Kishimoto⁶⁷, D. Kisielewska^{38a}, F. Kiss⁴⁸, K. Kiuchi¹⁶⁰, O. Kivernyk¹³⁶, E. Kladiva^{144b}, M.H. Klein³⁵, M. Klein⁷⁴, U. Klein⁷⁴, K. Kleinknecht⁸³, P. Klimek^{146a,146b}, A. Klimentov²⁵, R. Klingenberg⁴³, J.A. Klinger¹³⁹, T. Kliutchnikova³⁰, E.-E. Kluge^{58a}, P. Kluit¹⁰⁷, S. Kluth¹⁰¹, J. Knapik³⁹, E. Kneringer⁶², E.B.F.G. Knoop⁸⁵, A. Knue⁵³, A. Kobayashi¹⁵⁵, D. Kobayashi¹⁵⁷, T. Kobayashi¹⁵⁵, M. Kobel⁴⁴, M. Kocian¹⁴³, P. Kodys¹²⁹, T. Koffas²⁹, E. Koffeman¹⁰⁷, L.A. Kogan¹²⁰, S. Kohlmann¹⁷⁵, Z. Kohout¹²⁸, T. Kohriki⁶⁶, T. Koi¹⁴³, H. Kolanoski¹⁶, M. Kolb^{58b}, I. Koletsou⁵, A.A. Komar^{96,*}, Y. Komori¹⁵⁵, T. Kondo⁶⁶, N. Kondrashova⁴², K. Köneke⁴⁸, A.C. König¹⁰⁶, T. Kono⁶⁶, R. Konoplich^{110,w}, N. Konstantinidis⁷⁸, R. Kopeliansky¹⁵², S. Koperny^{38a}, L. Köpke⁸³, A.K. Kopp⁴⁸, K. Korcyl³⁹, K. Kordas¹⁵⁴, A. Korn⁷⁸, A.A. Korol^{109,c}, I. Korolkov¹², E.V. Korolkova¹³⁹, O. Kortner¹⁰¹, S. Kortner¹⁰¹, T. Kosek¹²⁹, V.V. Kostyukhin²¹, V.M. Kotov⁶⁵, A. Kotwal⁴⁵, A. Kourkouveli-Charalampidi¹⁵⁴, C. Kourkouvelis⁹, V. Kouskoura²⁵, A. Koutsman^{159a}, R. Kowalewski¹⁶⁹, T.Z. Kowalski^{38a}, W. Kozanecki¹³⁶, A.S. Kozhin¹³⁰, V.A. Kramarenko⁹⁹, G. Kramberger⁷⁵, D. Krasnopevtsev⁹⁸, M.W. Krasny⁸⁰, A. Krasznahorkay³⁰, J.K. Kraus²¹, A. Kravchenko²⁵, S. Kreiss¹¹⁰, M. Kretz^{58c}, J. Kretzschmar⁷⁴, K. Kreutzfeldt⁵², P. Krieger¹⁵⁸, K. Krizka³¹, K. Kroeninger⁴³, H. Kroha¹⁰¹, J. Kroll¹²², J. Kroseberg²¹, J. Krstic¹³, U. Kruchonak⁶⁵, H. Krüger²¹, N. Krumnack⁶⁴, A. Kruse¹⁷³, M.C. Kruse⁴⁵, M. Kruskal²², T. Kubota⁸⁸, H. Kucuk⁷⁸, S. Kuday^{4b}, S. Kuehn⁴⁸, A. Kugel^{58c}, F. Kuger¹⁷⁴, A. Kuhl¹³⁷, T. Kuhl⁴², V. Kukhtin⁶⁵, R. Kukla¹³⁶, Y. Kulchitsky⁹², S. Kuleshov^{32b}, M. Kuna^{132a,132b}, T. Kunigo⁶⁸, A. Kupco¹²⁷, H. Kurashige⁶⁷, Y.A. Kurochkin⁹², V. Kus¹²⁷, E.S. Kuwertz¹⁶⁹, M. Kuze¹⁵⁷, J. Kvita¹¹⁵, T. Kwan¹⁶⁹, D. Kyriazopoulos¹³⁹, A. La Rosa¹³⁷, J.L. La Rosa Navarro^{24d}, L. La Rotonda^{37a,37b}, C. Lacasta¹⁶⁷, F. Lacava^{132a,132b}, J. Lacey²⁹, H. Lacker¹⁶, D. Lacour⁸⁰, V.R. Lacuesta¹⁶⁷, E. Ladygin⁶⁵, R. Lafaye⁵, B. Laforge⁸⁰, T. Lagouri¹⁷⁶, S. Lai⁵⁴, L. Lambourne⁷⁸, S. Lammers⁶¹, C.L. Lampen⁷, W. Lampl⁷, E. Lançon¹³⁶, U. Landgraf⁴⁸, M.P.J. Landon⁷⁶, V.S. Lang^{58a}, J.C. Lange¹², A.J. Lankford¹⁶³, F. Lanni²⁵, K. Lantzscht²¹, A. Lanza^{121a}, S. Laplace⁸⁰, C. Lapoire³⁰, J.F. Laporte¹³⁶, T. Lari^{91a}, F. Lasagni Manghi^{20a,20b}, M. Lassnig³⁰, P. Laurelli⁴⁷, W. Lavrijsen¹⁵, A.T. Law¹³⁷, P. Laycock⁷⁴, T. Lazovich⁵⁷, O. Le Dortz⁸⁰, E. Le Guirriec⁸⁵, E. Le Menedeu¹², M. LeBlanc¹⁶⁹, T. LeCompte⁶, F. Ledroit-Guillon⁵⁵, C.A. Lee^{145b}, S.C. Lee¹⁵¹, L. Lee¹, G. Lefebvre⁸⁰, M. Lefebvre¹⁶⁹, F. Legger¹⁰⁰, C. Leggett¹⁵, A. Lehan⁷⁴, G. Lehmann Miotto³⁰, X. Lei⁷, W.A. Leight²⁹, A. Leisos^{154,x}, A.G. Leister¹⁷⁶,

M.A.L. Leite^{24d}, R. Leitner¹²⁹, D. Lellouch¹⁷², B. Lemmer⁵⁴, K.J.C. Leney⁷⁸, T. Lenz²¹, B. Lenzi³⁰,
R. Leone⁷, S. Leone^{124a,124b}, C. Leonidopoulos⁴⁶, S. Leontsinis¹⁰, C. Leroy⁹⁵, C.G. Lester²⁸,
M. Levchenko¹²³, J. Levêque⁵, D. Levin⁸⁹, L.J. Levinson¹⁷², M. Levy¹⁸, A. Lewis¹²⁰, A.M. Leyko²¹,
M. Leyton⁴¹, B. Li^{33b,y}, H. Li¹⁴⁸, H.L. Li³¹, L. Li⁴⁵, L. Li^{33e}, S. Li⁴⁵, X. Li⁸⁴, Y. Li^{33c,z}, Z. Liang¹³⁷,
H. Liao³⁴, B. Liberti^{133a}, A. Liblong¹⁵⁸, P. Lichard³⁰, K. Lie¹⁶⁵, J. Liebal²¹, W. Liebig¹⁴, C. Limbach²¹,
A. Limosani¹⁵⁰, S.C. Lin^{151,aa}, T.H. Lin⁸³, F. Linde¹⁰⁷, B.E. Lindquist¹⁴⁸, J.T. Linnemann⁹⁰,
E. Lipeles¹²², A. Lipniacka¹⁴, M. Lisovyi^{58b}, T.M. Liss¹⁶⁵, D. Lissauer²⁵, A. Lister¹⁶⁸, A.M. Litke¹³⁷,
B. Liu^{151,ab}, D. Liu¹⁵¹, H. Liu⁸⁹, J. Liu⁸⁵, J.B. Liu^{33b}, K. Liu⁸⁵, L. Liu¹⁶⁵, M. Liu⁴⁵, M. Liu^{33b},
Y. Liu^{33b}, M. Livan^{121a,121b}, A. Lleres⁵⁵, J. Llorente Merino⁸², S.L. Lloyd⁷⁶, F. Lo Sterzo¹⁵¹,
E. Lobodzinska⁴², P. Loch⁷, W.S. Lockman¹³⁷, F.K. Loebinger⁸⁴, A.E. Loevschall-Jensen³⁶,
K.M. Loew²³, A. Loginov¹⁷⁶, T. Lohse¹⁶, K. Lohwasser⁴², M. Lokajicek¹²⁷, B.A. Long²², J.D. Long¹⁶⁵,
R.E. Long⁷², K.A. Looper¹¹¹, L. Lopes^{126a}, D. Lopez Mateos⁵⁷, B. Lopez Paredes¹³⁹, I. Lopez Paz¹²,
J. Lorenz¹⁰⁰, N. Lorenzo Martinez⁶¹, M. Losada¹⁶², P.J. Lösel¹⁰⁰, X. Lou^{33a}, A. Lounis¹¹⁷, J. Love⁶,
P.A. Love⁷², N. Lu⁸⁹, H.J. Lubatti¹³⁸, C. Luci^{132a,132b}, A. Lucotte⁵⁵, C. Luedtke⁴⁸, F. Luehring⁶¹,
W. Lukas⁶², L. Luminari^{132a}, O. Lundberg^{146a,146b}, B. Lund-Jensen¹⁴⁷, D. Lynn²⁵, R. Lysak¹²⁷,
E. Lytken⁸¹, H. Ma²⁵, L.L. Ma^{33d}, G. Maccarrone⁴⁷, A. Macchiolo¹⁰¹, C.M. Macdonald¹³⁹, B. Maček⁷⁵,
J. Machado Miguens^{122,126b}, D. Macina³⁰, D. Madaffari⁸⁵, R. Madar³⁴, H.J. Maddocks⁷², W.F. Mader⁴⁴,
A. Madsen¹⁶⁶, J. Maeda⁶⁷, S. Maeland¹⁴, T. Maeno²⁵, A. Maevskiy⁹⁹, E. Magradze⁵⁴, K. Mahboubi⁴⁸,
J. Mahlstedt¹⁰⁷, C. Maiani¹³⁶, C. Maidantchik^{24a}, A.A. Maier¹⁰¹, T. Maier¹⁰⁰, A. Maio^{126a,126b,126d},
S. Majewski¹¹⁶, Y. Makida⁶⁶, N. Makovec¹¹⁷, B. Malaescu⁸⁰, Pa. Malecki³⁹, V.P. Maleev¹²³, F. Malek⁵⁵,
U. Mallik⁶³, D. Malon⁶, C. Malone¹⁴³, S. Maltezos¹⁰, V.M. Malyshev¹⁰⁹, S. Malyukov³⁰, J. Mamuzic⁴²,
G. Mancini⁴⁷, B. Mandelli³⁰, L. Mandelli^{91a}, I. Mandić⁷⁵, R. Mandrysch⁶³, J. Maneira^{126a,126b},
A. Manfredini¹⁰¹, L. Manhaes de Andrade Filho^{24b}, J. Manjarres Ramos^{159b}, A. Mann¹⁰⁰,
A. Manousakis-Katsikakis⁹, B. Mansoulie¹³⁶, R. Mantifel⁸⁷, M. Mantoani⁵⁴, L. Mapelli³⁰, L. March^{145c},
G. Marchiori⁸⁰, M. Marcisovsky¹²⁷, C.P. Marino¹⁶⁹, M. Marjanovic¹³, D.E. Marley⁸⁹, F. Marroquim^{24a},
S.P. Marsden⁸⁴, Z. Marshall¹⁵, L.F. Marti¹⁷, S. Marti-Garcia¹⁶⁷, B. Martin⁹⁰, T.A. Martin¹⁷⁰,
V.J. Martin⁴⁶, B. Martin dit Latour¹⁴, M. Martinez^{12,o}, S. Martin-Haugh¹³¹, V.S. Martoiu^{26b},
A.C. Martyniuk⁷⁸, M. Marx¹³⁸, F. Marzano^{132a}, A. Marzin³⁰, L. Masetti⁸³, T. Mashimo¹⁵⁵,
R. Mashinistov⁹⁶, J. Masik⁸⁴, A.L. Maslennikov^{109,c}, I. Massa^{20a,20b}, L. Massa^{20a,20b}, P. Mastrandrea¹⁴⁸,
A. Mastroberardino^{37a,37b}, T. Masubuchi¹⁵⁵, P. Mättig¹⁷⁵, J. Mattmann⁸³, J. Maurer^{26b}, S.J. Maxfield⁷⁴,
D.A. Maximov^{109,c}, R. Mazini¹⁵¹, S.M. Mazza^{91a,91b}, L. Mazzaferro^{133a,133b}, G. Mc Goldrick¹⁵⁸,
S.P. Mc Kee⁸⁹, A. McCarn⁸⁹, R.L. McCarthy¹⁴⁸, T.G. McCarthy²⁹, N.A. McCubbin¹³¹,
K.W. McFarlane^{56,*}, J.A. Mcfayden⁷⁸, G. Mchedlidze⁵⁴, S.J. McMahon¹³¹, R.A. McPherson^{169,k},
M. Medinnis⁴², S. Meehan^{145a}, S. Mehlhase¹⁰⁰, A. Mehta⁷⁴, K. Meier^{58a}, C. Meineck¹⁰⁰, B. Meirose⁴¹,
B.R. Mellado Garcia^{145c}, F. Meloni¹⁷, A. Mengarelli^{20a,20b}, S. Menke¹⁰¹, E. Meoni¹⁶¹, K.M. Mercurio⁵⁷,
S. Mergelmeyer²¹, P. Mermod⁴⁹, L. Merola^{104a,104b}, C. Meroni^{91a}, F.S. Merritt³¹, A. Messina^{132a,132b},
J. Metcalfe²⁵, A.S. Mete¹⁶³, C. Meyer⁸³, C. Meyer¹²², J-P. Meyer¹³⁶, J. Meyer¹⁰⁷,
H. Meyer Zu Theenhausen^{58a}, R.P. Middleton¹³¹, S. Miglioranza^{164a,164c}, L. Mijović²¹, G. Mikenberg¹⁷²,
M. Mikestikova¹²⁷, M. Mikuž⁷⁵, M. Milesi⁸⁸, A. Milic³⁰, D.W. Miller³¹, C. Mills⁴⁶, A. Milov¹⁷²,
D.A. Milstead^{146a,146b}, A.A. Minaenko¹³⁰, Y. Minami¹⁵⁵, I.A. Minashvili⁶⁵, A.I. Mincer¹¹⁰,
B. Mindur^{38a}, M. Mineev⁶⁵, Y. Ming¹⁷³, L.M. Mir¹², K.P. Mistry¹²², T. Mitani¹⁷¹, J. Mitrevski¹⁰⁰,
V.A. Mitsou¹⁶⁷, A. Miucci⁴⁹, P.S. Miyagawa¹³⁹, J.U. Mjörnmark⁸¹, T. Moa^{146a,146b}, K. Mochizuki⁸⁵,
S. Mohapatra³⁵, W. Mohr⁴⁸, S. Molander^{146a,146b}, R. Moles-Valls²¹, R. Monden⁶⁸, K. Mönig⁴²,
C. Monini⁵⁵, J. Monk³⁶, E. Monnier⁸⁵, J. Montejo Berlingen¹², F. Monticelli⁷¹, S. Monzani^{132a,132b},
R.W. Moore³, N. Morange¹¹⁷, D. Moreno¹⁶², M. Moreno Llácer⁵⁴, P. Morettini^{50a}, D. Mori¹⁴²,
T. Mori¹⁵⁵, M. Morii⁵⁷, M. Morinaga¹⁵⁵, V. Morisbak¹¹⁹, S. Moritz⁸³, A.K. Morley¹⁵⁰, G. Mornacchi³⁰,
J.D. Morris⁷⁶, S.S. Mortensen³⁶, A. Morton⁵³, L. Morvaj¹⁰³, M. Mosidze^{51b}, J. Moss¹⁴³,

K. Motohashi¹⁵⁷, R. Mount¹⁴³, E. Mountricha²⁵, S.V. Mouraviev^{96,*}, E.J.W. Moyse⁸⁶, S. Muanza⁸⁵, R.D. Mudd¹⁸, F. Mueller¹⁰¹, J. Mueller¹²⁵, R.S.P. Mueller¹⁰⁰, T. Mueller²⁸, D. Muenstermann⁴⁹, P. Mullen⁵³, G.A. Mullier¹⁷, J.A. Murillo Quijada¹⁸, W.J. Murray^{170,131}, H. Musheghyan⁵⁴, E. Musto¹⁵², A.G. Myagkov^{130,ac}, M. Myska¹²⁸, B.P. Nachman¹⁴³, O. Nackenhorst⁵⁴, J. Nadal⁵⁴, K. Nagai¹²⁰, R. Nagai¹⁵⁷, Y. Nagai⁸⁵, K. Nagano⁶⁶, A. Nagarkar¹¹¹, Y. Nagasaka⁵⁹, K. Nagata¹⁶⁰, M. Nagel¹⁰¹, E. Nagy⁸⁵, A.M. Nairz³⁰, Y. Nakahama³⁰, K. Nakamura⁶⁶, T. Nakamura¹⁵⁵, I. Nakano¹¹², H. Namasivayam⁴¹, R.F. Naranjo Garcia⁴², R. Narayan³¹, D.I. Narrias Villar^{58a}, T. Naumann⁴², G. Navarro¹⁶², R. Nayyar⁷, H.A. Neal⁸⁹, P.Yu. Nechaeva⁹⁶, T.J. Neep⁸⁴, P.D. Nef¹⁴³, A. Negri^{121a,121b}, M. Negrini^{20a}, S. Nektarijevic¹⁰⁶, C. Nellist¹¹⁷, A. Nelson¹⁶³, S. Nemecek¹²⁷, P. Nemethy¹¹⁰, A.A. Nepomuceno^{24a}, M. Nessi^{30,ad}, M.S. Neubauer¹⁶⁵, M. Neumann¹⁷⁵, R.M. Neves¹¹⁰, P. Nevski²⁵, P.R. Newman¹⁸, D.H. Nguyen⁶, R.B. Nickerson¹²⁰, R. Nicolaidou¹³⁶, B. Nicquevert³⁰, J. Nielsen¹³⁷, N. Nikiforou³⁵, A. Nikiforov¹⁶, V. Nikolaenko^{130,ac}, I. Nikolic-Audit⁸⁰, K. Nikolopoulos¹⁸, J.K. Nilsen¹¹⁹, P. Nilsson²⁵, Y. Ninomiya¹⁵⁵, A. Nisati^{132a}, R. Nisius¹⁰¹, T. Nobe¹⁵⁵, M. Nomachi¹¹⁸, I. Nomidis²⁹, T. Nooney⁷⁶, S. Norberg¹¹³, M. Nordberg³⁰, O. Novgorodova⁴⁴, S. Nowak¹⁰¹, M. Nozaki⁶⁶, L. Nozka¹¹⁵, K. Ntekas¹⁰, G. Nunes Hanninger⁸⁸, T. Nunnemann¹⁰⁰, E. Nurse⁷⁸, F. Nuti⁸⁸, B.J. O'Brien⁴⁶, F. O'grady⁷, D.C. O'Neil¹⁴², V. O'Shea⁵³, F.G. Oakham^{29,d}, H. Oberlack¹⁰¹, T. Obermann²¹, J. Ocariz⁸⁰, A. Ochi⁶⁷, I. Ochoa⁷⁸, J.P. Ochoa-Ricoux^{32a}, S. Oda⁷⁰, S. Odaka⁶⁶, H. Ogren⁶¹, A. Oh⁸⁴, S.H. Oh⁴⁵, C.C. Ohm¹⁵, H. Ohman¹⁶⁶, H. Oide³⁰, W. Okamura¹¹⁸, H. Okawa¹⁶⁰, Y. Okumura³¹, T. Okuyama⁶⁶, A. Olariu^{26b}, S.A. Olivares Pino⁴⁶, D. Oliveira Damazio²⁵, E. Oliver Garcia¹⁶⁷, A. Olszewski³⁹, J. Olszowska³⁹, A. Onofre^{126a,126e}, K. Onogi¹⁰³, P.U.E. Onyisi^{31,s}, C.J. Oram^{159a}, M.J. Oreglia³¹, Y. Oren¹⁵³, D. Orestano^{134a,134b}, N. Orlando¹⁵⁴, C. Oropeza Barrera⁵³, R.S. Orr¹⁵⁸, B. Osculati^{50a,50b}, R. Ospanov⁸⁴, G. Otero y Garzon²⁷, H. Otono⁷⁰, M. Ouchrif^{135d}, F. Ould-Saada¹¹⁹, A. Ouraou¹³⁶, K.P. Oussoren¹⁰⁷, Q. Ouyang^{33a}, A. Ovcharova¹⁵, M. Owen⁵³, R.E. Owen¹⁸, V.E. Ozcan^{19a}, N. Ozturk⁸, K. Pachal¹⁴², A. Pacheco Pages¹², C. Padilla Aranda¹², M. Pagáčová⁴⁸, S. Pagan Griso¹⁵, E. Paganis¹³⁹, F. Paige²⁵, P. Pais⁸⁶, K. Pajchel¹¹⁹, G. Palacino^{159b}, S. Palestini³⁰, M. Palka^{38b}, D. Pallin³⁴, A. Palma^{126a,126b}, Y.B. Pan¹⁷³, E.St. Panagiotopoulou¹⁰, C.E. Pandini⁸⁰, J.G. Panduro Vazquez⁷⁷, P. Pani^{146a,146b}, S. Panitkin²⁵, D. Pantea^{26b}, L. Paolozzi⁴⁹, Th.D. Papadopoulou¹⁰, K. Papageorgiou¹⁵⁴, A. Paramonov⁶, D. Paredes Hernandez¹⁵⁴, M.A. Parker²⁸, K.A. Parker¹³⁹, F. Parodi^{50a,50b}, J.A. Parsons³⁵, U. Parzefall¹⁴⁸, E. Pasqualucci^{132a}, S. Passaggio^{50a}, F. Pastore^{134a,134b,*}, Fr. Pastore⁷⁷, G. Pásztor²⁹, S. Pataria¹⁷⁵, N.D. Patel¹⁵⁰, J.R. Pater⁸⁴, T. Pauly³⁰, J. Pearce¹⁶⁹, B. Pearson¹¹³, L.E. Pedersen³⁶, M. Pedersen¹¹⁹, S. Pedraza Lopez¹⁶⁷, R. Pedro^{126a,126b}, S.V. Peleganchuk^{109,c}, D. Pelikan¹⁶⁶, O. Penc¹²⁷, C. Peng^{33a}, H. Peng^{33b}, B. Penning³¹, J. Penwell⁶¹, D.V. Perepelitsa²⁵, E. Perez Codina^{159a}, M.T. Pérez García-Están¹⁶⁷, L. Perini^{91a,91b}, H. Pernegger³⁰, S. Perrella^{104a,104b}, R. Peschke⁴², V.D. Peshekhonov⁶⁵, K. Peters³⁰, R.F.Y. Peters⁸⁴, B.A. Petersen³⁰, T.C. Petersen³⁶, E. Petit⁴², A. Petridis¹, C. Petridou¹⁵⁴, P. Petroff¹¹⁷, E. Petrolu^{132a}, F. Petrucci^{134a,134b}, N.E. Pettersson¹⁵⁷, R. Pezoa^{32b}, P.W. Phillips¹³¹, G. Piacquadio¹⁴³, E. Pianori¹⁷⁰, A. Picazio⁴⁹, E. Piccaro⁷⁶, M. Piccinini^{20a,20b}, M.A. Pickering¹²⁰, R. Piegaia²⁷, D.T. Pignotti¹¹¹, J.E. Pilcher³¹, A.D. Pilkington⁸⁴, A.W.J. Pin⁸⁴, J. Pina^{126a,126b,126d}, M. Pinamonti^{164a,164c,ae}, J.L. Pinfold³, A. Pingel³⁶, S. Pires⁸⁰, H. Pirumov⁴², M. Pitt¹⁷², C. Pizio^{91a,91b}, L. Plazak^{144a}, M.-A. Pleier²⁵, V. Pleskot¹²⁹, E. Plotnikova⁶⁵, P. Plucinski^{146a,146b}, D. Pluth⁶⁴, R. Poettgen^{146a,146b}, L. Poggioli¹¹⁷, D. Pohl²¹, G. Polesello^{121a}, A. Poley⁴², A. Policicchio^{37a,37b}, R. Polifka¹⁵⁸, A. Polini^{20a}, C.S. Pollard⁵³, V. Polychronakos²⁵, K. Pommès³⁰, L. Pontecorvo^{132a}, B.G. Pope⁹⁰, G.A. Popeneciu^{26c}, D.S. Popovic¹³, A. Poppleton³⁰, S. Pospisil¹²⁸, K. Potamianos¹⁵, I.N. Potrap⁶⁵, C.J. Potter¹⁴⁹, C.T. Potter¹¹⁶, G. Poulard³⁰, J. Poveda³⁰, V. Pozdnyakov⁶⁵, P. Pralavorio⁸⁵, A. Pranko¹⁵, S. Prasad³⁰, S. Prell⁶⁴, D. Price⁸⁴, L.E. Price⁶, M. Primavera^{73a}, S. Prince⁸⁷, M. Proissl⁴⁶, K. Prokofiev^{60c}, F. Prokoshin^{32b}, E. Protopapadaki¹³⁶, S. Protopopescu²⁵, J. Proudfoot⁶, M. Przybycien^{38a}, E. Ptacek¹¹⁶, D. Puddu^{134a,134b}, E. Pueschel⁸⁶, D. Puldon¹⁴⁸, M. Purohit^{25,af}, P. Puzo¹¹⁷, J. Qian⁸⁹, G. Qin⁵³, Y. Qin⁸⁴,

A. Quadt⁵⁴, D.R. Quarrie¹⁵, W.B. Quayle^{164a,164b}, M. Queitsch-Maitland⁸⁴, D. Quilty⁵³, S. Raddum¹¹⁹,
 V. Radeka²⁵, V. Radescu⁴², S.K. Radhakrishnan¹⁴⁸, P. Radloff¹¹⁶, P. Rados⁸⁸, F. Ragusa^{91a,91b},
 G. Rahal¹⁷⁸, S. Rajagopalan²⁵, M. Rammensee³⁰, C. Rangel-Smith¹⁶⁶, F. Rauscher¹⁰⁰, S. Rave⁸³,
 T. Ravenscroft⁵³, M. Raymond³⁰, A.L. Read¹¹⁹, N.P. Readioff⁷⁴, D.M. Rebutti^{121a,121b},
 A. Redelbach¹⁷⁴, G. Redlinger²⁵, R. Reece¹³⁷, K. Reeves⁴¹, L. Rehnisch¹⁶, J. Reichert¹²², H. Reisin²⁷,
 C. Rembser³⁰, H. Ren^{33a}, A. Renaud¹¹⁷, M. Rescigno^{132a}, S. Resconi^{91a}, O.L. Rezanova^{109,c},
 P. Reznicek¹²⁹, R. Rezvani⁹⁵, R. Richter¹⁰¹, S. Richter⁷⁸, E. Richter-Was^{38b}, O. Ricken²¹, M. Ridet⁸⁰,
 P. Rieck¹⁶, C.J. Riegel¹⁷⁵, J. Rieger⁵⁴, O. Rifki¹¹³, M. Rijssenbeek¹⁴⁸, A. Rimoldi^{121a,121b}, L. Rinaldi^{20a},
 B. Ristić⁴⁹, E. Ritsch³⁰, I. Riu¹², F. Rizatdinova¹¹⁴, E. Rizvi⁷⁶, S.H. Robertson^{87,k},
 A. Robichaud-Veronneau⁸⁷, D. Robinson²⁸, J.E.M. Robinson⁴², A. Robson⁵³, C. Roda^{124a,124b}, S. Roe³⁰,
 O. Røhne¹¹⁹, S. Rolli¹⁶¹, A. Romaniouk⁹⁸, M. Romano^{20a,20b}, S.M. Romano Saez³⁴,
 E. Romero Adam¹⁶⁷, N. Rompotis¹³⁸, M. Ronzani⁴⁸, L. Roos⁸⁰, E. Ros¹⁶⁷, S. Rosati^{132a}, K. Rosbach⁴⁸,
 P. Rose¹³⁷, P.L. Rosendahl¹⁴, O. Rosenthal¹⁴¹, V. Rossetti^{146a,146b}, E. Rossi^{104a,104b}, L.P. Rossi^{50a},
 J.H.N. Rosten²⁸, R. Rosten¹³⁸, M. Rotaru^{26b}, I. Roth¹⁷², J. Rothberg¹³⁸, D. Rousseau¹¹⁷, C.R. Royon¹³⁶,
 A. Rozanov⁸⁵, Y. Rozen¹⁵², X. Ruan^{145c}, F. Rubbo¹⁴³, I. Rubinskiy⁴², V.I. Rud⁹⁹, C. Rudolph⁴⁴,
 M.S. Rudolph¹⁵⁸, F. Rühr⁴⁸, A. Ruiz-Martinez³⁰, Z. Rurikova⁴⁸, N.A. Rusakovich⁶⁵, A. Ruschke¹⁰⁰,
 H.L. Russell¹³⁸, J.P. Rutherford⁷, N. Ruthmann⁴⁸, Y.F. Ryabov¹²³, M. Rybar¹⁶⁵, G. Rybkin¹¹⁷,
 N.C. Ryder¹²⁰, A.F. Saavedra¹⁵⁰, G. Sabato¹⁰⁷, S. Sacerdoti²⁷, A. Saddique³, H.F.-W. Sadrozinski¹³⁷,
 R. Sadykov⁶⁵, F. Safai Tehrani^{132a}, P. Saha¹⁰⁸, M. Sahinsoy^{58a}, M. Saimpert¹³⁶, T. Saito¹⁵⁵,
 H. Sakamoto¹⁵⁵, Y. Sakurai¹⁷¹, G. Salamanna^{134a,134b}, A. Salamon^{133a}, J.E. Salazar Loyola^{32b},
 M. Saleem¹¹³, D. Salek¹⁰⁷, P.H. Sales De Bruin¹³⁸, D. Salihagic¹⁰¹, A. Salnikov¹⁴³, J. Salt¹⁶⁷,
 D. Salvatore^{37a,37b}, F. Salvatore¹⁴⁹, A. Salvucci^{60a}, A. Salzburger³⁰, D. Sammel⁴⁸, D. Sampsonidis¹⁵⁴,
 A. Sanchez^{104a,104b}, J. Sánchez¹⁶⁷, V. Sanchez Martinez¹⁶⁷, H. Sandaker¹¹⁹, R.L. Sandbach⁷⁶,
 H.G. Sander⁸³, M.P. Sanders¹⁰⁰, M. Sandhoff¹⁷⁵, C. Sandoval¹⁶², R. Sandstroem¹⁰¹, D.P.C. Sankey¹³¹,
 M. Sannino^{50a,50b}, A. Sansoni⁴⁷, C. Santoni³⁴, R. Santonico^{133a,133b}, H. Santos^{126a},
 I. Santoyo Castillo¹⁴⁹, K. Sapp¹²⁵, A. Saponov⁶⁵, J.G. Saraiva^{126a,126d}, B. Sarrazin²¹, O. Sasaki⁶⁶,
 Y. Sasaki¹⁵⁵, K. Sato¹⁶⁰, G. Sauvage^{5,*}, E. Sauvan⁵, G. Savage⁷⁷, P. Savard^{158,d}, C. Sawyer¹³¹,
 L. Sawyer^{79,n}, J. Saxon³¹, C. Sbarra^{20a}, A. Sbrizzi^{20a,20b}, T. Scanlon⁷⁸, D.A. Scannicchio¹⁶³,
 M. Scarcella¹⁵⁰, V. Scarfone^{37a,37b}, J. Schaarschmidt¹⁷², P. Schacht¹⁰¹, D. Schaefer³⁰, R. Schaefer⁴²,
 J. Schaeffer⁸³, S. Schaepe²¹, S. Schaezel^{58b}, U. Schäfer⁸³, A.C. Schaffer¹¹⁷, D. Schaile¹⁰⁰,
 R.D. Schamberger¹⁴⁸, V. Scharf^{58a}, V.A. Schegelsky¹²³, D. Scheirich¹²⁹, M. Schernau¹⁶³,
 C. Schiavi^{50a,50b}, C. Schillo⁴⁸, M. Schioppa^{37a,37b}, S. Schlenker³⁰, K. Schmieden³⁰, C. Schmitt⁸³,
 S. Schmitt^{58b}, S. Schmitt⁴², B. Schneider^{159a}, Y.J. Schnellbach⁷⁴, U. Schnoor⁴⁴, L. Schoeffel¹³⁶,
 A. Schoening^{58b}, B.D. Schoenrock⁹⁰, E. Schopf²¹, A.L.S. Schorlemmer⁵⁴, M. Schott⁸³, D. Schouten^{159a},
 J. Schovancova⁸, S. Schramm⁴⁹, M. Schreyer¹⁷⁴, C. Schroeder⁸³, N. Schuh⁸³, M.J. Schultens²¹,
 H.-C. Schultz-Coulon^{58a}, H. Schulz¹⁶, M. Schumacher⁴⁸, B.A. Schumm¹³⁷, Ph. Schune¹³⁶,
 C. Schwanenberger⁸⁴, A. Schwartzman¹⁴³, T.A. Schwarz⁸⁹, Ph. Schwegler¹⁰¹, H. Schweiger⁸⁴,
 Ph. Schwemling¹³⁶, R. Schwienhorst⁹⁰, J. Schwindling¹³⁶, T. Schwindt²¹, F.G. Sciacca¹⁷, E. Scifo¹¹⁷,
 G. Sciolla²³, F. Scuri^{124a,124b}, F. Scutti²¹, J. Searcy⁸⁹, G. Sedov⁴², E. Sedykh¹²³, P. Seema²¹,
 S.C. Seidel¹⁰⁵, A. Seiden¹³⁷, F. Seifert¹²⁸, J.M. Seixas^{24a}, G. Sekhniaidze^{104a}, K. Sekhon⁸⁹,
 S.J. Sekula⁴⁰, D.M. Seliverstov^{123,*}, N. Semprini-Cesari^{20a,20b}, C. Serfon³⁰, L. Serin¹¹⁷,
 L. Serkin^{164a,164b}, T. Serre⁸⁵, M. Sessa^{134a,134b}, R. Seuster^{159a}, H. Severini¹¹³, T. Sfiligoj⁷⁵, F. Sforza³⁰,
 A. Sfyrila³⁰, E. Shabalina⁵⁴, M. Shamim¹¹⁶, L.Y. Shan^{33a}, R. Shang¹⁶⁵, J.T. Shank²², M. Shapiro¹⁵,
 P.B. Shatalov⁹⁷, K. Shaw^{164a,164b}, S.M. Shaw⁸⁴, A. Shcherbakova^{146a,146b}, C.Y. Shehu¹⁴⁹, P. Sherwood⁷⁸,
 L. Shi^{151,ag}, S. Shimizu⁶⁷, C.O. Shimmin¹⁶³, M. Shimojima¹⁰², M. Shiyakova⁶⁵, A. Shmeleva⁹⁶,
 D. Shoaleh Saadi⁹⁵, M.J. Shochet³¹, S. Shojai^{91a,91b}, S. Shrestha¹¹¹, E. Shulga⁹⁸, M.A. Shupe⁷,
 S. Shushkevich⁴², P. Sicho¹²⁷, P.E. Sidebo¹⁴⁷, O. Sidiropoulou¹⁷⁴, D. Sidorov¹¹⁴, A. Sidoti^{20a,20b},

F. Siegert⁴⁴, Dj. Sijacki¹³, J. Silva^{126a,126d}, Y. Silver¹⁵³, S.B. Silverstein^{146a}, V. Simak¹²⁸, O. Simard⁵, Lj. Simic¹³, S. Simion¹¹⁷, E. Simioni⁸³, B. Simmons⁷⁸, D. Simon³⁴, P. Sinervo¹⁵⁸, N.B. Sinev¹¹⁶, M. Sioli^{20a,20b}, G. Siragusa¹⁷⁴, A.N. Sisakyan^{65,*}, S.Yu. Sivoklov⁹⁹, J. Sjölin^{146a,146b}, T.B. Sjursen¹⁴, M.B. Skinner⁷², H.P. Skottowe⁵⁷, P. Skubic¹¹³, M. Slater¹⁸, T. Slavicek¹²⁸, M. Slawinska¹⁰⁷, K. Sliwa¹⁶¹, V. Smakhtin¹⁷², B.H. Smart⁴⁶, L. Smestad¹⁴, S.Yu. Smirnov⁹⁸, Y. Smirnov⁹⁸, L.N. Smirnova^{99,ah}, O. Smirnova⁸¹, M.N.K. Smith³⁵, R.W. Smith³⁵, M. Smizanska⁷², K. Smolek¹²⁸, A.A. Snesarev⁹⁶, G. Snidero⁷⁶, S. Snyder²⁵, R. Sobie^{169,k}, F. Socher⁴⁴, A. Soffer¹⁵³, D.A. Soh^{151,ag}, G. Sokhrannyi⁷⁵, C.A. Solans³⁰, M. Solar¹²⁸, J. Solc¹²⁸, E.Yu. Soldatov⁹⁸, U. Soldevila¹⁶⁷, A.A. Solodkov¹³⁰, A. Soloshenko⁶⁵, O.V. Solovyanov¹³⁰, V. Solovyev¹²³, P. Sommer⁴⁸, H.Y. Song^{33b,y}, N. Soni¹, A. Sood¹⁵, A. Sopczak¹²⁸, B. Sopko¹²⁸, V. Sopko¹²⁸, V. Sorin¹², D. Sosa^{58b}, M. Sosebee⁸, C.L. Sotiropoulou^{124a,124b}, R. Soualah^{164a,164c}, A.M. Soukharev^{109,c}, D. South⁴², B.C. Sowden⁷⁷, S. Spagnolo^{73a,73b}, M. Spalla^{124a,124b}, M. Spangenberg¹⁷⁰, F. Spanò⁷⁷, W.R. Spearman⁵⁷, D. Sperlich¹⁶, F. Spettel¹⁰¹, R. Spighi^{20a}, G. Spigo³⁰, L.A. Spiller⁸⁸, M. Spousta¹²⁹, T. Spreitzer¹⁵⁸, R.D. St. Denis^{53,*}, A. Stabile^{91a}, S. Staerz⁴⁴, J. Stahlman¹²², R. Stamen^{58a}, S. Stamm¹⁶, E. Stanecka³⁹, C. Stancu^{134a}, M. Stancu-Bellu⁴², M.M. Stanitzki⁴², S. Stapnes¹¹⁹, E.A. Starchenko¹³⁰, J. Stark⁵⁵, P. Staroba¹²⁷, P. Starovoitov^{58a}, R. Staszewski³⁹, P. Steinberg²⁵, B. Stelzer¹⁴², H.J. Stelzer³⁰, O. Stelzer-Chilton^{159a}, H. Stenzel⁵², G.A. Stewart⁵³, J.A. Stillings²¹, M.C. Stockton⁸⁷, M. Stoebe⁸⁷, G. Stoicea^{26b}, P. Stolte⁵⁴, S. Stonjek¹⁰¹, A.R. Stradling⁸, A. Straessner⁴⁴, M.E. Stramaglia¹⁷, J. Strandberg¹⁴⁷, S. Strandberg^{146a,146b}, A. Strandlie¹¹⁹, E. Strauss¹⁴³, M. Strauss¹¹³, P. Strizenec^{144b}, R. Ströhmer¹⁷⁴, D.M. Strom¹¹⁶, R. Stroynowski⁴⁰, A. Strubig¹⁰⁶, S.A. Stucci¹⁷, B. Stugu¹⁴, N.A. Styles⁴², D. Su¹⁴³, J. Su¹²⁵, R. Subramaniam⁷⁹, A. Succurro¹², S. Suchek^{58a}, Y. Sugaya¹¹⁸, M. Suk¹²⁸, V.V. Sulin⁹⁶, S. Sultansoy^{4c}, T. Sumida⁶⁸, S. Sun⁵⁷, X. Sun^{33a}, J.E. Sundermann⁴⁸, K. Suruliz¹⁴⁹, G. Susinno^{37a,37b}, M.R. Sutton¹⁴⁹, S. Suzuki⁶⁶, M. Svatos¹²⁷, M. Swiatlowski¹⁴³, I. Sykora^{144a}, T. Sykora¹²⁹, D. Ta⁴⁸, C. Taccini^{134a,134b}, K. Tackmann⁴², J. Taenzer¹⁵⁸, A. Taffard¹⁶³, R. Tafirout^{159a}, N. Taiblum¹⁵³, H. Takai²⁵, R. Takashima⁶⁹, H. Takeda⁶⁷, T. Takeshita¹⁴⁰, Y. Takubo⁶⁶, M. Talby⁸⁵, A.A. Talyshv^{109,c}, J.Y.C. Tam¹⁷⁴, K.G. Tan⁸⁸, J. Tanaka¹⁵⁵, R. Tanaka¹¹⁷, S. Tanaka⁶⁶, B.B. Tannenwald¹¹¹, N. Tannoury²¹, S. Tapprogge⁸³, S. Tarem¹⁵², F. Tarrade²⁹, G.F. Tartarelli^{91a}, P. Tas¹²⁹, M. Tasevsky¹²⁷, T. Tashiro⁶⁸, E. Tassi^{37a,37b}, A. Tavares Delgado^{126a,126b}, Y. Tayalati^{135d}, F.E. Taylor⁹⁴, G.N. Taylor⁸⁸, P.T.E. Taylor⁸⁸, W. Taylor^{159b}, F.A. Teischinger³⁰, M. Teixeira Dias Castanheira⁷⁶, P. Teixeira-Dias⁷⁷, K.K. Temming⁴⁸, D. Temple¹⁴², H. Ten Kate³⁰, P.K. Teng¹⁵¹, J.J. Teoh¹¹⁸, F. Tepel¹⁷⁵, S. Terada⁶⁶, K. Terashi¹⁵⁵, J. Terron⁸², S. Terzo¹⁰¹, M. Testa⁴⁷, R.J. Teuscher^{158,k}, T. Theveneaux-Pelzer³⁴, J.P. Thomas¹⁸, J. Thomas-Wilsker⁷⁷, E.N. Thompson³⁵, P.D. Thompson¹⁸, R.J. Thompson⁸⁴, A.S. Thompson⁵³, L.A. Thomsen¹⁷⁶, E. Thomson¹²², M. Thomson²⁸, R.P. Thun^{89,*}, M.J. Tibbetts¹⁵, R.E. Ticse Torres⁸⁵, V.O. Tikhomirov^{96,ai}, Yu.A. Tikhonov^{109,c}, S. Timoshenko⁹⁸, E. Tiouchichine⁸⁵, P. Tipton¹⁷⁶, S. Tisserant⁸⁵, K. Todome¹⁵⁷, T. Todorov^{5,*}, S. Todorova-Nova¹²⁹, J. Tojo⁷⁰, S. Tokár^{144a}, K. Tokushuku⁶⁶, K. Tollefson⁹⁰, E. Tolley⁵⁷, L. Tomlinson⁸⁴, M. Tomoto¹⁰³, L. Tompkins^{143,aj}, K. Toms¹⁰⁵, E. Torrence¹¹⁶, H. Torres¹⁴², E. Torró Pastor¹³⁸, J. Toth^{85,ak}, F. Touchard⁸⁵, D.R. Tovey¹³⁹, T. Trefzger¹⁷⁴, L. Tremblet³⁰, A. Tricoli³⁰, I.M. Trigger^{159a}, S. Trincas-Duvoid⁸⁰, M.F. Tripiana¹², W. Trischuk¹⁵⁸, B. Trocme⁵⁵, C. Troncon^{91a}, M. Trottier-McDonald¹⁵, M. Trovatelli¹⁶⁹, L. Truong^{164a,164c}, M. Trzebinski³⁹, A. Trzupek³⁹, C. Tsarouchas³⁰, J.C-L. Tseng¹²⁰, P.V. Tsiarashka⁹², D. Tsionou¹⁵⁴, G. Tsipolitis¹⁰, N. Tsirintanis⁹, S. Tsiskaridze¹², V. Tsiskaridze⁴⁸, E.G. Tskhadadze^{51a}, I.I. Tsukerman⁹⁷, V. Tsulaia¹⁵, S. Tsuno⁶⁶, D. Tsybychev¹⁴⁸, A. Tudorache^{26b}, V. Tudorache^{26b}, A.N. Tuna⁵⁷, S.A. Tupputi^{20a,20b}, S. Turchikhin^{99,ah}, D. Turecek¹²⁸, R. Turra^{91a,91b}, A.J. Turvey⁴⁰, P.M. Tuts³⁵, A. Tykhonov⁴⁹, M. Tylmad^{146a,146b}, M. Tyndel¹³¹, I. Ueda¹⁵⁵, R. Ueno²⁹, M. Ughetto^{146a,146b}, M. Ugland¹⁴, F. Ukegawa¹⁶⁰, G. Unal³⁰, A. Undrus²⁵, G. Unel¹⁶³, F.C. Ungaro⁴⁸, Y. Unno⁶⁶, C. Unverdorben¹⁰⁰, J. Urban^{144b}, P. Urquijo⁸⁸, P. Urrejola⁸³, G. Usai⁸, A. Usanova⁶², L. Vacavant⁸⁵, V. Vacek¹²⁸, B. Vachon⁸⁷, C. Valderanis⁸³, N. Valencic¹⁰⁷, S. Valentini^{20a,20b}, S. Valentini^{20a,20b}

A. Valero¹⁶⁷, L. Valery¹², S. Valkar¹²⁹, E. Valladolid Gallego¹⁶⁷, S. Vallecorsa⁴⁹, J.A. Valls Ferrer¹⁶⁷, W. Van Den Wollenberg¹⁰⁷, P.C. Van Der Deijl¹⁰⁷, R. van der Geer¹⁰⁷, H. van der Graaf¹⁰⁷, N. van Eldik¹⁵², P. van Gemmeren⁶, J. Van Nieuwkoop¹⁴², I. van Vulpen¹⁰⁷, M.C. van Woerden³⁰, M. Vanadia^{132a,132b}, W. Vandelli³⁰, R. Vanguri¹²², A. Vaniachine⁶, F. Vannucci⁸⁰, G. Vardanyan¹⁷⁷, R. Vari^{132a}, E.W. Varnes⁷, T. Varol⁴⁰, D. Varouchas⁸⁰, A. Vartapetian⁸, K.E. Varvell¹⁵⁰, F. Vazeille³⁴, T. Vazquez Schroeder⁸⁷, J. Veatch⁷, L.M. Veloce¹⁵⁸, F. Veloso^{126a,126c}, T. Velz²¹, S. Veneziano^{132a}, A. Ventura^{73a,73b}, D. Ventura⁸⁶, M. Venturi¹⁶⁹, N. Venturi¹⁵⁸, A. Venturini²³, V. Vercesi^{121a}, M. Verducci^{132a,132b}, W. Verkerke¹⁰⁷, J.C. Vermeulen¹⁰⁷, A. Vest⁴⁴, M.C. Vetterli^{142,d}, O. Viazlo⁸¹, I. Vichou¹⁶⁵, T. Vickey¹³⁹, O.E. Vickey Boeriu¹³⁹, G.H.A. Viehhauser¹²⁰, S. Viel¹⁵, R. Vigne⁶², M. Villa^{20a,20b}, M. Villaplana Perez^{91a,91b}, E. Vilucchi⁴⁷, M.G. Vinciter²⁹, V.B. Vinogradov⁶⁵, I. Vivarelli¹⁴⁹, F. Vives Vaque³, S. Vlachos¹⁰, D. Vladioiu¹⁰⁰, M. Vlasak¹²⁸, M. Vogel^{32a}, P. Vokac¹²⁸, G. Volpi^{124a,124b}, M. Volpi⁸⁸, H. von der Schmitt¹⁰¹, H. von Radziewski⁴⁸, E. von Toerne²¹, V. Vorobel¹²⁹, K. Vorobev⁹⁸, M. Vos¹⁶⁷, R. Voss³⁰, J.H. Vosseveld⁷⁴, N. Vranjes¹³, M. Vranjes Milosavljevic¹³, V. Vrba¹²⁷, M. Vreeswijk¹⁰⁷, R. Vuillermet³⁰, I. Vukotic³¹, Z. Vykydal¹²⁸, P. Wagner²¹, W. Wagner¹⁷⁵, H. Wahlberg⁷¹, S. Wahrmond⁴⁴, J. Wakabayashi¹⁰³, J. Walder⁷², R. Walker¹⁰⁰, W. Walkowiak¹⁴¹, C. Wang¹⁵¹, F. Wang¹⁷³, H. Wang¹⁵, H. Wang⁴⁰, J. Wang⁴², J. Wang¹⁵⁰, K. Wang⁸⁷, R. Wang⁶, S.M. Wang¹⁵¹, T. Wang²¹, T. Wang³⁵, X. Wang¹⁷⁶, C. Wanotayaroj¹¹⁶, A. Warburton⁸⁷, C.P. Ward²⁸, D.R. Wardrope⁷⁸, A. Washbrook⁴⁶, C. Wasicki⁴², P.M. Watkins¹⁸, A.T. Watson¹⁸, I.J. Watson¹⁵⁰, M.F. Watson¹⁸, G. Watts¹³⁸, S. Watts⁸⁴, B.M. Waugh⁷⁸, S. Webb⁸⁴, M.S. Weber¹⁷, S.W. Weber¹⁷⁴, J.S. Webster³¹, A.R. Weidberg¹²⁰, B. Weinert⁶¹, J. Weingarten⁵⁴, C. Weiser⁴⁸, H. Weits¹⁰⁷, P.S. Wells³⁰, T. Wenaus²⁵, T. Wengler³⁰, S. Wenig³⁰, N. Wermes²¹, M. Werner⁴⁸, P. Werner³⁰, M. Wessels^{58a}, J. Wetter¹⁶¹, K. Whalen¹¹⁶, A.M. Wharton⁷², A. White⁸, M.J. White¹, R. White^{32b}, S. White^{124a,124b}, D. Whiteson¹⁶³, F.J. Wickens¹³¹, W. Wiedenmann¹⁷³, M. Wielers¹³¹, P. Wienemann²¹, C. Wiglesworth³⁶, L.A.M. Wiik-Fuchs²¹, A. Wildauer¹⁰¹, H.G. Wilkens³⁰, H.H. Williams¹²², S. Williams¹⁰⁷, C. Willis⁹⁰, S. Willocq⁸⁶, A. Wilson⁸⁹, J.A. Wilson¹⁸, I. Wingerter-Seez⁵, F. Winklmeier¹¹⁶, B.T. Winter²¹, M. Wittgen¹⁴³, J. Wittkowski¹⁰⁰, S.J. Wollstadt⁸³, M.W. Wolter³⁹, H. Wolters^{126a,126c}, B.K. Wosiek³⁹, J. Wotschack³⁰, M.J. Woudstra⁸⁴, K.W. Wozniak³⁹, M. Wu⁵⁵, M. Wu³¹, S.L. Wu¹⁷³, X. Wu⁴⁹, Y. Wu⁸⁹, T.R. Wyatt⁸⁴, B.M. Wynne⁴⁶, S. Xella³⁶, D. Xu^{33a}, L. Xu²⁵, B. Yabsley¹⁵⁰, S. Yacoub^{145a}, R. Yakabe⁶⁷, M. Yamada⁶⁶, D. Yamaguchi¹⁵⁷, Y. Yamaguchi¹¹⁸, A. Yamamoto⁶⁶, S. Yamamoto¹⁵⁵, T. Yamanaka¹⁵⁵, K. Yamauchi¹⁰³, Y. Yamazaki⁶⁷, Z. Yan²², H. Yang^{33e}, H. Yang¹⁷³, Y. Yang¹⁵¹, W-M. Yao¹⁵, Y. Yasu⁶⁶, E. Yatsenko⁵, K.H. Yau Wong²¹, J. Ye⁴⁰, S. Ye²⁵, I. Yeletsikh⁶⁵, A.L. Yen⁵⁷, E. Yildirim⁴², K. Yorita¹⁷¹, R. Yoshida⁶, K. Yoshihara¹²², C. Young¹⁴³, C.J.S. Young³⁰, S. Youssef²², D.R. Yu¹⁵, J. Yu⁸, J.M. Yu⁸⁹, J. Yu¹¹⁴, L. Yuan⁶⁷, S.P.Y. Yuen²¹, A. Yurkewicz¹⁰⁸, I. Yusuff^{28,a1}, B. Zabinski³⁹, R. Zaidan⁶³, A.M. Zaitsev^{130,ac}, J. Zalieckas¹⁴, A. Zaman¹⁴⁸, S. Zambito⁵⁷, L. Zanello^{132a,132b}, D. Zanzi⁸⁸, C. Zeitnitz¹⁷⁵, M. Zeman¹²⁸, A. Zemla^{38a}, Q. Zeng¹⁴³, K. Zengel²³, O. Zenin¹³⁰, T. Ženiš^{144a}, D. Zerwas¹¹⁷, D. Zhang⁸⁹, F. Zhang¹⁷³, H. Zhang^{33c}, J. Zhang⁶, L. Zhang⁴⁸, R. Zhang^{33b,i}, X. Zhang^{33d}, Z. Zhang¹¹⁷, X. Zhao⁴⁰, Y. Zhao^{33d,117}, Z. Zhao^{33b}, A. Zhemchugov⁶⁵, J. Zhong¹²⁰, B. Zhou⁸⁹, C. Zhou⁴⁵, L. Zhou³⁵, L. Zhou⁴⁰, M. Zhou¹⁴⁸, N. Zhou^{33f}, C.G. Zhu^{33d}, H. Zhu^{33a}, J. Zhu⁸⁹, Y. Zhu^{33b}, X. Zhuang^{33a}, K. Zhukov⁹⁶, A. Zibell¹⁷⁴, D. Zieminska⁶¹, N.I. Zimine⁶⁵, C. Zimmermann⁸³, S. Zimmermann⁴⁸, Z. Zinonos⁵⁴, M. Zinser⁸³, M. Ziolkowski¹⁴¹, L. Živković¹³, G. Zobernig¹⁷³, A. Zoccoli^{20a,20b}, M. zur Nedden¹⁶, G. Zurzolo^{104a,104b}, L. Zwalinski³⁰.

¹ Department of Physics, University of Adelaide, Adelaide, Australia

² Physics Department, SUNY Albany, Albany NY, United States of America

³ Department of Physics, University of Alberta, Edmonton AB, Canada

⁴ (a) Department of Physics, Ankara University, Ankara; (b) Istanbul Aydin University, Istanbul; (c)

Division of Physics, TOBB University of Economics and Technology, Ankara, Turkey

⁵ LAPP, CNRS/IN2P3 and Université Savoie Mont Blanc, Annecy-le-Vieux, France

⁶ High Energy Physics Division, Argonne National Laboratory, Argonne IL, United States of America

⁷ Department of Physics, University of Arizona, Tucson AZ, United States of America

⁸ Department of Physics, The University of Texas at Arlington, Arlington TX, United States of America

⁹ Physics Department, University of Athens, Athens, Greece

¹⁰ Physics Department, National Technical University of Athens, Zografou, Greece

¹¹ Institute of Physics, Azerbaijan Academy of Sciences, Baku, Azerbaijan

¹² Institut de Física d'Altes Energies and Departament de Física de la Universitat Autònoma de Barcelona, Barcelona, Spain

¹³ Institute of Physics, University of Belgrade, Belgrade, Serbia

¹⁴ Department for Physics and Technology, University of Bergen, Bergen, Norway

¹⁵ Physics Division, Lawrence Berkeley National Laboratory and University of California, Berkeley CA, United States of America

¹⁶ Department of Physics, Humboldt University, Berlin, Germany

¹⁷ Albert Einstein Center for Fundamental Physics and Laboratory for High Energy Physics, University of Bern, Bern, Switzerland

¹⁸ School of Physics and Astronomy, University of Birmingham, Birmingham, United Kingdom

¹⁹ ^(a) Department of Physics, Bogazici University, Istanbul; ^(b) Department of Physics Engineering, Gaziantep University, Gaziantep; ^(c) Department of Physics, Dogus University, Istanbul, Turkey

²⁰ ^(a) INFN Sezione di Bologna; ^(b) Dipartimento di Fisica e Astronomia, Università di Bologna, Bologna, Italy

²¹ Physikalisches Institut, University of Bonn, Bonn, Germany

²² Department of Physics, Boston University, Boston MA, United States of America

²³ Department of Physics, Brandeis University, Waltham MA, United States of America

²⁴ ^(a) Universidade Federal do Rio De Janeiro COPPE/EE/IF, Rio de Janeiro; ^(b) Electrical Circuits Department, Federal University of Juiz de Fora (UFJF), Juiz de Fora; ^(c) Federal University of Sao Joao del Rei (UFSJ), Sao Joao del Rei; ^(d) Instituto de Fisica, Universidade de Sao Paulo, Sao Paulo, Brazil

²⁵ Physics Department, Brookhaven National Laboratory, Upton NY, United States of America

²⁶ ^(a) Transilvania University of Brasov, Brasov, Romania; ^(b) National Institute of Physics and Nuclear Engineering, Bucharest; ^(c) National Institute for Research and Development of Isotopic and Molecular Technologies, Physics Department, Cluj Napoca; ^(d) University Politehnica Bucharest, Bucharest; ^(e) West University in Timisoara, Timisoara, Romania

²⁷ Departamento de Física, Universidad de Buenos Aires, Buenos Aires, Argentina

²⁸ Cavendish Laboratory, University of Cambridge, Cambridge, United Kingdom

²⁹ Department of Physics, Carleton University, Ottawa ON, Canada

³⁰ CERN, Geneva, Switzerland

³¹ Enrico Fermi Institute, University of Chicago, Chicago IL, United States of America

³² ^(a) Departamento de Física, Pontificia Universidad Católica de Chile, Santiago; ^(b) Departamento de Física, Universidad Técnica Federico Santa María, Valparaíso, Chile

³³ ^(a) Institute of High Energy Physics, Chinese Academy of Sciences, Beijing; ^(b) Department of Modern Physics, University of Science and Technology of China, Anhui; ^(c) Department of Physics, Nanjing University, Jiangsu; ^(d) School of Physics, Shandong University, Shandong; ^(e) Department of Physics and Astronomy, Shanghai Key Laboratory for Particle Physics and Cosmology, Shanghai Jiao Tong University, Shanghai; ^(f) Physics Department, Tsinghua University, Beijing 100084, China

³⁴ Laboratoire de Physique Corpusculaire, Clermont Université and Université Blaise Pascal and CNRS/IN2P3, Clermont-Ferrand, France

- ³⁵ Nevis Laboratory, Columbia University, Irvington NY, United States of America
- ³⁶ Niels Bohr Institute, University of Copenhagen, Kobenhavn, Denmark
- ³⁷ ^(a) INFN Gruppo Collegato di Cosenza, Laboratori Nazionali di Frascati; ^(b) Dipartimento di Fisica, Università della Calabria, Rende, Italy
- ³⁸ ^(a) AGH University of Science and Technology, Faculty of Physics and Applied Computer Science, Krakow; ^(b) Marian Smoluchowski Institute of Physics, Jagiellonian University, Krakow, Poland
- ³⁹ Institute of Nuclear Physics Polish Academy of Sciences, Krakow, Poland
- ⁴⁰ Physics Department, Southern Methodist University, Dallas TX, United States of America
- ⁴¹ Physics Department, University of Texas at Dallas, Richardson TX, United States of America
- ⁴² DESY, Hamburg and Zeuthen, Germany
- ⁴³ Institut für Experimentelle Physik IV, Technische Universität Dortmund, Dortmund, Germany
- ⁴⁴ Institut für Kern- und Teilchenphysik, Technische Universität Dresden, Dresden, Germany
- ⁴⁵ Department of Physics, Duke University, Durham NC, United States of America
- ⁴⁶ SUPA - School of Physics and Astronomy, University of Edinburgh, Edinburgh, United Kingdom
- ⁴⁷ INFN Laboratori Nazionali di Frascati, Frascati, Italy
- ⁴⁸ Fakultät für Mathematik und Physik, Albert-Ludwigs-Universität, Freiburg, Germany
- ⁴⁹ Section de Physique, Université de Genève, Geneva, Switzerland
- ⁵⁰ ^(a) INFN Sezione di Genova; ^(b) Dipartimento di Fisica, Università di Genova, Genova, Italy
- ⁵¹ ^(a) E. Andronikashvili Institute of Physics, Iv. Javakhishvili Tbilisi State University, Tbilisi; ^(b) High Energy Physics Institute, Tbilisi State University, Tbilisi, Georgia
- ⁵² II Physikalisches Institut, Justus-Liebig-Universität Giessen, Giessen, Germany
- ⁵³ SUPA - School of Physics and Astronomy, University of Glasgow, Glasgow, United Kingdom
- ⁵⁴ II Physikalisches Institut, Georg-August-Universität, Göttingen, Germany
- ⁵⁵ Laboratoire de Physique Subatomique et de Cosmologie, Université Grenoble-Alpes, CNRS/IN2P3, Grenoble, France
- ⁵⁶ Department of Physics, Hampton University, Hampton VA, United States of America
- ⁵⁷ Laboratory for Particle Physics and Cosmology, Harvard University, Cambridge MA, United States of America
- ⁵⁸ ^(a) Kirchhoff-Institut für Physik, Ruprecht-Karls-Universität Heidelberg, Heidelberg; ^(b) Physikalisches Institut, Ruprecht-Karls-Universität Heidelberg, Heidelberg; ^(c) ZITI Institut für technische Informatik, Ruprecht-Karls-Universität Heidelberg, Mannheim, Germany
- ⁵⁹ Faculty of Applied Information Science, Hiroshima Institute of Technology, Hiroshima, Japan
- ⁶⁰ ^(a) Department of Physics, The Chinese University of Hong Kong, Shatin, N.T., Hong Kong; ^(b) Department of Physics, The University of Hong Kong, Hong Kong; ^(c) Department of Physics, The Hong Kong University of Science and Technology, Clear Water Bay, Kowloon, Hong Kong, China
- ⁶¹ Department of Physics, Indiana University, Bloomington IN, United States of America
- ⁶² Institut für Astro- und Teilchenphysik, Leopold-Franzens-Universität, Innsbruck, Austria
- ⁶³ University of Iowa, Iowa City IA, United States of America
- ⁶⁴ Department of Physics and Astronomy, Iowa State University, Ames IA, United States of America
- ⁶⁵ Joint Institute for Nuclear Research, JINR Dubna, Dubna, Russia
- ⁶⁶ KEK, High Energy Accelerator Research Organization, Tsukuba, Japan
- ⁶⁷ Graduate School of Science, Kobe University, Kobe, Japan
- ⁶⁸ Faculty of Science, Kyoto University, Kyoto, Japan
- ⁶⁹ Kyoto University of Education, Kyoto, Japan
- ⁷⁰ Department of Physics, Kyushu University, Fukuoka, Japan
- ⁷¹ Instituto de Física La Plata, Universidad Nacional de La Plata and CONICET, La Plata, Argentina
- ⁷² Physics Department, Lancaster University, Lancaster, United Kingdom

- ⁷³ ^(a) INFN Sezione di Lecce; ^(b) Dipartimento di Matematica e Fisica, Università del Salento, Lecce, Italy
- ⁷⁴ Oliver Lodge Laboratory, University of Liverpool, Liverpool, United Kingdom
- ⁷⁵ Department of Physics, Jožef Stefan Institute and University of Ljubljana, Ljubljana, Slovenia
- ⁷⁶ School of Physics and Astronomy, Queen Mary University of London, London, United Kingdom
- ⁷⁷ Department of Physics, Royal Holloway University of London, Surrey, United Kingdom
- ⁷⁸ Department of Physics and Astronomy, University College London, London, United Kingdom
- ⁷⁹ Louisiana Tech University, Ruston LA, United States of America
- ⁸⁰ Laboratoire de Physique Nucléaire et de Hautes Energies, UPMC and Université Paris-Diderot and CNRS/IN2P3, Paris, France
- ⁸¹ Fysiska institutionen, Lunds universitet, Lund, Sweden
- ⁸² Departamento de Física Teórica C-15, Universidad Autónoma de Madrid, Madrid, Spain
- ⁸³ Institut für Physik, Universität Mainz, Mainz, Germany
- ⁸⁴ School of Physics and Astronomy, University of Manchester, Manchester, United Kingdom
- ⁸⁵ CPPM, Aix-Marseille Université and CNRS/IN2P3, Marseille, France
- ⁸⁶ Department of Physics, University of Massachusetts, Amherst MA, United States of America
- ⁸⁷ Department of Physics, McGill University, Montreal QC, Canada
- ⁸⁸ School of Physics, University of Melbourne, Victoria, Australia
- ⁸⁹ Department of Physics, The University of Michigan, Ann Arbor MI, United States of America
- ⁹⁰ Department of Physics and Astronomy, Michigan State University, East Lansing MI, United States of America
- ⁹¹ ^(a) INFN Sezione di Milano; ^(b) Dipartimento di Fisica, Università di Milano, Milano, Italy
- ⁹² B.I. Stepanov Institute of Physics, National Academy of Sciences of Belarus, Minsk, Republic of Belarus
- ⁹³ National Scientific and Educational Centre for Particle and High Energy Physics, Minsk, Republic of Belarus
- ⁹⁴ Department of Physics, Massachusetts Institute of Technology, Cambridge MA, United States of America
- ⁹⁵ Group of Particle Physics, University of Montreal, Montreal QC, Canada
- ⁹⁶ P.N. Lebedev Institute of Physics, Academy of Sciences, Moscow, Russia
- ⁹⁷ Institute for Theoretical and Experimental Physics (ITEP), Moscow, Russia
- ⁹⁸ National Research Nuclear University MEPhI, Moscow, Russia
- ⁹⁹ D.V. Skobeltsyn Institute of Nuclear Physics, M.V. Lomonosov Moscow State University, Moscow, Russia
- ¹⁰⁰ Fakultät für Physik, Ludwig-Maximilians-Universität München, München, Germany
- ¹⁰¹ Max-Planck-Institut für Physik (Werner-Heisenberg-Institut), München, Germany
- ¹⁰² Nagasaki Institute of Applied Science, Nagasaki, Japan
- ¹⁰³ Graduate School of Science and Kobayashi-Maskawa Institute, Nagoya University, Nagoya, Japan
- ¹⁰⁴ ^(a) INFN Sezione di Napoli; ^(b) Dipartimento di Fisica, Università di Napoli, Napoli, Italy
- ¹⁰⁵ Department of Physics and Astronomy, University of New Mexico, Albuquerque NM, United States of America
- ¹⁰⁶ Institute for Mathematics, Astrophysics and Particle Physics, Radboud University Nijmegen/Nikhef, Nijmegen, Netherlands
- ¹⁰⁷ Nikhef National Institute for Subatomic Physics and University of Amsterdam, Amsterdam, Netherlands
- ¹⁰⁸ Department of Physics, Northern Illinois University, DeKalb IL, United States of America
- ¹⁰⁹ Budker Institute of Nuclear Physics, SB RAS, Novosibirsk, Russia

- ¹¹⁰ Department of Physics, New York University, New York NY, United States of America
- ¹¹¹ Ohio State University, Columbus OH, United States of America
- ¹¹² Faculty of Science, Okayama University, Okayama, Japan
- ¹¹³ Homer L. Dodge Department of Physics and Astronomy, University of Oklahoma, Norman OK, United States of America
- ¹¹⁴ Department of Physics, Oklahoma State University, Stillwater OK, United States of America
- ¹¹⁵ Palacký University, RCPTM, Olomouc, Czech Republic
- ¹¹⁶ Center for High Energy Physics, University of Oregon, Eugene OR, United States of America
- ¹¹⁷ LAL, Université Paris-Sud and CNRS/IN2P3, Orsay, France
- ¹¹⁸ Graduate School of Science, Osaka University, Osaka, Japan
- ¹¹⁹ Department of Physics, University of Oslo, Oslo, Norway
- ¹²⁰ Department of Physics, Oxford University, Oxford, United Kingdom
- ¹²¹ ^(a) INFN Sezione di Pavia; ^(b) Dipartimento di Fisica, Università di Pavia, Pavia, Italy
- ¹²² Department of Physics, University of Pennsylvania, Philadelphia PA, United States of America
- ¹²³ National Research Centre "Kurchatov Institute" B.P.Konstantinov Petersburg Nuclear Physics Institute, St. Petersburg, Russia
- ¹²⁴ ^(a) INFN Sezione di Pisa; ^(b) Dipartimento di Fisica E. Fermi, Università di Pisa, Pisa, Italy
- ¹²⁵ Department of Physics and Astronomy, University of Pittsburgh, Pittsburgh PA, United States of America
- ¹²⁶ ^(a) Laboratório de Instrumentação e Física Experimental de Partículas - LIP, Lisboa; ^(b) Faculdade de Ciências, Universidade de Lisboa, Lisboa; ^(c) Department of Physics, University of Coimbra, Coimbra; ^(d) Centro de Física Nuclear da Universidade de Lisboa, Lisboa; ^(e) Departamento de Física, Universidade do Minho, Braga; ^(f) Departamento de Física Teórica y del Cosmos and CAFPE, Universidad de Granada, Granada (Spain); ^(g) Dep Física and CEFITEC of Faculdade de Ciências e Tecnologia, Universidade Nova de Lisboa, Caparica, Portugal
- ¹²⁷ Institute of Physics, Academy of Sciences of the Czech Republic, Praha, Czech Republic
- ¹²⁸ Czech Technical University in Prague, Praha, Czech Republic
- ¹²⁹ Faculty of Mathematics and Physics, Charles University in Prague, Praha, Czech Republic
- ¹³⁰ State Research Center Institute for High Energy Physics (Protvino), NRC KI, Russia, Russia
- ¹³¹ Particle Physics Department, Rutherford Appleton Laboratory, Didcot, United Kingdom
- ¹³² ^(a) INFN Sezione di Roma; ^(b) Dipartimento di Fisica, Sapienza Università di Roma, Roma, Italy
- ¹³³ ^(a) INFN Sezione di Roma Tor Vergata; ^(b) Dipartimento di Fisica, Università di Roma Tor Vergata, Roma, Italy
- ¹³⁴ ^(a) INFN Sezione di Roma Tre; ^(b) Dipartimento di Matematica e Fisica, Università Roma Tre, Roma, Italy
- ¹³⁵ ^(a) Faculté des Sciences Ain Chock, Réseau Universitaire de Physique des Hautes Energies - Université Hassan II, Casablanca; ^(b) Centre National de l'Energie des Sciences Techniques Nucleaires, Rabat; ^(c) Faculté des Sciences Semlalia, Université Cadi Ayyad, LPHEA-Marrakech; ^(d) Faculté des Sciences, Université Mohamed Premier and LPTPM, Oujda; ^(e) Faculté des sciences, Université Mohammed V, Rabat, Morocco
- ¹³⁶ DSM/IRFU (Institut de Recherches sur les Lois Fondamentales de l'Univers), CEA Saclay (Commissariat à l'Energie Atomique et aux Energies Alternatives), Gif-sur-Yvette, France
- ¹³⁷ Santa Cruz Institute for Particle Physics, University of California Santa Cruz, Santa Cruz CA, United States of America
- ¹³⁸ Department of Physics, University of Washington, Seattle WA, United States of America
- ¹³⁹ Department of Physics and Astronomy, University of Sheffield, Sheffield, United Kingdom
- ¹⁴⁰ Department of Physics, Shinshu University, Nagano, Japan

- ¹⁴¹ Fachbereich Physik, Universität Siegen, Siegen, Germany
- ¹⁴² Department of Physics, Simon Fraser University, Burnaby BC, Canada
- ¹⁴³ SLAC National Accelerator Laboratory, Stanford CA, United States of America
- ¹⁴⁴ ^(a) Faculty of Mathematics, Physics & Informatics, Comenius University, Bratislava; ^(b) Department of Subnuclear Physics, Institute of Experimental Physics of the Slovak Academy of Sciences, Kosice, Slovak Republic
- ¹⁴⁵ ^(a) Department of Physics, University of Cape Town, Cape Town; ^(b) Department of Physics, University of Johannesburg, Johannesburg; ^(c) School of Physics, University of the Witwatersrand, Johannesburg, South Africa
- ¹⁴⁶ ^(a) Department of Physics, Stockholm University; ^(b) The Oskar Klein Centre, Stockholm, Sweden
- ¹⁴⁷ Physics Department, Royal Institute of Technology, Stockholm, Sweden
- ¹⁴⁸ Departments of Physics & Astronomy and Chemistry, Stony Brook University, Stony Brook NY, United States of America
- ¹⁴⁹ Department of Physics and Astronomy, University of Sussex, Brighton, United Kingdom
- ¹⁵⁰ School of Physics, University of Sydney, Sydney, Australia
- ¹⁵¹ Institute of Physics, Academia Sinica, Taipei, Taiwan
- ¹⁵² Department of Physics, Technion: Israel Institute of Technology, Haifa, Israel
- ¹⁵³ Raymond and Beverly Sackler School of Physics and Astronomy, Tel Aviv University, Tel Aviv, Israel
- ¹⁵⁴ Department of Physics, Aristotle University of Thessaloniki, Thessaloniki, Greece
- ¹⁵⁵ International Center for Elementary Particle Physics and Department of Physics, The University of Tokyo, Tokyo, Japan
- ¹⁵⁶ Graduate School of Science and Technology, Tokyo Metropolitan University, Tokyo, Japan
- ¹⁵⁷ Department of Physics, Tokyo Institute of Technology, Tokyo, Japan
- ¹⁵⁸ Department of Physics, University of Toronto, Toronto ON, Canada
- ¹⁵⁹ ^(a) TRIUMF, Vancouver BC; ^(b) Department of Physics and Astronomy, York University, Toronto ON, Canada
- ¹⁶⁰ Faculty of Pure and Applied Sciences, and Center for Integrated Research in Fundamental Science and Engineering, University of Tsukuba, Tsukuba, Japan
- ¹⁶¹ Department of Physics and Astronomy, Tufts University, Medford MA, United States of America
- ¹⁶² Centro de Investigaciones, Universidad Antonio Narino, Bogota, Colombia
- ¹⁶³ Department of Physics and Astronomy, University of California Irvine, Irvine CA, United States of America
- ¹⁶⁴ ^(a) INFN Gruppo Collegato di Udine, Sezione di Trieste, Udine; ^(b) ICTP, Trieste; ^(c) Dipartimento di Chimica, Fisica e Ambiente, Università di Udine, Udine, Italy
- ¹⁶⁵ Department of Physics, University of Illinois, Urbana IL, United States of America
- ¹⁶⁶ Department of Physics and Astronomy, University of Uppsala, Uppsala, Sweden
- ¹⁶⁷ Instituto de Física Corpuscular (IFIC) and Departamento de Física Atómica, Molecular y Nuclear and Departamento de Ingeniería Electrónica and Instituto de Microelectrónica de Barcelona (IMB-CNM), University of Valencia and CSIC, Valencia, Spain
- ¹⁶⁸ Department of Physics, University of British Columbia, Vancouver BC, Canada
- ¹⁶⁹ Department of Physics and Astronomy, University of Victoria, Victoria BC, Canada
- ¹⁷⁰ Department of Physics, University of Warwick, Coventry, United Kingdom
- ¹⁷¹ Waseda University, Tokyo, Japan
- ¹⁷² Department of Particle Physics, The Weizmann Institute of Science, Rehovot, Israel
- ¹⁷³ Department of Physics, University of Wisconsin, Madison WI, United States of America
- ¹⁷⁴ Fakultät für Physik und Astronomie, Julius-Maximilians-Universität, Würzburg, Germany

- ¹⁷⁵ Fachbereich C Physik, Bergische Universität Wuppertal, Wuppertal, Germany
- ¹⁷⁶ Department of Physics, Yale University, New Haven CT, United States of America
- ¹⁷⁷ Yerevan Physics Institute, Yerevan, Armenia
- ¹⁷⁸ Centre de Calcul de l'Institut National de Physique Nucléaire et de Physique des Particules (IN2P3), Villeurbanne, France
- ^a Also at Department of Physics, King's College London, London, United Kingdom
- ^b Also at Institute of Physics, Azerbaijan Academy of Sciences, Baku, Azerbaijan
- ^c Also at Novosibirsk State University, Novosibirsk, Russia
- ^d Also at TRIUMF, Vancouver BC, Canada
- ^e Also at Department of Physics, California State University, Fresno CA, United States of America
- ^f Also at Department of Physics, University of Fribourg, Fribourg, Switzerland
- ^g Also at Departamento de Física e Astronomia, Faculdade de Ciências, Universidade do Porto, Portugal
- ^h Also at Tomsk State University, Tomsk, Russia
- ⁱ Also at CPPM, Aix-Marseille Université and CNRS/IN2P3, Marseille, France
- ^j Also at Università di Napoli Parthenope, Napoli, Italy
- ^k Also at Institute of Particle Physics (IPP), Canada
- ^l Also at Particle Physics Department, Rutherford Appleton Laboratory, Didcot, United Kingdom
- ^m Also at Department of Physics, St. Petersburg State Polytechnical University, St. Petersburg, Russia
- ⁿ Also at Louisiana Tech University, Ruston LA, United States of America
- ^o Also at Institució Catalana de Recerca i Estudis Avançats, ICREA, Barcelona, Spain
- ^p Also at Department of Physics, The University of Michigan, Ann Arbor MI, United States of America
- ^q Also at Graduate School of Science, Osaka University, Osaka, Japan
- ^r Also at Department of Physics, National Tsing Hua University, Taiwan
- ^s Also at Department of Physics, The University of Texas at Austin, Austin TX, United States of America
- ^t Also at Institute of Theoretical Physics, Ilia State University, Tbilisi, Georgia
- ^u Also at CERN, Geneva, Switzerland
- ^v Also at Georgian Technical University (GTU), Tbilisi, Georgia
- ^w Also at Manhattan College, New York NY, United States of America
- ^x Also at Hellenic Open University, Patras, Greece
- ^y Also at Institute of Physics, Academia Sinica, Taipei, Taiwan
- ^z Also at LAL, Université Paris-Sud and CNRS/IN2P3, Orsay, France
- ^{aa} Also at Academia Sinica Grid Computing, Institute of Physics, Academia Sinica, Taipei, Taiwan
- ^{ab} Also at School of Physics, Shandong University, Shandong, China
- ^{ac} Also at Moscow Institute of Physics and Technology State University, Dolgoprudny, Russia
- ^{ad} Also at Section de Physique, Université de Genève, Geneva, Switzerland
- ^{ae} Also at International School for Advanced Studies (SISSA), Trieste, Italy
- ^{af} Also at Department of Physics and Astronomy, University of South Carolina, Columbia SC, United States of America
- ^{ag} Also at School of Physics and Engineering, Sun Yat-sen University, Guangzhou, China
- ^{ah} Also at Faculty of Physics, M.V.Lomonosov Moscow State University, Moscow, Russia
- ^{ai} Also at National Research Nuclear University MEPhI, Moscow, Russia
- ^{aj} Also at Department of Physics, Stanford University, Stanford CA, United States of America
- ^{ak} Also at Institute for Particle and Nuclear Physics, Wigner Research Centre for Physics, Budapest, Hungary
- ^{al} Also at University of Malaya, Department of Physics, Kuala Lumpur, Malaysia
- * Deceased